Cellular and molecular impacts of copper exposure in parental and resistant human intestinal Caco-2 cells

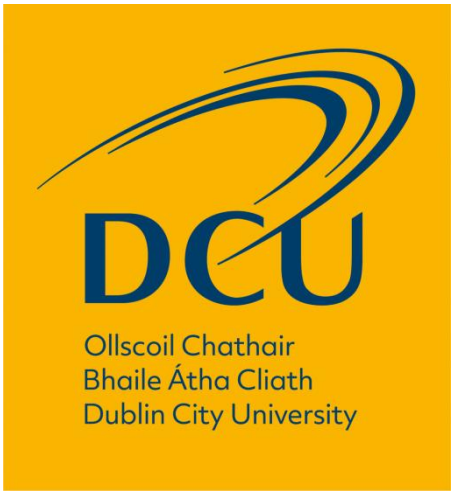

A thesis by publication submitted for the degree of PhD

By **Charles O'Doherty, B.Sc. (Hons)**

The work described herein was conducted under the supervision of

Dr Joanne Keenan & Dr Finbarr O'Sullivan

School of Biotechnology,

Dublin City University

August 2020

I hereby certify that this material, which I now submit for assessment on the programme of study leading to the award of PhD is entirely my own work, that I have exercised reasonable care to ensure that the work is original, and does not to the best of my knowledge breach any law of copyright, and has not been taken from the work of others save and to the extent that such work has been cited and acknowledged within the text of my work.

Signed:  (Candidate) ID No.: 57366230

Date: 31/08/2020

Now the dust settles all around me,

I want to dedicate this thesis to two wonderful people,

My late father Manus,

Without whom, I would not have started,

And my mother Pauline,

Without whom, I would not have finished.

Acknowledgements

Firstly I would like to thank my supervisors at the NICB; Prof Martin Clynes, Dr Joanne Keenan and Dr Finbarr O'Sullivan and at Alltech; Prof Richard Murphy and Dr Karina Horgan. This work was only made possible with your guidance, encouragement and wisdom. I am grateful for the opportunity and deeply appreciate all the support over the years, especially the last two when papers were flying.

I would like to thank Dr Michael Henry and Dr Paula Meleady for their help during the proteomics studies and expertise in all things protein related. I want to extend my gratitude also to Dr Fiona O'Neill who was essential in generating all the microarray data and for being so patient when the RNA would not behave.

I would like to thank those who are essential to keeping the NICB standing and everything running so smoothly behind the scenes, particularly Mairead Callan and Gillan Smith for their help in accessing everything I needed to complete my work.

A massive thank you to the amazing people I've had the joy of getting to know these last few years, you've made this journey far easier and for that I will be forever grateful. I want to thank Neil, Nicola, John, Shannon, Ciara and the rest of the first floor gang; the way you guys looked out for me and each other kept me going to the end. A special shout out to my G119 co-conspirator Ali Coyle, for sharing all the ups and downs of a PhD including many rants, rambles and eclectic music choices, it has been an experience! Thanks also to those past and present, for getting me out to clear to the cobwebs when cell culture and paper writing seemed endless, particularly Anto, Sam, Berta, Charlotte, Agata and Prashant.

I also want to thank my girlfriend Vanessa whom I met in my final year and is somehow still with me, testament to your patience and love. Finally, thanks to my family - my mum Pauline for doing more than anyone could ask from the start of this journey, and to my sister Catherine for her love and support. You've been with me for the whole roller-coaster, from the highs at each publication acceptance to the lows when I had to start something again from scratch. I couldn't have done it without you guys. Lastly, I thank my inspiration for taking this on, my father Manus. I looked to his wisdom, strength and stubbornness during the toughest times. Thank you for believing in me. I can only imagine how proud you'd be.

Table of Contents

Abbreviations and Acronyms

AMP	-	Antimicrobial peptide
BSA	-	Bovine serum albumin
CCS	-	Copper chaperone to superoxide dismutase
cDNA	-	Complementary deoxyribonucleic acid
CTR1	-	Copper transporter 1
$CuSO_4$	-	Copper sulfate
Cu Pro	-	Copper chelate to soy protein hydrolysate (Cu Proteinate)
DCFDA	-	2, 7-dichlorofluorescein diacetate
DMEM	-	Dulbecco's modified Eagle medium
DMSO	-	Dimethyl sulfoxide
DMT1	-	Divalent metal transporter 1
DNA	-	Deoxyribonucleic acid
EDTA	-	Ethylenediaminetetraacetic acid
FAE	-	Follicle associated epithelium
FBS	-	Fetal bovine serum
GALT	-	Gut associated lymphoid tissue
H_2O_2	-	Hydrogen peroxide
HEPES	-	2-[4-(2-hydroxyethyl) piperazin-1-yl] ethanesulfonic acid
HIO	-	Human intestinal organoid
IE	-	In exposure (copper selection pressure)
IESC	-	Intestinal epithelial stem cell
IF	-	Immunofluorescence

LGR5	-	Leucine-rich repeat-containing G protein-coupled receptor 5
M-cell	-	Microfold cell
MEM	-	Eagle's minimal essential medium
MT	-	Metallothionein
MTX	-	Methotrexate
NMDR	-	Non-monotonic dose-responses
OOE	-	Out of exposure (removed from selection pressure)
PBS	-	Phosphate buffered saline
PCR	-	Polymerase chain reaction
PepT	-	Peptide transporter
RNA	-	Ribonucleic acid
ROH_2O	-	Reverse osmosis treated water
ROS	-	Reactive oxygen species
RT	-	Reverse transcription
SCO	-	Cytochrome c oxidase assembly protein
SI	-	Small intestine
TA	-	Transit-amplifying
TEER	-	Transepithelial electrical resistance
THIO	-	Thioglycollate broth
TJ	-	Tight junction
TSB	-	Tryptone soya broth
ZnT	-	Zinc transporter
ZO	-	Zonula-occludens

Thesis Structure

Section	Title	Status of publication	Authors	Contribution
Chapter 1	Introduction - theory and literature review	-	-	-
Chapter 2	Copper-induced non-monotonic dose response in Caco-2 cells	Accepted and published in In Vitro Cellular & Developmental Biology – Animal, DOI: 10.1007/s11626-019-00333-8	Charles O'Doherty, Joanne Keenan, Karina Horgan, Richard Murphy, Finbarr O'Sullivan and Martin Clynes	All authors contributed to the experimental design. Primary contributor to execution.
Chapter 3	Characterisation and proteomic profiling of continuously exposed Cu-resistant variants of the Caco-2 cell line	Accepted and published in Toxicology In Vitro, DOI: 10.1016/j.tiv.2020.104773	Charles O'Doherty, Joanne Keenan, Michael Henry, Paula Meleady, Indre Sinkunaite, Martin Clynes, Finbarr O'Sullivan, Karina Horgan and Richard Murphy	All authors contributed to the experimental design. Primary contributor to execution. MH carried out Mass Spec; JK carried out data acquisition and generation of DEP lists
Chapter 4	Gene expression profiling of copper-resistant Caco-2 clones	Accepted and published in Metallomics, DOI: 10.1039/D0MT00126K	Charles O'Doherty, Joanne Keenan, Fiona O'Neill, Martin Clynes, Indre Sinkunaite, Karina Horgan, Richard Murphy and Finbarr O'Sullivan	All authors contributed to the experimental design. Primary contributor to execution. FON and COD carried out microarray analysis
Chapter 5	LC-MS proteomic profiling of Caco-2 human intestinal cells exposed to the copper-chelating agent, triethylenetetramine: A preliminary study	Accepted and published in Biochemical and Biophysical Research Communications, DOI: 10.1016/j.bbrc.2020.01.138	Charles O'Doherty, Finbarr O'Sullivan, Michael Henry, Paula Meleady, Martin Clynes, Karina Horgan, Joanne Keenan and Richard Murphy	All authors contributed to the experimental design. Primary contributor to execution. MH carried out Mass Spec; JK carried out data acquisition and generation of DEP lists
Chapter 6	Overview, future perspectives and concluding remarks	-	-	-

Research outputs:

- Apr 2015 - Invent Commercialisation award "Innovation Partnership with Alltech"

- Jan 2017 - BRS research day presentation "Cell culture models for micronutrient interactions and tolerance"

- Sep 2017 - Blog, publication and profile write-up in Silicon Republic
  - https://www.siliconrepublic.com/innovation/nicb-alltech-food-production

- Aug 2018 - Travel award - selected to participate in Roche Continents programme in Salzburg

- Oct 2018 - Expose your research competition - 1st prize Researcher Life category

- Dec 2018 - Invention disclosure of intellectual property 'know-how': "An in vitro system for examining changes at a genetic and protein level in intestinal cells in copper restriction and subsequent repletion of Cu levels"

- Dec 2018 - Invention disclosure of intellectual property 'know-how': "Intestinal Caco-2 cells resistant to copper sulfate and to copper proteinate"

Abstract

Copper is an essential dietary micronutrient for a wide range of structural, regulatory, and catalytic functions but even moderately increased concentrations may result in toxicity to cells and tissues. Recent research has greatly enhanced our understanding of metal micronutrients in biological systems, but gaps still exist regarding copper metabolism and regulation and a combination of approaches towards furthering this knowledge are required.

To obtain a better understanding of micronutrient interactions within living cells, the research presented in this thesis investigated copper toxicity, resistance and homeostasis by examining the responses of human intestinal Caco-2 cells to exposure of inorganic copper sulfate ($CuSO_4$), organic copper proteinate (Cu Pro) and a chelator used to treat copper overload in Wilson's disease (triethylenetetramine). The work features: (i) the discovery of non-monotonic dose responses to copper exposure in the Caco-2 cell line; (ii) the establishment of copper tolerant variants in Caco-2 cells and their subsequent characterisation, including proteomic analysis; (iii) microarray profiling of five phenotypically different clones subsequently selected from the copper-resistant Caco-2 variants and investigations of their cross-resistance to other compounds and (iv) proteomic profiling of Caco-2 cells following exposure to triethylenetetramine and subsequent restoration in growth media. These results are detailed in the published research and submitted manuscripts and possible future directions are discussed.

1 Introduction

The effect micronutrients have on the site of uptake, the intestinal epithelium, remains poorly characterised in terms of proteomic and transcriptomic expression, particularly during prolonged exposure of different copper forms and extended depletion. Models of intestinal tissue have represented the mainstay of uptake, transport and toxicity studies for pharmaceuticals, xenobiotics and nutrients for decades. These models range from single cell monolayer design to complex co-cultured 3D-architecture designs to closely mimic the in vivo intestinal epithelium. To set the publications included in this thesis in context, the literature review presented focusses on the current understandings of copper homeostasis, acquisition and toxicity with a particular emphasis on research examining intestinal *in vitro* models. The use of models that explore copper and other metal interactions in biological systems is further evaluated and the effect of copper overload and deficiency is presented in the context of their relevance towards diagnosing abnormal copper status and the associated pathologies. Finally, publications which assess the effects of various metals and their different chemical formulations and consequent effects on proteomic and transcriptomic expression are also discussed.

1.1 Overview of theory and literature review

The small intestinal epithelium is a complex tissue, populated by several essential cell types which interact with each other and the surrounding microenvironment. It consists of intestinal stem cells located within protective crypts which give rise to mature functional populations that migrate, differentiate and dynamically regulate the manifold responsibilities of the small intestine. The primary responsibilities

include the digestion and absorption of nutrients from the diet and immunoregulation; acting as a barrier to gut flora and relaying information regarding xenobiotics to the immune system.

It is due to the complexity of the small intestine and the difficulties associated with establishing primary cell cultures, poor reproducibility and limited life span for example, that immortalised and cancerous cell lines are used. One such line – adenocarcinoma derived Caco-2 cells, have been employed in toxicity, absorption and transport studies to represent gastrointestinal tissues for over 30 years as models of the small intestinal enterocytes. The Caco-2 cell line expresses markers of intestinal epithelial tissue and possesses the ability to differentiate into polarised enterocyte-like cells over a 3 week period (Sambuy *et al.*, 2005). Enterocyte-like Caco-2 cells are often co-cultured with other intestinal cell populations, such as goblet cells, in an effort to better represent small intestinal tissues. These models have been utilised extensively in research to increase our understanding of the intestinal epithelium, including its role in protection against pathogenic microorganisms and in the uptake of various micronutrients and drugs. Despite decades of research using these models, many discoveries are still being made and many gaps in our understanding remain such as the elucidation of mechanisms conferring tolerance to constantly fluctuating drugs and micronutrients at this primary site of uptake.

Enterocytes of the small intestine are responsible for absorption of copper (Cu), an essential micronutrient with diverse biological functions including mitochondrial respiration, antioxidant defence and regulation of systemic iron through its incorporation as a cofactor in metalloproteins and cuproenzymes (Barceloux and Barceloux, 1999; Kozlowski *et al.*, 2009). The current understanding regarding

copper suggests uptake and transport are strictly regulated in the body due the potential for copper accumulation in tissues which can lead to tissue-damaging excess oxidative stress or equally copper deficiency which can cause neurological disorders and anaemia (Waggoner, Bartnikas and Gitlin, 1999; Jaiser and Winston, 2010).

1.2 Copper in biological systems

"Today morbidity and mortality related to trace element deficiencies or toxicities affect more than half of the world's population"

- Editorial for the Journal of Trace Elements in Medicine and Biology (Andersen and Freeland-Graves, 2012).

The study of bioinorganic chemistry began half a century ago and has since developed to identify the evident importance of metal ions in biological systems. This relationship has been established to be a double-edged sword, as many metal ions are essential to the physiological functioning of organisms, yet can cause adverse effects and toxicity at elevated concentrations (Kozlowski *et al.*, 2009).

Importantly, the Scientific Committee on Food and the Scientific Panel on Dietetic Products, Nutrition and Allergies noted that when determining the recommended upper limits for human consumption, consideration must be given for supplementary-derived nutrients as they are potentially different from food-derived nutrients in terms of individual dosage size, frequency, interactions with other luminal contents and chemical form (European Food Safety Authority 2006).

The structure, function and interactions of metalloproteins, covering metallo-enzymes, chaperones and cofactors, represent a focus of increasing interest. Advances in analytical techniques and tools such as x-ray crystallography and nuclear magnetic resonance (NMR) have allowed the determination of coordination sites and metal ion ligation in protein complexes, strengthening our understanding of these ions in the biological setting (Zheng *et al.*, 2008; Erdman Jr. *et al.*, 2014). As discussed later, genomic sequencing and the range of "omics" tools have

furthered this pursuit and theoretically has resulted in access to all proteins, DNA and RNA in living organisms.

However, much remains to be understood due to the complexity of the 'copper interactome'. To examine the copper interactome in living cells, this study focusses on the current understanding of copper transport, storage, distribution and the relationship of copper in nutrition, health and disease, with particular emphasis on copper toxicity, tolerance and deprivation in individual systems.

1.2.1 Overview of copper in humans

The transition metal copper is required for survival by all aerobic eukaryotic organisms. In humans, copper is found associated with proteins and prosthetic groups of enzymes. Cellular homeostasis of copper is strictly maintained by a network of transporters, chaperones and antioxidant proteins due to its participation in Haber–Weiss and Fenton chemistry (reactions 1-3 below). These reactions can lead to the accumulation of highly reactive hydroxyl radicals (OH•) through redox cycling between cuprous copper (Cu^{+}) and cupric copper (Cu^{2+}) with hydrogen peroxide and result in the formation of excess reactive oxygen species (ROS), which are damaging to cells and tissues (Koch, O Pena and Thiele, 1997; Kozlowski *et al.*, 2009; Linder, 2012).

1. $Cu^{2+} + H_2O_2 \rightarrow Cu^{+} \bullet O_2H + H^{+}$
2. $Cu^{+} \bullet O_2H + H_2O_2 \rightarrow Cu^{+} + O_2 + OH\bullet + H_2O$
3. $H^{+} + Cu^{+} + H_2O_2 \rightarrow Cu^{2+} + OH\bullet + H_2O$

It is long established that copper is essential for multiple cellular processes, causing toxicity when present in excess and has various deleterious health implications when deficient. Dysfunction of copper homeostasis has been observed in the genetic conditions: Menkes syndrome and Wilson's disease, associated with severe deficiency and overload respectively (Waggoner, Bartnikas and Gitlin, 1999). As such, these conditions have contributed much of the current understanding surrounding copper status and have helped in the identification of important proteins associated with copper. No robust individual biomarker sensitive for early diagnosis of marginal deficiency or toxicity in humans has yet been identified. Instead, the use of a biomarker suite – through combination of several markers in plasma, urine and sera have been proposed to aid in this diagnosis, but development of such systems has yet to be realised (Danzeisen *et al.*, 2007; Harvey and McArdle, 2008; Bertinato, Sherrard and Plouffe, 2010).

1.2.2 Copper in Nutrition

Most western diets are within the safe range (for adults) to avoid deficiency (0.9mg min RDA) and overload (10mg - upper tolerable limit) of copper, typically ranging between 1 – 5 mg/day. Unless contaminated with a source of copper, a small percent (6-13%) of total dietary Cu intake is absorbed from drinking water (Gaetke, Chow-Johnson and Chow, 2014).

Two primary sources of systemic Cu exist; dietary intake and environmental exposure. Dietary sources with the highest copper concentrations include shellfish and liver, while other Cu rich sources more common to the Western diet include chocolate, legumes,

nuts, grains and seeds (Osredkar and Sustar, 2011). As a whole, the majority of dietary Cu originates from plant sources (Johnson and Kays, 1990). Importantly, dairy products contain very little Cu and this may play a critical role on the impact of developing infants who require higher Cu intake than adults (Johnson and Kays, 1990; Linder and Hazegh-Azam, 1996; DiNicolantonio, Mangan and O'Keefe, 2018). Environmental exposure to copper comes from water pipes, cookware, medication for birth control (intrauterine devices) and fungicides. In cases of suspected deficiency, various forms of over-the-counter Cu supplements are available from pharmacies and health stores.

Although awareness of subclinical deficiency and toxicity of Cu is increasing, the majority of diets include sufficient Cu (1–5 mg) to prevent health issues without causing toxicity. However, a recent study suggests subclinical copper deficiency may be more common than previously assumed and may have serious health implications, particularly regarding heart disease (DiNicolantonio, Mangan and O'Keefe, 2018). The safe upper and lower ranges for copper intake are based on gastrointestinal effects resulting from overexposure and deficient conditions (Araya *et al.*, 2002). However, individual variability primarily arising from genetic, cultural and environmental differences such as diet and geographical location complicates the development of overarching copper intake guidelines.

1.2.3 Copper Absorption

Copper absorption from food takes place primarily in duodenal enterocytes of the small intestine but also in small parts in the stomach (particularly in drinking water), jejunum and ileum (Mason, 1979; Gaetke, Chow-Johnson and Chow, 2014) and is regulated

at two levels; whole body and at the cellular level i.e. the enterocytes. This absorption varies in efficiency between individuals and fluctuates depending on other factors, such as diet, age and sex (Van den Berghe and Klomp, 2009).

At the cellular level, uptake and transport of copper is regulated by expression and translocation of proteins such as copper transporter 1 (CTR1) and Menkes' protein (ATP7A) and storage proteins such as metallothionein (MT). The primary copper transporter on the mammalian cell membrane, CTR1, allows intestinal absorption of dietary cupric copper (Cu^{2+}) following its reduction to cuprous copper (Cu^{+}) by cell-surface metalloreductase proteins, suggested to be facilitated by STEAP (6-transmembrane epithelial antigen of prostate) proteins (Fig. 1.2.1) (Lönnerdal, 2008; Gomes, Maia and Santos, 2012).

In biological systems, no copper ions are left unbound due to their participation in Fenton reactions. Thus, once transported across the apical membrane, Cu is quickly bound by specific compounds and chaperones (GSH, ATOX1, CCS and Cox17, Fig. 1.2.1) which shuttle the metal to destinations of requirement, while excess Cu is sequestered in cytoprotective metal-binding proteins, such as glutathione (GSH) and metallothioneins.

Copper transfer to other components is facilitated by metallochaperones through three separate pathways. Human antioxidant protein 1 (ATOX1) delivers copper to the ATPases, ATP7A and ATP7B (primarily located to the *trans*-Golgi network), which facilitate organelle transport and extracellular export to the bloodstream (Hatori and Lutsenko, 2016).

Copper chaperone to superoxide dismutase (CCS) is responsible for shuttling Cu into the first-line antioxidant defence enzyme, Cu, Zn superoxide dismutase (SOD1), which

serves as a scavenger of superoxide ($O_2 \cdot -$), catalysing dismutation of the superoxide radical into less harmful hydrogen peroxide (H_2O_2) and molecular oxygen (O_2) (Bertinato and L'Abbé, 2003).

Cytochrome c oxidase copper chaperone (COX17) is responsible for Cu transport to mitochondria, where it is crucially incorporated by a cytochrome c oxidase assembly protein (SCO1/2) as a cofactor in respiratory chain complex IV (Cytochrome C oxidase, COX) (Prohaska, 2008; Suazo *et al.*, 2008; Nishito and Kambe, 2018).

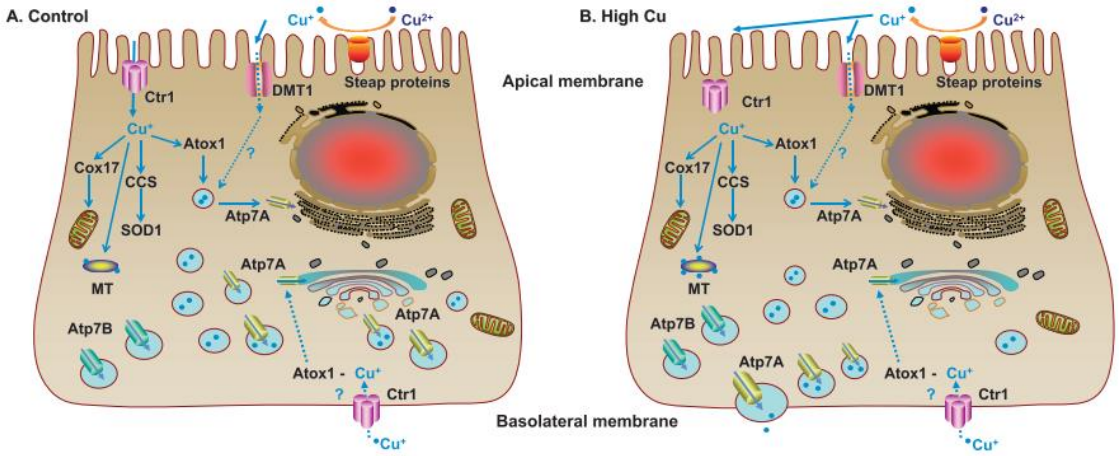

Figure 1.2.1*: Overview of copper transport through enterocytes of the intestinal epithelium, under: A – normal physiological copper concentrations, B – high extracellular copper loading in the intestinal lumen. CCS, copper chaperone to SOD; MT, metallothionein; SOD1, Cu/Zn superoxide dismutase (from Lönnerdal 2008)*

Uptake of Cu^+ by CTR1 accounts for approximately 60-70% of total Cu absorption (Hasan and Lutsenko, 2012; Nishito and Kambe, 2018). Other transporters also play a

role in Cu uptake, such as divalent metal transporter 1 (DMT1), which can transport multiple metal ions in the 2+ valence state (Fe, Zn, Cu etc.) (Espinoza *et al.*, 2012).

Extracellular transport from the basal side of the intestinal epithelium is required to allow copper transport to the rest of the body. Evidence has shown the ATPases (ATP7a/7b) ATP7a and ATP7b predominantly localise to the trans-Golgi network (TGN) during physiological copper levels (Puig and Thiele, 2002) but may also directly facilitate transport across membranes depending on copper status. Their major function during physiological intracellular copper levels is facilitating copper transport to the TGN for incorporation into enzymes. During elevated intracellular Cu however, both ATP7a/7b relocate towards the plasma membrane to mediate extracellular copper transport from the cell (Van den Berghe and Klomp, 2009; Kaler, 2011). This is discussed in further detail in section 1.5.

1.2.4 Systemic copper distribution

Following intestinal enterocyte export, albumin and α-2-macroglobulin (also known as transcuperin) rapidly bind and exchange portal blood Cu, likely by direct interaction, to facilitate extracellular copper transport to the liver (Liu *et al.*, 2007). Hepatocytes incorporate Cu into ceruloplasmin (Cp), the major circulating Cu storage molecule/ferroxidase, which is exported into the blood for systemic distribution and accounts for approximately two thirds of total body copper (Linder, 2016). Thus, Cu is delivered to sites of requirement throughout the body in two phases; firstly, by intestinal uptake and transport to the liver and secondly by Cp synthesis and export to other tissues (Linder and Hazegh-Azam, 1996).

Ceruloplasmin catalyses ferrous iron (Fe^{2+}) oxidation to ferric iron (Fe^{3+}) which may then be loaded into transferrin for membrane transport. As with Cu ions, free ferrous ions may cause free radical damage via Fenton chemistry as previously described; as such, the importance of Cp is highlighted by the monogenic disease, aceruloplasminemia, which results in loss of protein ferroxidase activity and subsequent iron deposition in the liver, pancreas, retina and brain with associated diabetes, retinal degeneration and neurodegeneration (Gulec and Collins, 2014).

While copper in systemic circulation is primarily bound to ceruloplasmin, alternative copper-binding molecules such as albumin, transcuperin and histidine represent the exchangeable pool of circulating Cu (Gaetke, Chow-Johnson and Chow, 2014). Other copper-binding molecules found in smaller concentrations include clotting factors V and VIII, extracellular superoxide dismutase (SOD3), amine and diamine oxidases, ferroxidase II, metallothionein and an unidentified 45 kDa protein (Linder, 2016).

1.2.5 Copper storage mechanisms

Although present in all tissues of the body, there is no single established mechanism for cellular storage of copper outside of the liver, with lower amounts found in kidney, brain, heart, and muscles. The liver serves to store systemic copper for distribution in hepatocytes where it is bound by cysteine-rich low molecular weight metallothionein (MT) until incorporated into ceruloplasmin for secretion into blood plasma. It has been proposed that MT fulfils this role particularly in neonates where excretion in bile has not fully developed (Prohaska, Broderius and

Brokate, 2003). MTs also serve a protective role by mopping up excess free metal ions intracellularly (cadmium, copper, lead, mercury and zinc) (Valko, Morris and Cronin, 2005; Ruttkay-Nedecky *et al.*, 2013) rendering them biologically inactive.

1.2.6 Whole body regulation of copper excretion

In healthy adults, copper excretion normally occurs via the bile (approximately 1 mg per day) with small amounts accounted for in urine (approximately 50 μg) (Linder, 2016). When copper is present in excessive concentrations in the body, a copper-glutathione complex is formed in the liver and excreted in the bile (Araya *et al.*, 2005). A gastrointestinal excretion mechanism exists in intestinal epithelial cells, whereby excess copper may be sequestered by MT and ultimately sloughed off during desquamation, a normal part of the life-cycle of intestinal epithelial cells. An additional mechanism, whereby copper is excreted by a 2 kDa small copper carrier (SCC) into urine was identified when the liver is unable to handle excess concentrations; SCC has not been confirmed as a peptide but is suspected as such (Gray *et al.*, 2012).

1.2.7 Copper and neurodegenerative diseases

Due to its participation in redox biology, increased copper is implicated as a mediator of oxidative stress in neurodegenerative diseases. Many of the neurological disorders associated with secreted or membrane bound polypeptide chains are exemplified by protein misfolding and aggregate formation and copper demonstrates binding action

with proteins such as β-amyloid in Alzheimer's and prion protein (Maynard *et al.*, 2005)). It is therefore understandable that complex machinery has evolved to counteract mistakes in protein processing (Stefani and Dobson, 2003). Heat shock proteins (HSP's) are evolutionarily conserved molecular chaperones of the heat shock factor family which maintain protein homeostasis in response to cell stress. Normally induced by hyperthermia, HSP's can also be upregulated during changes in environmental conditions such as redox status and during exposure to a variety of stressors including cytotoxic drugs, viral infection and heavy metals such as arsenic, cadmium, copper, silver, and zinc (Leung *et al.*, 1990; Santoro, 2000; Y. Wang *et al.*, 2018).

Furthermore, copper deficiency results in reduced cuproenzyme activity. Biochemical pathways associated with neurologic deficit and neurodegenerative pathologies have been linked with decreased cuproenzyme activity including cytochrome c oxidase, required for high-energy phosphate in nerve cell maintenance and function (Meguro *et al.*, 1991).

1.2.8 Copper and ocular health and disease

As with neurologic disorders, levels of cuproenzyme activity may have an impact on the eye. Electron microscopic analysis of ocular tissues from Menkes' disease patients revealed retinal ganglion cell degeneration, nerve fiber loss, atrophy of the optic nerve and irregular elastin in Bruch's membrane (Wray, Kuwabara and Sanderson, 1976). Tyrosinase, a cuproenzyme responsible for melanin synthesis is produced by melanocytes and loss of function is a hallmark of albinism which results in a loss of melanin in the skin and uveal tissues of the eye (Mason, 1979).

Multiple cancers including lymphocytic leukaemia and lung adenocarcinoma have been associated with copper deposits forming in the eyes (Denoyer *et al.*, 2015). In the case of leukaemia, one case study reported copper mistakenly bound to IgG secreted by cancer cells in elevated concentrations which subsequently formed deposits in the eye instead of being eliminated via the liver (Aldave *et al.*, 2006).

1.2.9 Copper in the biopharmaceutical industry

The role of copper and other trace elements in the production of biopharmaceuticals by Chinese hamster ovary (CHO) cells has been covered extensively in a recent review by Graham et. al (2019).

In short, the production of monoclonal antibodies (mAbs) has grown exponentially in recent decades and now represents 48% of total worldwide biopharmaceuticals sold (>$102 billion). Studies to maximise productivity of this process include manipulation of trace element content of various cell culture media during manufacture. It has emerged that copper content plays a vital role in CHO cell culture (Qian *et al.*, 2011). Increasing copper content to a threshold in cell culture media allowed for increased productivity, lowered glucose consumption (Luo *et al.*, 2012) and resulted in an increase in basic charge variants (Yuk *et al.*, 2015), particularly under conditions of hypoxic stress through the induction of protective hypoxia inducible factor 1 α (Qian *et al.*, 2014).

1.3 Primary site of micronutrient absorption

In this section, particular focus is given to enterocytes of the small intestinal epithelia as these represent the primary cell type accounting for uptake of micronutrients. The role and biological significance of several intestinal epithelial cell types are discussed to place them into context of micronutrient acquisition. Barriers restricting uptake of micronutrients are also examined.

1.3.1 Intestinal epithelium

The primary site of absorption for many micronutrients and the barrier regulating uptake and transport is the epithelium of the small intestine (SI) (Linder and Hazegh-Azam, 1996). The SI epithelium is a one-cell-layer thick regulator of absorption and consists of several different cell types, with multiple functions including absorption, secretion and immunoregulation. A crypt and villus structure maximizes surface area for optimal absorption and digestion; in humans the average surface area of the 9 m long gastrointestinal tract is approximately 32 m^2, about 2 m^2 of which refers to the large intestine (Helander and Fändriks, 2014, Fig. 1.3.1). This figure was revised by a tenfold decrease from a previously reported estimate of 250-300 m^2 (Tlaskalová-Hogenová *et al.*, 2004), a consequence of overestimated macro-anatomy from biopsies from the SI.

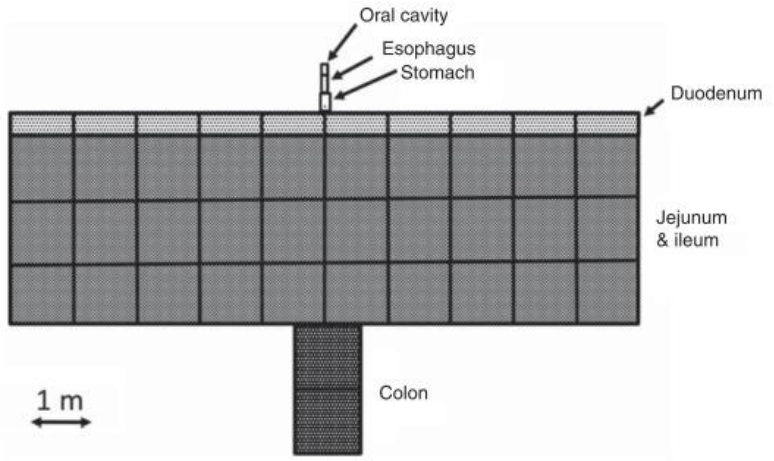

Figure 1.3.1: Approximate distribution of absorptive surface areas along the gastrointestinal tract. Adapted from Helander & Fändriks (2014)

The intestinal epithelium is organised into a crypt and villi structure which serves to protect and house critical LGR5+ (Leucine-rich repeat-containing G protein-coupled receptor 5-expressing) intestinal epithelial stem cells (IESC) in the crypt base. At the fourth position from the crypt base a population of stem cells known as '+4 reserve' cells can restore the LGR5+ IESCs following injury (Umar, 2011). Rapidly cycling daughter cells of LGR5+ cells, also known as transit-amplifying (TA) cells, undergo a limited number of divisions as they predominantly migrate from the crypt towards the villus tip and terminally differentiate into various intestinal epithelial cells on the villi (Peterson and Artis, 2014). When fully differentiated intestinal epithelial cells reach the tips of the villi and the end of their life cycle, they undergo apoptosis and are released into the intestinal lumen by desquamation (Fig. 1.3.2, left panel). This epithelial turnover takes between 3-7 days (De Santa Barbara, Van Den Brink and Roberts, 2003).

The most dominant type of cell to which LGR5+ IESCs gives rise are the absorptive enterocytes, representing 90% of the overall population. During their differentiation, these cells adopt a columnar appearance, form junctional complexes between neighbouring cells and develop microvilli on apical surfaces, further increasing surface area. The primary function of enterocytes is the uptake and transport of nutrients specifically required by the organism. To facilitate and regulate this absorption, assorted mechanisms have evolved which control chaperones, transporters and storage proteins located both intracellularly and at the cell membrane and digestive tract.

In addition to enterocytes, IESCs give rise to all the other cell types present in the SI, including secretory lineages: mucin-producing goblet cells; hormone-regulating enteroendocrine cells; and antimicrobial-producing Paneth cells (Sato *et al.*, 2009; Umar, 2011). Additional lineages include microfold cells (M-cells), contained in Peyer´s patches scattered throughout the intestinal epithelium; tuft cells, with a recently established function in initiating immune responses; and cup cells, the function of which has remained unknown (Mabbott *et al.*, 2013; Gerbe and Jay, 2016) (Fig. 1.3.2).

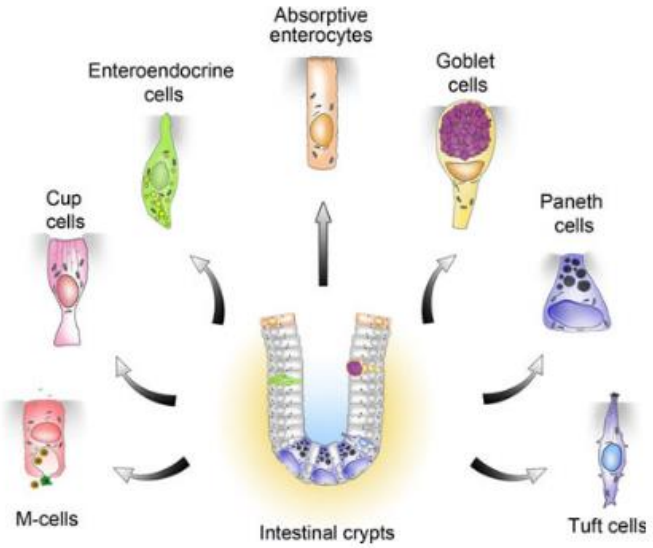

Figure 1.3.2*: Schematic diagram demonstrating all known intestinal epithelial lineages originating from Lgr5-expressing crypt base columnar stem cells (from Gerbe, Legraverend and Jay, 2012)*

There are also cells with critical immunoregulatory functions in the underlying lamina propria such as macrophages and dendritic cells, these cells coordinate to routinely sample antigens present in the intestinal lumen and direct appropriate immune responses to protect against infection directly and via microfold cells (Gerbe, Legraverend and Jay, 2012; Peterson and Artis, 2014). Paneth cells migrate into the crypt base (Sato *et al.*, 2009), as they serve to supply the crypts with antimicrobial peptides (AMPs), protecting the critical LGR5+ IESCs (Barker, 2014) (Fig. 1.3.3).

Scattered throughout the ileum of the SI are Peyer's patches of the follicle associated epithelium (FAE), also known as gut associated lymphoid tissue (GALT) (Mabbott *et al.*, 2013). These essential dome-like structures house large populations of immune cells and specific phagocytic M-cells which allow sampling of the

surrounding intestinal lumen. M-cells also perform functions of transcytosis/phagocytosis to allow macromolecules, particulate antigens and microorganisms traverse the intestinal barrier to the cells of the underlying mucosal immune system (Mabbott *et al.*, 2013). An anti-inflammatory response occurs when antigens of pathogenic organisms, such as commensal bacteria, are presented to the underlying immune cells, which can then mount an appropriate response (Fig. 1.3.3, middle panel). Human M-cells currently remain largely uncharacterised in *in vitro* intestinal models, due to a lack of specific markers although interest in this area is increasing (des Rieux *et al.*, 2007; Beloqui *et al.*, 2017).

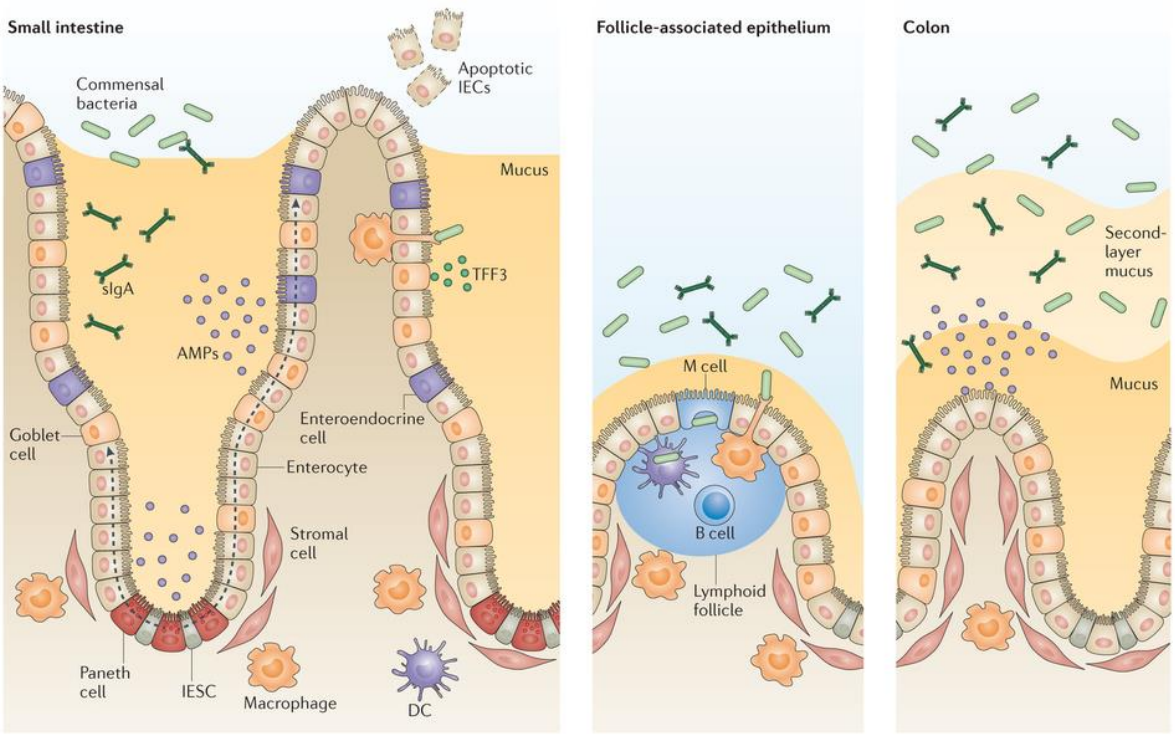

Figure 1.3.3*: Schematic diagrams demonstrating structural and organisational differences in SI, FAE and colon tissues (left, middle and right panels, respectively). Dotted arrows in the left panel designate direction of migration and*

differentiation of LGR5+ IESCs towards villus tip and finally desquamation of intestinal epithelial cells by apoptosis. Stromal cells and immune cells (B-cells, dendritic cells and macrophages) in the underlying lamina propria and FAE are represented in each panel (from Peterson and Artis, 2014)

Separating intestinal epithelial cells into apical and basolateral sections are three junctional complexes: tight junctions (TJ), adherent junctions and desmosomes. Apical TJ proteins seal the intercellular space and regulate cellular permeability of the intestinal epithelial barrier (Fig. 1.3.4). Epithelial cells employ adherent junctions and desmosomes for anchorage and to confer mechanical strength to the intestinal epithelial barrier. The enteric nervous system (comprising enteric neurons and glial cells) has been observed to manipulate these complexes in order to regulate factors such as wound healing, rate of differentiation and epithelial permeability (Bauer *et al.*, 2010; Neunlist *et al.*, 2013).

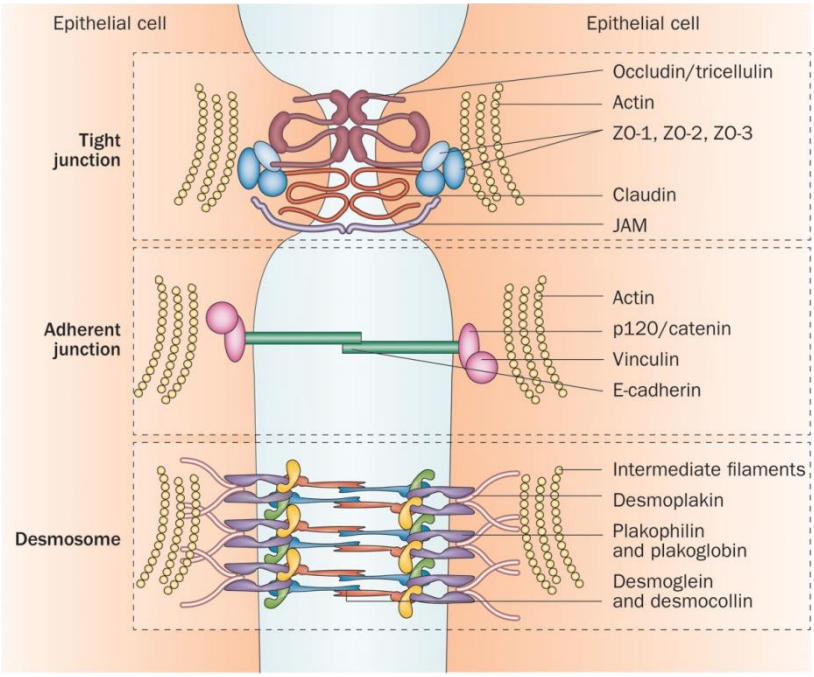

Figure 1.3.4*: Junctional complexes; tight junctions, adherent junctions and desmosomes facilitating anchorage and cross-talk in epithelial cells of intestinal tissue. JAM - junctional adhesion molecule, ZO - zona occludens (from Neunlist et al., 2013)*

1.3.2 Barriers to micronutrient acquisition

Mucin layers are provided by goblet cells of the SI and are critical to segregation of host and microorganisms (Tlaskalová-Hogenová *et al.*, 2004). However, micronutrient permeability is directly affected by this mucin barrier adjacent to absorptive enterocytes. When Mahler et al. (2009) examined a mixed cell culture *in vitro*/digestion model, they found differences between the effect of different types of mucin on the absorption of iron using mono and co-cultures. The group determined that models predicting iron bioavailability could be enhanced through the addition of a physiologically realistic mucus layer and goblet-type cells to their model.

Goblet cells account for 8-10% of the total cell population in the SI epithelium (Umar, 2011). The main purpose of these cells is to secrete large glycoprotein molecules (mucin) with a net negative charge. This mucin forms complex polymeric structures via disulphide bonds which traps and slows the interaction between the intestinal barrier and the contents of the lumen such as microorganisms, lipids, proteins and cell debris alongside immunoglobulins and antimicrobial peptides (AMPs) secreted by goblet and Paneth cells of the intestinal epithelium (Fig. 1.3.3).

Commensal bacteria trapped in the mucus of the small intestinal lumen are crucial for the development and function of the immune system alongside facilitating digestion (Tlaskalová-Hogenová *et al.*, 2004). Immunoglobulins such as IgA undergo transcytosis across the intestinal epithelial barrier from underlying immune cells in the lamina propria into the surrounding intestinal lumen (Peterson and Artis, 2014). In addition, goblet cells also secrete trefoil factors (TFFs) such as TFF3 (Fig. 1.3.3), responsible for growth and repair of the intestinal epithelial barrier (Taupin and Podolsky, 2003).

In addition to the physical barrier provided by mucins, dietary barriers may also interfere with adequate micronutrient absorption; increased intake of tannins and phytates can decrease available transition metal ion uptake (Mason, 1979; Fuqua, Vulpe and Anderson, 2012; Prasad, 2012). Furthermore, competition for direct uptake between metal micronutrients is well established and can lower bioavailability (Inglett and Solomons, 1998; Espinoza *et al.*, 2012).

1.4 Models for studying micronutrient interactions in intestinal tissues

Various models exist to study micronutrient acquisition and toxicity in animal cells *in vitro.* These models range from simple mono-cultures to complex scaffold-supported intestinal organoids originating from induced pluripotent stem cells. The most common cell line used in such models is the human Caco-2 cell line and its established clonal populations.

1.4.1 *In vitro* mono-cultures

Caco-2 cells

Caco-2 cells were established from the colon adenocarcinoma of a 72 year old male (Fogh et al. 1977). These cells were observed to differentiate and resemble enterocytes when cultured over approximately 20 days (Hidalgo, Raub and Borchardt, 1989). Following differentiation and polarization, Caco-2 cells form junctional complexes and express brush border enzymes and markers of differentiation in mature enterocytes: aminopeptidase, sucrase isomaltase, alkaline phosphatase and P27 (Natoli *et al.*, 2011). Due to their correlation with the intestinal epithelial membrane (Artursson, Palm and Luthman, 2001; Natoli *et al.*, 2011), Caco-2 cells have been utilised for over three decades to study the uptake and permeability of drugs and micronutrients in both academia and industry areas. When fully differentiated, Caco-2 cells demonstrate a barrier function resulting in increased transepithelial electrical resistance (TEER, a measure of barrier integrity in cell monolayers), with values greater than 200 $\Omega.cm^2$ and a low permeability (<0.25 % per hour) of fluid phase markers: Lucifer yellow (mol wt. 457.2), polyethylene glycol (mol wt. 4,000), inulin (mol wt. 5,200), and dextran (mol wt.

70,000) (Hidalgo, Raub and Borchardt, 1989; Arredondo, Uauy and González, 2000).

The Caco-2 cell line features a heterogenous mix of cells from which multiple clones representing different phenotypes have been established. Woodcock et al. (1991) reported the characterisation of several Caco-2 clonal populations, focussing on the study of an individual clone (clone 40) which displayed increased transport of taurocholic acid, a bile acid product arising from taurine and cholic acid conjugation. To isolate clones, the group employed a limited dilution technique combined with cloning rings. These clones were then characterised by their growth profiles, TEER, taurocholic transport and morphology. Only TEER and taurocholic transport were found to fluctuate between clones, whereas growth profiles were similar to the parental population. One of the clones (clone 12) demonstrated multilayered overlapping growth during differentiation, while the other clones displayed a relatively homogenous morphology compared to the parental population. This study demonstrated that the basal level of parental Caco-2 characteristics (such as of taurocholic acid transport) were a combined sum of the sub-populations within the heterogeneous patental population.

Caro *et al.* (1995) established three clones from parental Caco-2 cells, including the clone TC7. This clone was generated at a high passage count and demonstrated suitability in representing absorption and transport of specific compounds in the small intestine. The benefits of Caco-2/TC7 included: increased taurocholic acid transport activity, similar to Clone 40 by Woodcock et al. (1991), increased cytochrome 3A activity and increased brush-border associated hydrolase sucrase-isomaltase activity.

A subsequent study reported the promising potential of Caco-2/TC7 as a short term accelerated *in vitro* differentiation model, requiring only 3 days (Iolante *et al.*, 2004), however, at least 15 days were necessary in other models to complete differentiation sufficiently for Fe transport (Mahler, Shuler and Glahn, 2009). Terminal differentiation models using up to 21 days are still more common as determined by analysis of different stages of development (Chen, Elisia and Kitts, 2010).

1.4.2 *In vitro* co-cultures

To better represent the individual cell populations of the small intestine in their native state *in vivo*, mixed cell models can be produced *in vitro* through the co-culture of multiple cell lines.

The parental lines and various clones from absorptive Caco-2 and secretory HT29 cells represent the most extensively studied lines due to their suitability in a mixed cell culture model. HT29 cells were initially established from a human adenocarcinoma from which several mucus producing / absorptive sublines were isolated in the years that followed (Huet *et al.*, 1987). When cultured in the presence of galactose, the HT29 parental line differentiates to resemble both absorptive and goblet cells *in vitro*. However, the sublines were observed to retain most of their differentiated qualities when cultured outside of galactose (Huet *et al.*, 1987). Adaptation in media containing methotrexate (MTX) allowed the selection of HT29-MTX. This subline was established from the parental HT29 and acts as a mucus secreting line resembling goblet cells in vivo (Lesuffleur *et al.*, 1990; Keely

et al., 2005). In that study, MTX was chosen due to its ability to select subpopulations by interfering with folate metabolism.

Mucin-secreting HT29-H were also established as a subpopulation of HT29 cells and demonstrated monolayer formation comprising approximately 80% mature goblet cells with large mucin granules and 20% absorptive and immature goblet-like cells when cultured on polycarbonate cell culture inserts (Wikman *et al.*, 1993). Wikman-Larhed and Artursson (1995) described the first co-culture model reporting the formation of TJ between the Caco-2 and HT29 cells, which highlighted the requirement for further research to improve the presence of mucin barrier in the system. Subsequently, Walter *et al.* (1996) described the use of the HT29-MTX clone in a co-culture model with Caco-2 cells and found good drug permeability correlation with rat and human *in vivo* studies. Results for TEER and paracellular permeability also correlated better in these cell culture models as demonstrated by Meaney and O'Driscoll (1999) with the co-culture between Caco-2 and HT29-H.

In such complex co-culture systems, one of the factors influencing the suitability of small intestine models is seeding ratio. The predominant cell type in the small intestine are enterocytes, with reports in the literature for enterocyte fraction ranging from up to 80% (De Santa Barbara, Van Den Brink and Roberts, 2003) to more than 90% of total intestinal epithelial cells (Q. Wang *et al.*, 2018). This leaves the remaining 10 - 20% between all the other cell types. Hilgendorf *et al.* (2000) investigated how different ratios of Caco-2:HT29-MTX co-cultures impacted transport and permeability of several compounds involved in paracellular- (passing between intercellular cell spaces), transcellular- (directly through the cell) and carrier-mediated absorption and secretion. Using a range of ratios (100:0, 90:10,

70:30, 50:50 and 0:100 Caco-2:HT29-MTX) the group reported the impact of increasing HT29-MTX proportions on the permeability of the cell monolayer barrier by reducing both TEER and secretory transport via efflux transporter P-glycoprotein (also known as ABCB1, MDR1). Later, Mahler, Shuler and Glahn (2009) analysed various seeding ratios in a co-culture system for prediction of dietary iron bioavailability and determined the most suitable ratio to be between 90:10 and 75:25 (Caco-2:HT29-MTX) in their model.

Later, Chen, Elisia and Kitts (2010) attempted to simultaneously predict optimum conditions for drug transport, TEER and cell permeability using a Taguchi design, a statistical method applied to improve design quality of their experiment. By varying 11 parameters of the Caco-2:HT29-MTX co-culture model, the group reported that using 'an initial seeding density of 1×10^5 Caco-2 and HT29-MTX cells/cm^2 at a ratio of 90:10, followed by a 21 day culture time in MEM medium', delivered the best results from the range of variables tested.

Much variation remains between laboratories in intestinal *in vitro* culture conditions and no standard models have been set. Due to their complexity, co-culture models of epithelial uptake and transport show advantages over conventional monolayer systems. Ideal co-culture conditions are continually being proposed, although many laboratories often first optimise their own systems before generating results due to the lack of commonly agreed standards.

The human Burkitt's lymphoma cell line Raji B has been shown to induce M-cell-like morphology when introduced at a late stage of Caco-2 differentiation (Gullberg *et al.*, 2000). This induction of M-cells by Raji B lymphocytes has been exploited in recent mixed cell culture designs to study peptide drug absorption (Antunes *et al*,

2012) and the subsequent characterisation of the permeability of this model by Araújo et al. (2013).

In order to characterise hepatic iron regulation by hepcidin, a protein which restricts enterocyte basolateral export of iron, Scheers, Almgren and Sandberg (2014) incorporated a hepatocyte-like cancer cell line (HepG2) with the Caco-2 model (cultured in a transwell support insert) and designed a Caco-2/HepG2 co-culture. This model responded to increased iron exposure by increased hepcidin levels and ferritin formation in the Caco-2 cell line.

1.4.3 Use of devices to simulate intestinal tissue architecture

A downside of cell-based 2D models cultured on tissue culture flasks and Transwell® membranes is the lack of intestinal crypt-villus architecture. In an attempt to mimic the crypt-villus structure *in vitro*, various groups have manipulated the architecture of synthetic materials to provide 3D microenvironments similar to that present in the small intestine. Yu et al. (2012) designed a collagen scaffold which resulted in the first controlled microenvironment 3D villous platform facilitating cellular differentiation and absorption. They compared Caco-2 differentiation in their system against traditional 2D models, resulting in a more physiologically representative permeability and TEER (< 50 $\Omega.cm^2$). The group illustrated that collagen hydrogel was not suitable for rapidly permeable drug testing, indicating that further investigations on alternative surfaces were required.

More recently, a mixed cell culture protocol using synthetic polymethyl methacrylate (PMMA) scaffolds was developed (Costello *et al.*, 2014). Caco-

2:HT29-MTX cell lines (3:1) were co-cultured with intestinal crypts isolated from mice on a purpose-designed porous poly-lactic-glycolic acid (PLGA) scaffold. This design led to the formation of crypt-villus like structures that supported differentiation and migration towards villus tip. Mucus production increase with basolateral stimulation using epidermal growth factor (EGF) was also achieved. Confocal imagery of the design demonstrated appropriate crypt niche generation and differentiation towards four intestinal epithelial cell lineages by incorporating cultured intestinal stem cells in the model.

Chen et al. (2015) co-cultured Caco-2:HT29-MTX (3:1) in a 3D porous silk protein scaffold model with a hollow lumen, representing the intestinal tissue architecture. Their model allowed the injection of Caco-2 and HT29-MTX cells for attachment to the lumen alongside the growth of human intestinal myofibroblasts (H-InMyoFibs) in the porous scaffold bulk space, supplying cytokines and growth factors necessary to support intestinal epithelial cell growth and differentiation. The group demonstrated physiological properties of human intestinal tissue such as layered mucus covering, detected by MUC2 and Alcian blue staining after terminal differentiation on day 21, measuring 11-17 µm by comparison to 4 µm in a traditional 2D model. *In vivo,* mucosal barriers measure as low as 10 µm thick but may reach up to 700 µm in the intestine (Linden *et al.*, 2008). The 3D model also presented a low oxygen gradient (ranging from 0.1% - 5%) similar to that observed in proximal to distal gastrointestinal tract. The group then confirmed oxygen tension and examined the potential for simulating bacterial infections using *Yersinia pseudotuberculosis* tagged with oxygen-dependant and independent fluorescent proteins. Their system allowed for long term culture lasting for 8 weeks

before a decrease in differentiation markers was observed, compared to the maximum 4 week reported for 2D models.

1.4.4 *In vivo* scaling of intestinal models

Levin et al. (2013) investigated the use of postnatally-derived human small intestinal organoid units on poly-glycolic acid/poly-L-lactic acid (PGA/PLLA) scaffolds for the generation of tissue engineered small intestine (TESI) constructs. The group loaded the scaffolds with the organoid units before implanting into the omentum of irradiated NSG mice. As a result, tissue displaying all cell types of the intestinal mucosa, including surrounding mesenchyme and nerve cells, was obtained. This experiment was the first step towards a bioengineered intestinal replacement, with the potential goal of developing a suitable solution to small bowel syndrome.

Recently, Finkbeiner et al. (2015) expanded on the techniques developed by Levin et al. (2013) in seeding PGA/PLLA scaffolds with human intestinal organoids (HIO), which were then immediately implanted in NOD SCID gamma mice before harvesting at 12 weeks. These implants were compared to implanted HIOs and pluripotent stem cells on acellular porcine intestinal matrices. The pluripotent stem cells on scaffold experiments were unsuccessful as the acellular matrix failed to induce differentiation and HIOs loaded onto acellular matrix survived *in vitro* conditions only. However, when implanted on PGA/PLLA scaffolds, HIOs thrived *in vivo* and demonstrated development of tissues mimicking adult human SI. This

work serves as a progression on the Levin *et al.* (2013) paper, as it provides an alternative to the limited sources of organoid units from patient specific tissues.

1.4.5 Induced pluripotent stem cells

Takahashi and Yamanaka (2006) described the first procedure for re-programming mouse embryonic and adult fibroblast cultures towards an embryonic-like stage, thus inducing pluripotent stem cells (iPSCs). Importantly, iPSCs offered the opportunity to study stem cells without the ethical difficulties associated with the use of human embryos. These cells hold the capability to proliferate indefinitely in culture and retain pluripotency when supplemented with specific factors (including Oct3/4, Sox2 and Nanog). iPSCs are defined by their ability to differentiate into the three definitive lineages; endoderm, mesoderm and ectoderm.

iPSCs may be differentiated towards intestinal tissues in a stepwise manner. Initially, pluripotent stem cells are directed towards human intestinal organoids through induction of SOX17, FOXA2 and CDX2 expression by incorporating specific components into culture media. One method includes induction of definitive endoderm using Activin-A and stimulation towards hindgut endoderm differentiation and spheroid formation using a WNT-activator (Chiron99021, a potent glycogen synthase kinase-3 inhibitor). Maturation of spheroids may be completed by culture in B27+insulin and N2 supplemented (Sato crypt) culture media (Sato *et al.*, 2009; Spence *et al.*, 2011).

This process ultimately results in human intestinal organoid (HIO) generation. HIO's possess most of the cells types (absorptive, secretory and crypt cells) and

possess many functional and structural features of the human SI (Wells & Spence 2014). The HIO process develops from initial definitive endoderm formation, hindgut patterning and gut tube morphogenesis, followed by spheroid generation and embedding in 3D Matrigel® before scaling and passaging HIO's for maturation. Several weeks are required before mature HIOs can be harvested (Fig. 1.4.1). Mature HIOs represent *in vitro* models to study the microenvironment of developing small intestine and represent responses comparable to some *in vivo* physiological reactions (Watson *et al.*, 2014).

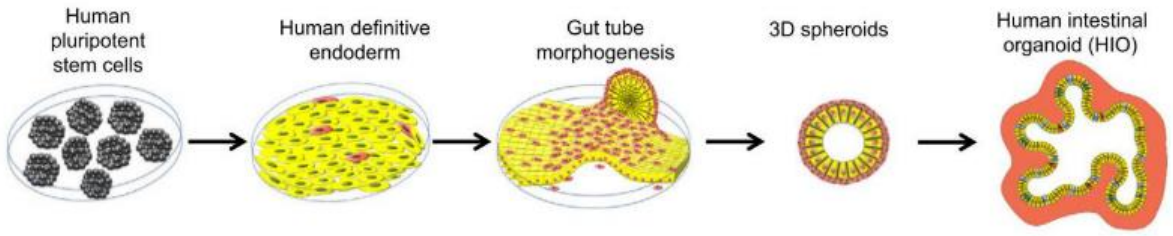

Figure 1.4.1: Directed intestinal differentiation of human iPSCs into human intestinal organoids (HIOs). From Wells and Spence (2014).

1.4.6 *Ex vivo* human and mouse models of the small gut

Ideally, to accurately simulate 3D architecture and interactions in the intestinal niche, *in vitro* examination of micronutrients would be performed using primary intestinal epithelial cells. However, culture time of primary tissues is severely limited and measuring the effects of exposure to micronutrients using *ex vivo* models is challenging. Recent developments to address this limitation have advanced our access to longer surviving *ex vivo* intestinal tissue models.

Following isolation and culture of mouse primary intestinal crypts, Grabinger *et al.* (2014) demonstrated increased survival and organoid development *ex vivo* using supplementation with R-spondin-1. The group then examined apoptosis and organoid death using exposure to TNFα. Later, Tsuruta *et al.* (2016) cultured *ex vivo* murine small intestine and colonic organoids to examine gene expression of 5-hydroxytryptamine (5-HT) serotonin factors and demonstrated the model would be suitable for examination of the 5-HT system. In contrast to Grabinger *et al*, Tsuruta *et al.* supplemented embedded organoids with R-spondin 3 and Noggin (with Wnt-3a for colonic organoids). More recently, mouse and human intestinal organoids have been used to study detoxification of ammonia by citrulline production (X. Wang *et al.*, 2018) and the immune system responses related to Major Histocompatibility Complex II (Wosen *et al.*, 2019).

Recent reviews by Almeqdadi *et al.* (2019) and Wallach and Bayrer (2017) detail additional current advances in intestinal organoid technology, exploring the different models in development, their applications and limitations. These reviews emphasise that promising research in this area has the potential to transform gastrointestinal investigations. However, the nature of these models remain still both specialised and expensive and several challenges have yet to be overcome before they will replace the use of traditional two-dimensional models such as Caco-2.

Evidently, elaborate developments have allowed for more complex representations of gastrointestinal cell types and architecture. However, much remains to be

overcome regarding the generation of a robust physiological *in vitro* SI model, such as the lack of incorporated enteroendocrine system in co-cultured models or the persisting difficulty in using iPSCs to represent mature enterocytes and not tissues resembling early embryonic development. Despite the emergence of alternative cell lines and techniques allowing the use of pluripotent stem cells, Caco-2 cells have remained the predominant models to study the uptake and transport of the small intestine, largely due to the fact of being established, well characterised and can readily be manipulated to fit a range of purposes.

1.5 Issues related to abnormal copper status

Malnutrition due to copper deficiency is prevalent in the developing world where it affects quality of life for millions of individuals and premature infants with higher intake requirements during early development (de Romaña *et al.*, 2011), highlighting the need for adequate copper intake. However, over supplementation can equally cause harm, thus a sensitive marker of copper status would be beneficial, particularly in at-risk populations (Muita, 2001).

Copper status is controlled in part by other minerals, vitamins and activity levels of hormones. For example, high zinc supplementation has been shown to deplete copper levels and is indeed used as a therapy for Wilson's disease (Hoffman, Richard and Phyliky, 1988). In cases of adrenal gland or liver malfunction, copper may accumulate in various tissues around the body, as adrenal hormones promote hepatic production of the main Cu-binding protein in the body, ceruloplasmin, which can complicate status assessment (Gaetke, Chow-Johnson and Chow, 2014).

The genetic copper disorders, Menkes and Wilson's diseases, are characterised by mutations in ATP7a and ATP7b, respectively. Both ATP7a and ATP7b share similar structural and functional components (Figure 1.5.1). Structurally, they are both comprised of eight trans-membrane domains, six copper-binding cytosolic N-terminal domains, C-terminal tails (ensuring proper protein targeting) and a highly conserved nucleotide-binding domain, phosphorylation domain and actuator domain (Hasan and Lutsenko, 2012). ATP7a and ATP7b each have many different phosphorylation sites essential for their function and ATP7b contains a specific N-terminal region essential for trans-Golgi network (TGN) apical targeting and retention (Braiterman *et al.*, 2011).

In intestinal cells, both ATP7a and ATP7b may undergo translocation dependant on Cu status. During normal physiological Cu levels, ATP7a and ATP7b are localised to the TGN. However, high intracellular Cu concentrations prompt the release of ATP7a/7b from the TGN, where they relocate to intracellular vesicles to facilitate export of excess Cu at the plasma membrane. Post-translational modifications such as kinase mediated phosphorylation are likely to influence the regulation of Cu by ATP7a/7b (Braiterman *et al.*, 2011; Hasan and Lutsenko, 2012). It was recently discovered that ATP7a is regulated in an organ-specific manner dependant on copper status, with high intestinal Cu resulting in a decrease of ATP7a and vice versa, while high Cu concentrations in other organs, including heart, spleen, and liver, cause concurrent increases in ATP7a (Chun *et al.*, 2017).

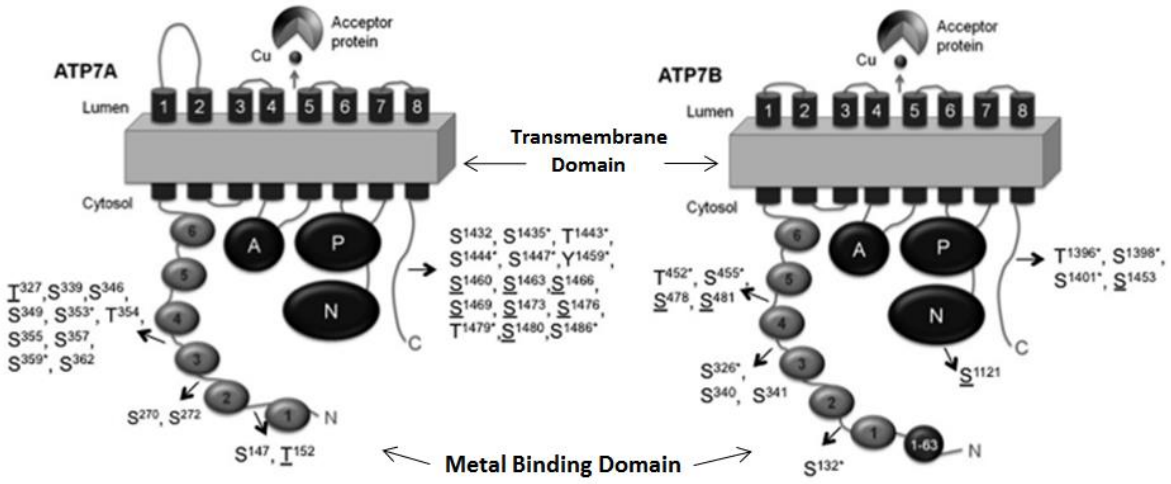

Figure 1.5.1: Structural configuration of ATP7a and ATP7b indicating eight shared transmembrane domains and six metal binding domains and individual phosphorylation sites. N: nucleotide-binding domain, P: phosphorylation domain, A: actuator domain. Adapted from Hasan and Lutsenko (2012)

1.5.1 Copper deficiency

No sensitive marker yet exists for diagnosing of subclinical copper deficiency. Cuproenzymes are commonly affected due to the lack of copper co-factor availability and, as a result, their activities may be decreased. For example, both ceruloplasmin (Cp) activity and rate of synthesis are reduced during low copper status, as such Cp activity measurements may be useful in the diagnosis of severe Cu deficiency (Danzeisen *et al.*, 2007; Linder, 2016).

Deficiency of copper is primarily observed in the genetic disorder Menkes syndrome, a X-linked recessive mutation of the gene encoding P_{1b}-type ATPase (ATP7a) that results in an inability to properly absorb copper, leading to clinical deficiency (Smith, Smith and Rosenzweig, 2014). Menkes manifests with severe cerebellar degeneration occurring early in childhood, with many associated neurological implications such as seizures and hypothermia, as well as neuronal loss in the cerebellum (primarily Purkinje cells).

Interestingly, the use of chelators to induce copper deficiency is increasing and has demonstrated promise in a range of applications such as the treatment of diabetes mellitus and Alzheimer's disease (Garth J.S. Cooper, 2011) and as an anti-cancer therapy (Antoniades *et al.*, 2013; Fatfat *et al.*, 2014). Additionally, copper uptake is inhibited by high concentrations of other metal ions. High dietary zinc and iron can both inhibit copper uptake and reduce copper availability in blood (Linder and Hazegh-Azam, 1996).

1.5.2 Copper overload

Copper overload (hypercupremia) is demonstrated in Wilson's disease, which, without adequate therapy, may result in copper accumulation in various tissues (liver, heart and pancreas) and can cause copper deposits to form in the basal ganglia, ultimately leading to Parkinsonian-like disorders (Waggoner, Bartnikas and Gitlin, 1999). Wilson's disease is caused by mutations in the gene encoding ATP7b, a cation transporting P_{1b}-type ATPase homologous to ATP7a, although not ubiquitously expressed. Mutations of ATP7b expression lead to an inability to utilise the primary method for copper excretion, the bile, and thus toxic accumulation of copper in the liver is observed (Waggoner, Bartnikas and Gitlin, 1999).

As previously stated, hydroxyl radical formation via Fenton and Haber–Weiss reactions and reactive oxygen species (ROS) formed during excess copper can cause damage to intracellular components, particularly phospholipid bilayers of the cell membrane and organelles (Kozlowski *et al.*, 2009; Linder, 2012; Gaetke, Chow-Johnson and Chow, 2014). To overcome hypercupremia resulting from, for instance, accidental exposure or Wilson's disease, chelators have been employed for decades to reduce uptake in the intestine and increase excreted copper concentration. The primary chelators used in hypercupremia are D-penicillamine (DPA) and triethylenetetramine (TETA) while zinc supplementation may be employed as maintenance therapy (Purchase, 2013). These chelators are covered in detail in Section 2.8.

1.5.3 Progress on markers of copper status

A copper biomarker sensitive to slight changes in concentration, which also responds to excess as well as deficiency has not been found yet. Several cuproenzymes have been suggested as possible biomarkers of mild Cu deficit, as their activities have been shown to modify during deficiency. However, further research is still required to determine whether standardised assays can be developed, as variability exists across different populations. Danzeisen et al. (2007) envisaged the use of a novel array of biomarkers for the indication of copper status: "the biomarker suite". This group proposed utilising high-throughput technologies to develop different sets of biomarkers for different population subgroups, determined by the proposed examples of gender, nutritional status and age – important due to the inherent variability in copper biomarker prevalence across these categories.

Previously investigated methods for diagnosis of toxicity and deficiency included blood, hair and urine copper analysis, although these have failed to produce substantial contribution in the identification of copper status. The commonly used indicators include ceruloplasmin (a copper containing ferroxidase) and serum copper concentrations, though these are only sensitive to marked increases and moderate or severe copper deficiency (Olivares *et al.*, 2008).

The ideal biomarker for body "copper load" would be sensitive to small changes in copper status, sufficiently early to allow intervention before the onset of clinical symptoms. Liver concentrations of copper stores – the most reliable indicator for measuring total body copper - have proven impractical as biopsy is required for measurement. Therefore this is only performed when clear signs of liver disease are

presented. Other traditional biomarkers of copper status include serum copper, serum ceruloplasmin (Cp) and erythrocyte Cu,Zn superoxide dismutase (Cu,Zn SOD1), although a study by Araya et al. (2005) reported that these markers are not sensitive enough to detect changes in subjects exposed to the upper limit of established tolerance (10mg) for 60 days. Instead, significant but transient changes were observed in various serum aminotransferases, aspartate and alanine aminotransferase. The group also detected increases in peripheral blood cell concentrations of glutathione, which they believe may have resulted from an adaptation to increased copper (Araya *et al.*, 2005).

In other studies, Cu,Zn superoxide dismutase (SOD1) and its chaperone (CCS) have been producing encouraging results as potential early biomarkers of copper status. Suazo et al. (2008) conducted research over two months analysing copper supplementation in adults at 10mg/day, which identified reduced mRNA concentrations of both SOD1 and CCS following exposure. They also examined cellular copper content alongside relative mRNA concentrations of metallothionein 2A (MT2A), prion protein (PrP) and amyloid precursor-like protein 2 (APLP2) but found no significant differences between them following Cu exposure. The group suggested further assessment of SOD1 and CCS as potential biomarkers of copper status. Animal studies agree with the current understanding of CCS behaviour; erythrocyte CCS was examined as a biomarker for copper status in rats and mice and has been shown to decrease in conditions of excess (Bertinato, Sherrard and Plouffe, 2010) and increase when deficient (Prohaska, Broderius and Brokate, 2003). The evidence for CCS as a potential biomarker of copper status appears to be promising in preliminary studies. However, performance and characterisation of

CCS in milder conditions is critical before controlled population wide studies are justified.

1.6 Cell culture studies of copper interactions i*n vitro*

The understanding of copper and other metals in biological systems has advanced exponentially within the last few decades. The growing interest may be thought of as partly due to the desire to aid populations suffering from deficiencies and toxic exposures or the many genetic disorders which can cause issues with metal homeostasis. Notwithstanding are other influences, such as the optimisation of agricultural practices, concerns for the environment and to boost health and performance. This section focusses on studies of copper interactions *in vitro*, models of copper uptake and introduces the non-monotonic dose response, as reported in section 2.

1.6.1 Models to examine copper interactions *in vitro*

Much has been gleaned regarding copper homeostasis and interactions with biological systems from the use of various *in vitro* models. The most important cupro-protein discoveries in recent decades included the major Cu transporters CTR1, ATP7a and ATP7b and were facilitated by a combination of advances in genetics and biochemical studies with microbial (bacterial and yeast) model systems (Puig and Thiele, 2002). Subsequent advances were predominantly facilitated by human *in vitro* models, such as Caco-2, and examined the localisation of copper transporters (CTR1, ATP7a and ATP7b) alongside the effects of toxic copper concentrations on the antioxidant response element/NRF2 pathways.

However, not all of the studies regarding copper interactions agree with each other and controversy remains with respect to CTR1 localisation in Caco-2 cells (Zimnicka, Maryon and Kaplan, 2007; Nose *et al.*, 2010). Furthermore, the impact of basal media

used for cell culture has recently been shown, with discrepancies reported between batches and formulations in a metal-dependant manner which has been observed to influence the expression of proteins associated with autophagy (LC3, sequestosome) and apoptosis (caspase 3) (Keenan *et al.*, 2018). In addition, the impact of exposure to different forms of copper to Caco-2 and HT29 cells was recently examined, revealing changes dependant on cell type and metal chosen (Keenan *et al.*, 2018). Inorganic copper sulfate and organic forms of copper (glycinate, organic acid chelate and proteinate) were shown to have different impacts on ROS generation and aggresome formation alongside protein expression, such as heat shock proteins (HSPA6/A1), metallothionein and ubiquitination of high-molecular weight proteins.

1.6.2 Copper uptake studies

Recent analysis of copper uptake in two different systems revealed that Cu uptake occurs via CTR1 (see section 1.2.3) and an as yet unidentified transporter (Kidane *et al.*, 2012; Ramos *et al.*, 2016). These studies demonstrated that both knockdown and knockout of CTR1 mRNA expression by siRNA was not capable of reducing the rate of Cu uptake in multiple cell lines (human hepatoma HepG2; human mammary PMC42; and mouse embryonic fibroblasts MEFs).

Gao *et al.* (2014) examined the effect of Caco-2 cell exposure to different forms of copper ($CuSO_4$, micron copper oxide and nano copper oxide) and reported increased intracellular copper accumulation during exposure to nano Cu oxide relative to other forms of Cu. The group suggested higher Cu content during nano Cu oxide was likely due to increased endocytosis.

1.6.3 Non-monotonic dose-responses

Dose-responses relationships which do not show 'classical' linear toxicity curves are termed as non-monotonic dose-responses (NMDRs) and were first described in the late 1800's (Schulz, 1888). The study of NMDR relationships has expanded our understanding of biological and environmental responses to various sources of stress and has contributed to the knowledgebase surrounding phenotypic plasticity (Michael Davis and Svendsgaard, 1990; Vandenberg *et al.*, 2012; Calabrese, 2014). However, NMDRs are still generating much attention and their causes and effects are widely debated in the literature.

Conolly & Lutz (2004) previously outlined four mechanisms based on fundamental biochemistry which may result in an observed NMDR. These included: (*a*) opposing regulatory effects by membrane receptor subtypes, (*b*) modulation of gene-expression by homodimers but not mixed dimers in increasing xenobiotic concentration (*c*) DNA damage repair induced by xenobiotic in a saturable manner and (*d*) concentration-dependant DNA damage leading to two opposing monotonic responses (cell cycle delay/cell cycle acceleration) which generate NMDR curves when superimposed.

Hormesis is a type of NMDR whereby a stimulatory response (such as metabolic activity or growth) during low concentration exposure of a stressor is observed, succeeded by toxicity at higher concentrations (Calabrese *et al.*, 2001) leading to a "hormetic profile". Such a response was described by Bartłomiejczyk *et al.* (2013), who attributed the effect to activation of growth factor receptor tyrosine kinases through inactivation of upstream tyrosine phosphatase by ROS, leading to growth stimulation at

low concentrations. NMDRs have been classified according to a number of causes, including receptor mediated-responses or resulting from an overlay of two opposing monotonic profiles simultaneously observed (Conolly and Lutz, 2004; Calabrese, 2013).

NMDR profiles are commonly reported in endocrine disruption (Vandenberg *et al.*, 2012; Lagarde *et al.*, 2015) and during heavy metal exposure (Chaube, Mishra and Singh, 2010; Helmestam, Stavreus-Evers and Olovsson, 2010). Hormetic profiles have been identified during exposure of cadmium in Caco-2 cells and genistein to Caco-2 BBE (Chen and Donovan, 2004; Mantha and Jumarie, 2010) but have not been reported previously for copper exposure in Caco-2 cells. However, other metals including metal nanoparticles (Mn, Sb, Ti) have displayed hormetic effects in Caco-2 cells (Titma *et al.*, 2016).

In summary, non-linear dose–response relationships are a common phenomenon observed during exposure to a wide range of substances (including metals), resulting in multiple effects and originating from several different mechanisms. The nature of NMDRs challenges traditional models of toxicology and has far reached implications for study design and risk assessment (Calabrese and Blain, 2004).

The identification of a non-linear dose-response relationship in intestinal Caco-2 cells during exposure to different sources of copper is discussed in chapter 2.

1.7 Models of tolerance and resistance in biological systems

As discussed below a number of techniques for producing metal resistant variants using *in vitro* cell lines exist. Resistant cells have predominantly been generated by continuous selection in high concentrations of micronutrients or mutagenicity of targeted proteins related to cellular micronutrient processing. These models can demonstrate cross-resistance to other metals due to common mechanisms associated with intracellular metal handling (Garrick *et al.*, 2006). Multiple models of copper resistance in eukaryotic cells have been established and mechanistic data from these studies have revealed the importance of copper transporter and storage proteins in imparting Cu resistance in some models (Freedman et al. 1986; Schilsky et al. 1998), while several changes in tandem have been observed in others such as increased expression of oxidative stress proteins (SOD1, catalase) and reduced production of ROS (Adamo *et al.*, 2012). Furthermore, metal resistant cell lines generated via long-term exposure to high metal concentration have shown changes in transcriptome and proteome associated with metal binding (Adamo *et al.*, 2012).

1.7.1 Resistance induction by increasing exposure concentration

Freedman, Weiner and Peisachst, (1986) induced copper resistance in Morris rat hepatoma (H4AzC2) cells through exposure and maintenance at increasing concentrations of Cu^{2+} acetate up to 500 µM (and higher using Cu^{2+}- His2, due to precipitate nature). Resistance was initially thought to be conferred by sequestration of copper to a cysteine-rich protein (18 kDa), not then believed to be metallothionein, due to MTs smaller molecular weight. This cysteine-rich protein was still highly expressed

outside of copper treatment, despite a decrease in intracellular copper concentrations. The resistant cells generated during this study demonstrated long-term resistance to copper and a number of other metals ions (zinc, cadmium and mercury). Subsequent validation confirmed the expression of MTs conferred protection in the rat hepatoma model (Freedman and Peisach, 1989).

1.7.2 Resistance induction by transfection

Schilsky *et al.*, (1998) established another method for resistance to copper in hepatoblastoma cells, through overexpression of Wilson disease protein, ATP7B. The group found that upregulated ATP7B gene and protein expression (3 - 5 fold) conferred copper resistance to two HuH7 cell lines. The resistant lines demonstrated reduction of MT mRNA expression, which leads the group to postulate that unlike the copper resistant rat hepatoma cells generated by Freedman et al. (1986), ATP7B and not MT was the primary mechanism conferring resistance. Both cell lines showed no cross-resistance to cadmium or zinc exposure.

1.7.3 Resistance induction by subcloning and concentration selection

Chimienti *et al.*, (2001) developed a zinc-resistant HeLa variant (HZR) by subcloning the parental HeLa cell line and culturing in 200 µM $ZnSO_4$. A single resistant clone was selected and routinely subcultured in a zinc-enriched medium. Through depletion of intracellular zinc by culturing in normal growth media for 3 or 7 days, the group demonstrated that Zn-induced metal-free MT contributed to cellular protection from

oxidative stress. The generated clone demonstrated high levels of Zn (determined by electrothermal atomic absorption spectrophotometry) in intracellular vesicles and increased expression of cytoplasmic metallothionein.

Rousselet *et al.*, (2008) used the HZR clone to characterise the influence of cadmium (Cd) and manganese (Mn) exposure on resistant zinc-adapted cells. Both metals compete with Zn for uptake into HeLa cells, however in the Zn resistant HZR cell line the mechanism for Cd and Mn uptake was impaired, thus cross-conferring resistance. This was the first instance that interference of uptake for a toxic metal such as cadmium was demonstrated in a resistant line. The same group examined differentially expressed proteins using 2-DE and MALDI-TOF MS and determined co-chaperones, oxidoreductase related proteins and ubiquitin as the main factors responsible for resistance in their investigation (Rousselet, Martelli, *et al.*, 2008).

Many studies have since documented proteins associated with metal resistance. These proteins implicated in studies of metal resistance are listed in Table 1.7.1. The work in this thesis focusses on further exploration of such proteomic differences in intestinal-like Caco-2 cells in chapter 3.

Symbol	Protein Name	Resistant Metal	Cell Type	Reference
ABCC1	Multidrug resistance-associated protein (MRP1)	Antimony/arsenic	KB-3-1 and C-A120 cells	Mutoh *et al.*, 1997
ATP7B	Wilsons Disease Protein	Copper	HuH7	Schilsky *et al.* 1998
MT1	Metallothionein 1	Copper	H4AzC2 (rat)	Freedman *et al.* 1989
MT1	Metallothionein 1	Zinc	HeLa	Chimienti *et al.*, 2001
ABCC1	Multidrug resistance-associated protein (MRP1)	Antimony	GLC4/Sb30 cells	Vernhet *et al.*, 2002
HPPD	4-Hydroxyphenylpyruvate dioxygenase	Zinc/ Cadmium/ Manganese	HeLa	Rousselet *et al.*, 2008
GRIM-12	Thioredoxin reductase GRIM-12	Zinc/ Cadmium/ Manganese	HeLa	Rousselet *et al.*, 2008
STIP-1	Stress-induced-phosphoprotein 1	Zinc/ Cadmium/ Manganese	HeLa	Rousselet *et al.*, 2008
SDHA	Succinate dehydrogenase flavoprotein subunit, mitochondrial precursor	Zinc/ Cadmium/ Manganese	HeLa	Rousselet *et al.*, 2008
CA2	Carbonic anhydrase II	Zinc/ Cadmium/ Manganese	HeLa	Rousselet *et al.*, 2008
UBB	Ubiquitin	Zinc/ Cadmium/ Manganese	HeLa	Rousselet *et al.*, 2008
SXM1	Importin beta SMX1	Copper	*S. Cerevisae* (Yeast)	Jo *et al.* 2010
CUP1	Metallothionein 1	Copper	*S. Cerevisae*	Adamo *et al.*, 2012
TRK	Transketolase 1		*S. Cerevisae*	Adamo *et al.*, 2012
GLUD1	NADP glutamate dehydrogenase	Copper	*S. Cerevisae*	Adamo *et al.*, 2012
PDIA	Protein disulfide-isomerase	Copper	*S. Cerevisae*	Adamo *et al.*, 2012
EEF1B2	Elongation factor 1-beta	Copper	*S. Cerevisae*	Adamo *et al.*, 2012
SOD1	Cu, Zn-superoxide dismutase	Copper	*S. Cerevisae*	Adamo *et al.*, 2012
TSA1	Peroxiredoxin	Copper	*C. humilis* (yeast)	Adamo *et al.*, 2012
RPS31	Ubiquitin-40S ribosomal protein S31	Copper	*C. humilis*	Adamo *et al.*, 2012
ABCB1	Multidrug resistance protein (MDR1, P-gp)	Bismuth	HK-2 cells	Hong *et al.*, 2015
GSH	Glutathione	Bismuth	HK-2 cells	Hong *et al.*, 2015

Table 1.7.1: List of proteins associated with the generation of metal resistance in metal resistant models reported in the literature. All proteins listed were determined as upregulated in their relevant study. Species other than human are indicated in brackets

1.8 Gene and protein changes induced by micronutrient exposure - *In vitro* studies

Molecular changes associated with copper supplementation have been studied *in vitro* from sub-nanomolar range to toxic concentrations in millimolar range to understand various avenues of metal supplementation such as the rate of copper uptake, the effect on cell permeability, gene and protein expression changes, and resistance generation. This section focusses on changes observed in gene and protein expression during exposure to micronutrients, with particular attention to studies involving copper or Caco-2 cells. Also discussed are developments in proteomic and transcriptomic techniques, which have allowed the simultaneous identification of differentially regulated proteins and genes during exposure to stressors and represent highly valuable tools in deciphering the remaining unknowns regarding micronutrient homeostasis. These can be further enhanced to include the idea of microRNAs – a triomics approach (O'Sullivan *et al.*, 2017).

In a recent study, a top-down approach was used to generate the 'human Cu proteome': a list of Cu-binding proteins and their putative participation in cancer development (Fierro-González *et al.*, 2016). A total of 54 Cu-binding proteins were identified using a combination of literature review, manual curation and searching Cu related targets in Uniprot.org (Appendix Fig. 1). The expression patterns for the Cu-binding proteins were then mapped in different cancers by Ward2's hierarchical clustering method. In that study, the Cu chaperone ATOX1 was proposed as the only Cu-binding protein with transcription factor activity connected to cancer progression. This type of research combined with studies utilising the ranges of 'omics' suites and bioinformatics tools in

order to examine copper interactions both *in vitro* and *in vivo,* continues to contribute to molecular studies of Cu-dependent processes in cancer, neurodegenerative disorders, metabolomics disorders and nutritional disorders, and will hopefully one day allow for a better picture of the dynamic nature of cellular micronutrient homeostasis.

1.8.1 Copper-regulated gene and protein expression

As discussed in section 1.2, transition metals such as Cu are capable of generating increased intracellular reactive oxygen species (ROS) due to Fenton and Haber-Weiss reactions. Importantly, ROS are a by-product of aerobic metabolism and therefore, a wide range of genes which encode for proteins, enzymes and chaperones with antioxidant, detoxifying and transporting capacity have evolved to maintain redox homeostasis. Copper overexposure can also result in oxidative damage of cellular components through binding sulfhydryl residues (Valko, Morris and Cronin, 2005) and compounds which react with sulfhydryl groups are potent inducers of antioxidant response elements (Nguyen, Nioi and Pickett, 2009).

Under conditions of excess ROS, cis-acting sequences called antioxidant response elements (AREs) in the promoter regions of target genes play critical roles in controlling constitutive gene expression of detoxifying proteins involved in oxidative damage response (Raghunath *et al.*, 2018). AREs are regulated primarily by nuclear factor receptor 1 and 2 (NRF1 and NRF2) through the cis-acting elements. NRF2 activity is controlled partly by cytosolic Keap1 which triggers its ubiquitination, thus signalling NRF2 proteasomal degradation before transcription of antioxidant proteins may be initiated. This system of Keap1/Nrf2/ARE encompasses many targets which

play roles as mediators of adaptive responses to cell stress by regulating transcription of cytoprotective genes encoding for detoxification enzymes such as heme oxygenase or glutathione S transferases and elevating cellular glutathione (Hayes and McLellan, 1999; Nguyen, Nioi and Pickett, 2009).

Simmons *et al.* (2011) examined effects of exposure to twenty alkali, transition and heavy metals to determine which metals activated the transcription factor NRF2 in response to oxidative stress in different tissue and cell line models: HEK293T (kidney), A172 (brain), A549 (lung), HepG2 (liver) and MCF7 (breast). Their study found that only three of the heavy metals induced NRF2 activation in all cell lines: cadmium, copper and sodium arsenite. Fischbach, Sabbioni and Bromley (1993) had previously examined a panel of 31 metals in mouse NIH3T3 cells and cadmium, copper and sodium arsenite were among others (lead, gold, zinc and silver) identified as inducers of human heat shock 70 promoter.

Mattie, McElwee and Freedma (2008) examined 400 μM copper exposure in COS-7 cells and found elevated protein expression for multiple transcription factors; c-Fos, c-Jun and c-Myc were highly overexpressed (28-, 30- and 16- fold increases, respectively) after 4 hours, returning to levels not significantly different from unexposed control cells after 24 hours.

Recently, experimental evidence has shown copper exposure (100 - 600 μM) initiates ARE driven responses through NRF2 activation by restoring ectopic expression in Nrf2−/− cells (Song *et al.*, 2014). Interestingly, for short Cu exposure (4 h), Nrf1 and Nrf2 were both equally responsible for metallothionein expression, whereas NRF1 was required following longer exposures (24 h). The group demonstrated that while ARE-mediated transcription is initiated by copper exposure, Nrf1 and Nrf2 trigger different

antioxidant processes through this response and identified multiple genes associated specifically with these transcription factors (Song *et al.*, 2014).

1.8.2 Microarray analysis during micronutrient exposure

Analysis of the transcriptome has been used to examine the effect of copper exposure in various tissues previously, especially in cancer studies. Recently, a microarray analysis of colorectal cancer patients and *in vitro* tissues revealed that some colorectal cancers are linked to upregulated expression of copper homeostasis genes (Barresi *et al.*, 2016), but perhaps not surprisingly, given that the small intestine is the main site of Cu absorption.

Early microarray methods indicated the increased expression of the prion protein and the amyloid-β precursor protein during chronic copper overload in C57BL/6 cells (Armendariz *et al.*, 2004). In this study, the group detected no evidence of oxidative stress-related gene expression and this may be due to the Atp7a mutated mouse fibroblast cell model which is often used to simulate copper overload by restricting copper export.

Bigagli *et al.* (2010) used microarray analysis to study copper concentrations in the sub-nanomolar range (10^{-6} to 10^{-17} M) to determine the effect on gene expression profiles of human prostate epithelial cell lines. Their findings indicated that similar patterns in transcriptomic profile expression were obtained for copper exposure regardless of copper concentrations due to tight regulation mechanisms controlling free copper ions intracellularly to restrict excess oxidative stress. Functional genes belonging to families associated with oxidative stress, including metallothioneins and heat shock proteins

(HSP90Ad, HSP90B1 HSPD1, HSP90AB1 and HSPA8) were over-expressed at all copper concentrations, suggesting constitutively expressed mechanisms were present intracellularly in order to deal with any free copper ions. In this thesis, Chapter 4 describes microarray analysis of multiple Caco-2 clones resistant to Cu exposure and reports differential expression of over 4,000 genes.

1.8.3 Proteomic analysis during micronutrient exposure

The capacity to correctly identify proteins is essential to any investigation involving the proteome. Recent advances in high throughput protein profiling such as tandem mass spectrometry (MS/MS) have significantly improved resolution and mass accuracy and have allowed the field to open up to even more applications such as in vivo signalling analysis, enhanced protein biomarker detection and integrative structural analysis (Aebersold and Mann, 2016).

Recently, Keenan *et al.* (2018) used a 2-hour acute exposure with 10-hour recovery for multiple forms of copper in both Caco-2 and HT29 cells. In addition to increases in ROS generation, proteomic profiling identified upregulated expression of multiple stress response proteins including metallothionein (MT1), sulfiredoxin 1 (SRXN1) and heme oxygenase 1 (HMOX1), common between the copper sources. Additionally, increases in LC3 and SQSTM1 without changes in autophagy suggested the presence of aggresomes (depots of aggregated misfolded proteins). Aggresomal formation and protein ubiquitination correlated with decreased growth during exposure to copper organic acid chelate, while copper proteinate showed the least impact on aggresome formation and growth for both cell lines (Keenan *et al.*, 2018).

Proteomic analysis has also been used to further characterise protein dysregulation *in vivo* using animal models during the development of Wilsons disease in response to copper overload. In liver samples taken from a rat model of Wilsons disease, proteomic analysis identified multiple differentially expressed proteins as a result of age related copper-induced injury including downregulated mitochondrial matrix proteins (agmatinase and cytochrome b5) in the very early stage and highly upregulated apoptosis marker annexin 5A in the late stages of development (Lee *et al.*, 2011).

An earlier proteomics study by Park *et al.* (2009) examined the sera of heathy and young Wilsons disease patients in early stages of the disease and found differentially expressed proteins linked to oxidative stress and inflammation (complement component C3, complement factor B and alpha-2 macroglobulin). More recently, Cabras *et al.* (2015) looked at proteomic expression in Wilsons disease patient saliva and likewise identified increased levels of proteins related to oxidative stress (including oxidised S100A9 and S100A8) and inflammation (α-defensin 2 and α-defensin 4). These identified targets were proposed by the group as potential indicators of disease and stage of progression in Wilsons disease patients.

1.8.4 Effect of other metals on Caco-2 cells

Due to a rapid increase in the use of metal nanoparticles (NPs) and their incorporation into a growing number of consumer products within the last decade, studies assessing the effects of nanoparticle exposure on humans have also increased. Notably, Caco-2 cells are often the cell line model for nanoparticles studies due to their simulation of the intestinal route of exposure. Bajak *et al.* (2015) examined gold nanoparticle (AuNP)

exposure to proliferating Caco-2 cells to determine transcriptomic changes to the intestinal epithelial cell line. The gene expression profiles generated using microarrays revealed multiple upregulated metallothioneins alongside other genes including HMOX, and gastrointestinal glutathione peroxidase (GPX2). Interestingly, expression of multiple selenoproteins was also negatively affected, suggesting an influence of AuNP exposure on selenium homeostasis.

Recently, Gioria *et al.* (2018) examined 1 and 10 μg/mL silver nanoparticle (AgNP) exposure to Caco-2 cells using two proteomic approaches to decipher the copper-binding proteome resulting from AgNP exposure. Using different quantification methods and studying various time-points this study finds the major Heat shock 70 kDa protein (HSPA1A) as commonly expressed between all conditions tested, suggesting sustained changes in HSPA1A to counteract oxidative stress generated by AgNP exposure to Caco-2 cells. This group also identified time-specific deregulation of proteins involved in the neutralisation of excess oxidative stress including glutathione synthetase, glutaredoxin-1 and peroxiredoxin-1. From the resulting proteomic profiles of AgNP exposed Caco-2, the group also described changes to cell cycle and morphology, cellular function and maintenance using bioinformatics analysis tools.

All living organisms experience and respond to a diverse range of stress stimuli. When subjected to stressors exceeding homeostatic capacity, eukaryotic cells react to stimuli by eliciting adaptive or stress responses or die (Chovatiya and Medzhitov, 2014). Metal micronutrient studies are continuing to discover more pathways involved in cellular responses to stress exposure using complementary ‘omics’ based research platforms. Caco-2 cells appear to be a common choice in these studies due to their popularity as a

model of intestinal enterocytes to support informed decision-making when assessing the potential health effects of stressors including micronutrients in an *in vivo* setting. For these reasons, this thesis examines the approach of characterization of biological responses at molecular levels by combining *in vitro* Caco-2 models and powerful proteomic/transcriptomic tools in chapters 3 and 4.

1.9 The effect of micronutrient chelation in vitro

Chelators of metal micronutrients have been used to treat animals and humans suffering from metal overload for decades. Chelation remains the mainstay for treatment of many genetic conditions such as in Wilson's disease, where it is used to reduce Cu uptake in the intestine and increase excretion. Other conditions where copper chelators have been utilised in a clinical setting include Huntington disease, Alzheimer's disease, rheumatoid arthritis, kidney stones/cystinuria, in anticancer therapies and copper intoxication (Ogra, 2011, Flora and Pachauri, 2010). Some chelators demonstrate different effects on toxicity and effectiveness of copper depletion and many have been used in *in vitro* studies to examine uptake and transport studies. Some of the primary copper-binding chelators used in both research and a clinical setting are described below:

DPA - D-Penicillamine (formerly marketed as Cuprimine) is an amino acid metabolic product of penicillin and was the first discovered treatment suitable for Wilson's disease patients (Purchase, 2013). DPA is used to decrease copper intake and has been used during lead and mercury poisoning (Ogra 2011).

TETA – Triethylenetetramine (marketed as trientine) is a chelation agent used to treat Wilson's disease and copper intoxication. TETA is normally administered in the range of 750 – 2,000 mg daily, with copper excretion in urine reported to increase following administration, preventing the development of hepatitis and subsequent development of hepatocellular carcinoma (Sone *et al.*, 1996). Hepatic and renal DNA damage and renal

copper concentration are also reduced during TETA treatment (Sone *et al.*, 1996; Reed, Lutsenko and Bandmann, 2019). Following TETA administration, recently evaluated plasma concentrations vary over time at 35.6 ± 25 μM per hour (Pfeiffenberger *et al.*, 2018) and this range is within the concentration used in examinations of Caco-2 cell exposure to TETA (25 μM), carried out in chapter 5. Furthermore, TETA has demonstrated less toxicity than D-penicillamine in children with Wilson's disease, but also reduced effectiveness (Flora & Pachauri 2010). TETA has been used previously to induce copper depletion in Caco-2 cells *in vitro* (Zerounian and Linder, 2002) and increased iron transport.

TTM - Tetrathiomolybdate has specific affinity for copper. It depletes systemic copper levels and leads to excretion via the normal bilary pathway. It has been used to treat Wilson's disease patients presenting with neurological implications. DPA and TETA are ineffective in removing copper from metallothionein (MT) (Juarez *et al.*, 2006), however TTM is able to remove copper bound to MT. TTM has been examined as a therapeutic agent for angiogenesis and has undergone trials as an antitumor and anticancer agent (Juarez *et al.*, 2006).

BCS - Bathocuproine sulfonate is a Cu^{+} specific chelator. BCS has been utilised previously to induce Cu deficiency in cultured embryonic fibroblasts of 129Sv MT-WT and MT-null mice leading to an increase in intracellular zinc (Ogra, Aoyama and Suzuki, 2006).

More recently, Rakshit *et al.* (2018) developed two Cu^{2+} chelators with binding constants 10^8 times higher than that for other biologically relevant metal ions including Cu^{+}. Structural insights indicated that the chelators complexed Cu^{2+} with a pseudo-square-planar geometry, where two N-and phenolate O-donor atoms each are coordinated to the central metal ion. The cell-permeable chelators demonstrated reduction in Cu^{2+}-generated oxidative stress by limiting the Fenton reaction *in vitro* and *in vivo* while through binding with excess labile copper without affecting copper bound to cellular enzymes.

Evidently, studies incorporating Cu chelators are increasing due to their ability to modulate Cu homeostatic pathways and Cu induced oxidative stress responses. The use of chelators has shown benefit in the treatment of various conditions such as Alzheimer's disease and Wilson's disease and potential has been observed in a clinical setting for Huntington disorder, several cancers and other neurological conditions. The influence of exposure to Cu chelators on mRNA and protein expression profiles in cells is lesser known however and further studies are warranted to elucidate these effects. Chapter 5 examines the effect on the Caco-2 proteome both during exposure to TETA, exhibiting a decrease in cell viability and after removal of TETA, exhibiting restoration of cell viability.

Aims of the study

The heterogeneous Caco-2 cell line and its clones have long served in models of intestinal toxicity, absorption and homeostasis for drugs and micronutrients due to their versatility and the fact they are easily maintained and manipulated. Importantly, using this cell line, many attempts have been made to reduce variability and standardise culture conditions but much remains to be explored regarding their potential to yield new knowledge in intestinal biology.

Our understanding regarding how intestinal cells react during prolonged exposure to copper supplementation and restriction is not fully explored. Ultimately, the aim of this thesis was to further characterise copper interactions in intestinal-like Caco-2 cells, to examine the effect of copper-overload and restriction in the parental population and to use 'omics' tools to derive greater insight regarding copper homeostasis. In the publications, the following investigations were undertaken:

1) Characterisation of the Cu-induced non-monotonic dose response by comparing inorganic versus organic copper and Cu-induced toxicity in Caco-2 cells against cell lines from multiple tissues.

2) Development and study of Cu-resistant variants of Caco-2 cells by: i) determining their toxicity relative to parental Caco-2 and ii) investigating the mechanisms contributing towards tolerance using proteomic analysis in Cu-resistant Caco-2 variants both out-of-exposure and in-exposure.

3) Isolation of multiple clones from the Cu-resistant variants and further characterisation of their cross-resistance to additional metals and chemotherapeutics by using human gene microarrays to examine mechanisms of Cu-tolerance.

4) Examination of the effect on the Caco-2 proteome by exposure to a micronutrient chelator (TETA).

2 Copper-induced non-monotonic dose response in Caco-2 cells

Authors: Charles O'Doherty[1,a], Joanne Keenan[1,a], Karina Horgan[2], Richard Murphy[2], Finbarr O'Sullivan[1,b] and Martin Clynes[1,b]

[1] National Institute for Cellular Biotechnology, Dublin City University, Glasnevin, Dublin D09 W6Y4, Ireland

[2] Alltech, Dunboyne, Meath, Ireland

[a] O'Doherty C and Keenan J were involved at all stages of the research, co-wrote the manuscript and are joint-first authors;

[b] O'Sullivan F and Clynes M contributed equally to this work

Journal: In Vitro Cellular & Developmental Biology – Animal

Status: Accepted February 2019

DOI: 10.1007/s11626-019-00333-8

I participated in all stages of this study as lead co-author with Dr Joanne Keenan, from conception and design, acquisition, analysis and interpretation of data, to drafting, revising and submitting the manuscript. All authors participated in design, review and revision of the manuscript.

Abstract

Copper is an essential dietary micronutrient in humans for proper cell function, however in excess it is toxic. The human cell line Caco-2 is popular as an *in vitro* model for intestinal absorption and toxicology. This study investigated the response of exponentially growing Caco-2 cells to prolonged copper exposure (120 hours). An unexpected non-monotonic dose-response profile was observed in Caco-2 cells. Exposure to media supplemented with 3.125 µM $CuSO_4$ resulted in decreased cell yield versus untreated. However, toxicity was progressively reduced from 90% at 3.125 µM, to 60% at 25 µM. This effect was documented between 48 and 120 hours continuous exposure ($p < 0.05$). This triphasic toxicity curve was observed to be specific to copper in Caco-2 cells, as iron, manganese and zinc displayed monotonic dose-response profiles. Two inorganic copper forms: copper sulfate and copper chloride were shown to conserve the non-monotonic dose-response curve. The triphasic effect was shown to be specific to Caco-2 cells. These results have implications for research investigating the effect of copper and other micronutrients using Caco-2 cells.

2.1 Introduction

Copper is a redox active transition metal required for survival by all aerobic eukaryotic organisms, yet causes toxicity when present in excess, due to catalytic Fenton and Haber–Weiss reactions leading to hydroxyl radical formation (Kozlowski *et al.*, 2009; Linder, 2012; Gaetke, Chow-Johnson and Chow, 2014). Copper (Cu) is involved in numerous biological processes including embryogenesis, heme synthesis, iron absorption and mitochondrial respiration (Barceloux and Barceloux, 1999), and is predominantly associated with proteins and the prosthetic groups of enzymes. Shuttling of intracellular Cu is strictly controlled by transporters and chaperone proteins (Nishito and Kambe, 2018).

The intestinal epithelial barrier consists of a complex mix of cell types that work in tandem to regulate uptake for most nutrients following digestion. The adenocarcinoma derived Caco-2 cell line exhibits similar characteristics to enterocytes of intestinal epithelia when cultured as a monolayer or in co-cultured differentiated systems (Hidalgo, Raub and Borchardt, 1989; Natoli *et al.*, 2011). While recent developments including gut-on-a-chip (Kim *et al.*, 2012), intestinal organoids (Spence *et al.*, 2011) and *ex-vivo* xenografts have shown potential, use of Caco-2 cells in a differentiated form has represented the workhorse of food and pharmaceutical industries to study toxicity, permeability and uptake of nutrients, pharmaceuticals and xenobiotics for over four decades (Fogh and Trempe, 1975; Shah *et al.*, 2006; Shao *et al.*, 2017).

Non-monotonic dose-responses (NMDR) are dose/effect phenomena which do not show linear or threshold dose-response relationships and their discovery precedes the 1900's (Schulz, 1888). NMDR curves introduce paradoxical effects such as hormesis; an adaptive response in which stimulation is observed during exposure to low

concentration of a stressor followed by a toxicity at higher ranges (Calabrese *et al.*, 2001). These responses have shaped our understanding of pharmacology and toxicology to biological and environmental systems and have implications for understanding phenotypic plasticity and predicting dose-response effects during exposure to a wide variety of stressors (Michael Davis and Svendsgaard, 1990; Vandenberg *et al.*, 2012; Calabrese, 2014). Exposure of a stressor which results in a NMDR profile has been attributed to multiple factors, such as receptor-mediated interactions (Bartłomiejczyk *et al.*, 2013) or via an overlay of two opposing monotonic profiles (Conolly and Lutz, 2004; Calabrese, 2013). Recently, fluctuating copper levels in basal media were demonstrated to have a notable influence on the expression of apoptosis and autophagy related proteins in Caco-2 cells (Keenan, Horgan, *et al.*, 2018). Indeed, the expression or location of multiple transporters including divalent metal transporter 1 (DMT1) and copper transporter 1 (CTR1) and sequestration proteins (ATP7A/ATP7B, metallothionein) are also known to be modulated by Cu exposure (Tennant *et al.*, 2002; Gao *et al.*, 2014).

Focussing over a wide range of concentrations, a triphasic NMDR profile was observed in this study which has not been previously reported. The effect was seen in two copper formulations, was specific to Caco-2 and also appeared to be copper-specific as Fe, Mn and Zn did not display NMDR profiles.

2.2 Materials and Methods

2.2.1 Materials

Irradiated $CuSO_4$ and Cu proteinate (a product resulting from the chelation of soluble Cu with soy hydrolysate, Byrne, 2010) were supplied by Alltech Ireland Ltd. Inorganic sulfate and organic proteinate forms of iron, manganese and zinc were supplied by Alltech Ireland Ltd. All metal micronutrients were validated by ICP-MS analysis.

2.2.2 Cell culture conditions

Exponentially growing Caco-2 cells (HTB-37 ™; American Type Culture Collection) were cultivated at 37 °C under 5% CO_2, in MEM (Gibco, 21090022) supplemented with 10% fetal bovine serum (FBS, Gibco, 10270-106), 10 mM HEPES (Sigma Aldrich, H3537) and 2 mM L-glutamine (Sigma Aldrich, G7513). Cells were passaged approximately every 4 days, not allowing cells to reach confluence (Natoli *et al.*, 2011). HT29 cells were obtained from Public Health England Culture collection and were cultured in MEM supplemented with 10% fetal bovine serum, 10mM HEPES and 2mM L-glutamine. HT29-MTX-E12 cell line was obtained from Sigma Aldrich, porcine IPEC-J2 was obtained from DSMZ, HCC1954, BT-474, HCT116, porcine IPEC-J2, HEP-G2, and Mia-PaCa were obtained from the American Type Culture Collection and were cultured in DMEM high glucose GlutaMAX™ Supplement (Gibco, Cat: 61965026) supplemented with 10% Fetal bovine serum and 10mM HEPES. BxPC3 (ATCC) were cultured in RPMI-1640 (Sigma Aldrich, R8758) supplemented with 10% Fetal bovine serum, 10mM HEPES. Cells were routinely tested and found to be negative for *Mycoplasma* contamination.

2.2.3 Cell survival determination

Cells were seeded at 3125 cells/cm^2 and exposed after 24 hours for up to 120 hours before assaying by (A) acid phosphatase activity in 96-well microtiter plates (adapted from Martin and Clynes, 1993, 1991) and (B) in 75 cm^2 tissue culture flasks by viable cell count using haemocytometer and trypan blue exclusion method.

2.2.4 Statistical analysis

To evaluate statistical significance between any two populations, *P*-values were calculated by two-tailed Students' t-test with 2-tailed distribution and two-sample heteroscedastic unequal variance (Microsoft Excel®). Significance was set at *P*-values less than 0.05. Error bars in all figures indicate standard error of the arithmetic mean. Relative values in all figures are expressed as percentage of untreated controls, unless otherwise noted. All experiments were repeated at least three times.

2.3 Results and discussion

2.3.1 Identification of Cu-induced NMDR in Caco-2

We identified a triphasic dose-response profile in proliferating Caco-2 cells (ATCC® HTB37™) during copper exposure not detected in other cell lines or micronutrients tested and not previously explored in the literature to the best of our knowledge.

In the course of this study, increasing Cu concentration to proliferating Caco-2 cells was shown to generate a triphasic non-monotonic dose-response (NMDR) after 120 hr (cultured in basal medium with serum, together containing 0.3 µM Cu). The curve consisted of a linear dose-response from 0 µM to 3.125 µM added $CuSO_4$, followed by significantly reduced toxicity between 6.25 µM and 25 µM (Fig. 2.2.1A), resulting in two points of inflection within the range tested (1.56 µM to 100 µM). Above the first point of inflection at 3.125 µM (Cell survival was 12.33 ± 1.31%), progressively decreasing toxicity was identified up to 25 µM; cell toxicity was significantly reduced at 6.25 µM, 12.5 µM and 25 µM vs. 3.125 µM ($p < 0.05$). At the second point of inflection, increased dose-response toxicity was generated with exposures above 25 µM $CuSO_4$ (Fig. 2.2.1A) up to 100 µM.

Caco-2 cell growth was measured every 24 hr in Cu between 3.125 - 25 µM (Fig. 2.3.1B). No change was observed during temporal measurements of viable cell counts for cells cultured in 3.125 µM supplemented $CuSO_4$ over the time course (coefficient of variation: 10.9%), however, morphological observations showed clonal growth and much cell death at this concentration (not shown). Significant increases in growth were present in the other Cu concentrations added ($p < 0.05$). From 72 – 120 hours exposure,

25 µM $CuSO_4$ presented a significantly increased yield every 24 hours vs. 3.125, 6.25 and 12.5 µM ($p < 0.05$). Importantly, direct correlation was observed between viable cell count and acid phosphatase at the NMDR concentrations, demonstrating the Cu-induced response was not assay specific (Fig. 2.3.1C). Furthermore, the concentrations are within the range of reference values for serum copper, at approximately 1 µg/ml (15.73 µM) and this varies widely depending on many factors including age and diet (Bost *et al.*, 2016).

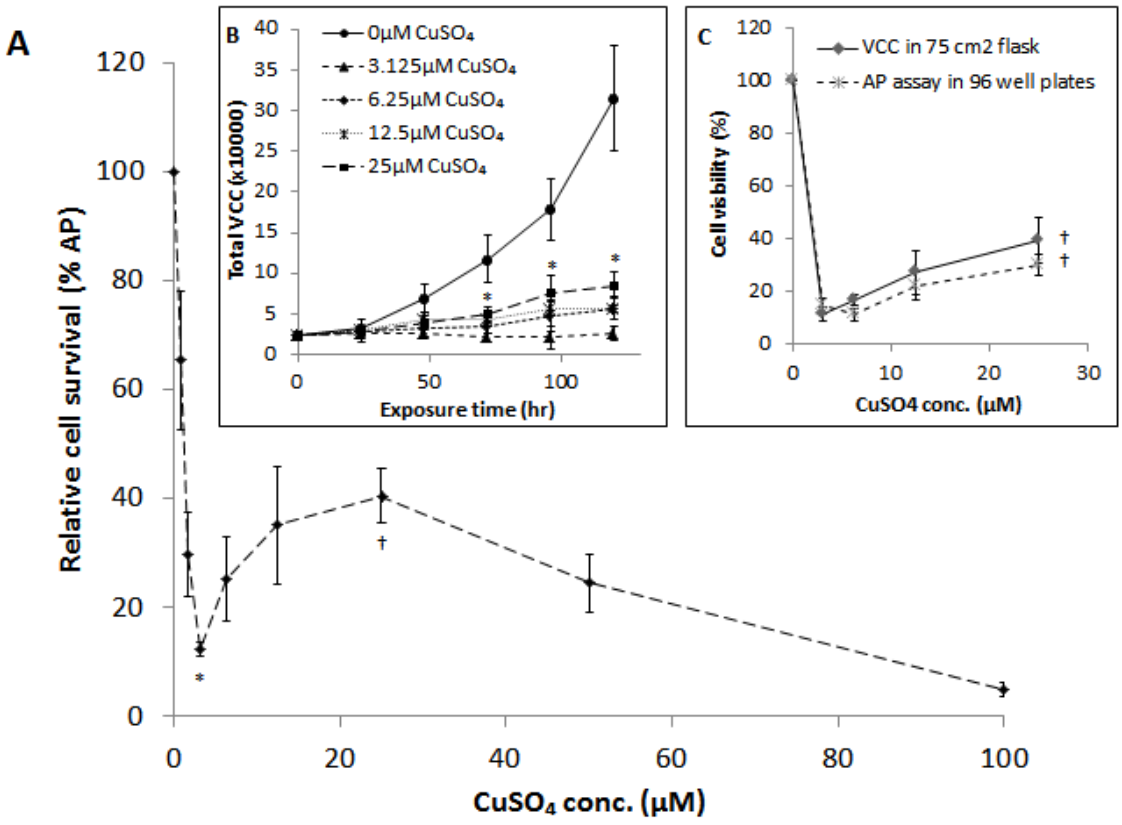

Figure 2.3.1: A) Caco-2 cells exposed to increasing $CuSO_4$, cultured in 96-well plates, assayed by acid phosphatase (AP) after 120 hrs continuous exposure (n=3). B) Time-course of Caco-2 cells cultured in 6-well plates exposed to $CuSO_4$ at 0, 3.125, 6.25, 12.5 and 25 µM, assayed by daily viable cell counts (VCC) (n=5). C) Caco-2 cells exposed

to increasing $CuSO_4$, demonstrating correlation between VCC and AP assays (n=3). All results are presented as relative to untreated control. Asterisk indicates significant difference from all ($p < 0.05$), dagger (†) indicates significant difference from 3.125 µM $CuSO_4$ exposure ($P < 0.05$).

2.3.2 Characterisation of cell specificity for the Cu-induced NMDR

NMDR profiles are commonly reported in endocrine disruption (Vandenberg *et al.*, 2012; Lagarde *et al.*, 2015) and during heavy metal exposure (Chaube, Mishra and Singh, 2010; Helmestam, Stavreus-Evers and Olovsson, 2010), but have not been reported previously for copper exposure in Caco-2 cells. However, profiles including stimulatory hormesis have been identified during exposure to cadmium in Caco-2 cells and genistein exposed Caco-2 BBE (Chen and Donovan, 2004; Mantha and Jumarie, 2010). Metal nanoparticles (Mn, Sb, Ti) displayed a hormetic effect on Caco-2 cells which was attributed to the activation of growth factor receptors indirectly by ROS formed during low concentration exposure (Titma *et al.*, 2016).

To investigate if the copper induced triphasic toxicity curve was specific to Caco-2, cells derived from breast (HCC1954, BT-474), colon (HT29, HT29-MTX-E12, HCT116), intestine (porcine IPEC-J2), liver (Hep-G2) and pancreas (Mia-PaCa, BxPC3) were exposed to increasing $CuSO_4$ (Fig. 2.3.2). The toxicity profiles obtained showed Caco-2 cells were considerably more sensitive to copper exposure; IC50 value for Caco-2 cells was 1.3 µM added $CuSO_4$ compared to lowest IC50 of 118.7 µM in HT29 cells.

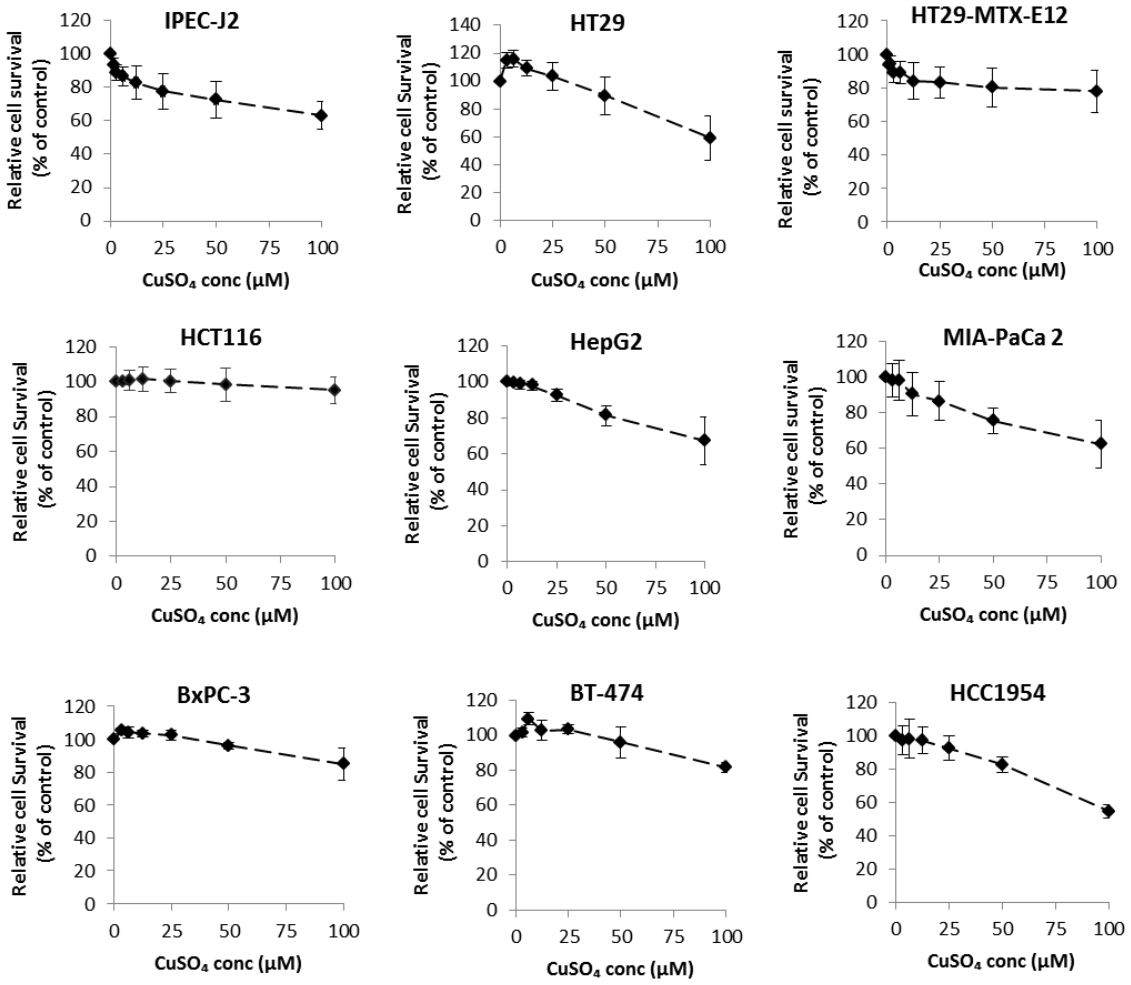

Figure 2.3.2: IPEC-J2, HT29, HT29-MTX-E12, HCT116, HepG2, MIA-PaCa 2, BxPC-3, BT-474 and HCC1954 cells exposed to increasing copper sulfate, assayed by acid phosphatase after 120 hrs continuous exposure. Results are presented as relative to untreated control (n=3).

With the exception of HT29 and BT-474 cells, the other cell lines examined displayed monotonic dose-response curves with IC50 values greater than 50 µM. Low concentration $CuSO_4$ exposure (3.125 - 6.25 µM) to HT29 and BT-474 demonstrated a small but significant stimulation in cell growth (15 and 10%, respectively, $p < 0.05$).

This slight hormetic response may indicate that Cu concentration in the growth media was too low or may suggest indirect growth factor receptor activation by ROS generation as described previously (Bartłomiejczyk et al. 2013). From the panel examined, this Cu-induced NMDR curve appeared specific to Caco-2 cells.

2.3.3 Characterisation of metal specificity for the Cu-induced NMDR

Inorganic $CuCl_2$ also demonstrated a triphasic Cu-induced NMDR curve (Fig. 2.3.3A), supporting the notion that toxicity was due to the copper component and not the chemical form of copper. Metal micronutrients other than copper including iron, manganese and zinc are also absorbed by intestinal epithelial cells and display interactions that may affect uptake and homeostasis (Goddard *et al.*, 1997; Arredondo *et al.*, 2006; Collins and Knutson, 2010). Exposure of iron, manganese or zinc to Caco-2 cells did not cause a significant NMDR curve (Fig. 2.2.3 B/C/D) between 3.125 µM and 800 µM. Increasing exposures of these micronutrients resulted in linear dose-response profiles after 120 hr continuous exposure. Additionally, Cu exposure was noticeably more toxic to the cells; IC50 values for Fe, Mn and Zn were greater than 50 µM and reflects toxicity noted previously (Zödl *et al.*, 2003; He *et al.*, 2008) . In Caco-2 cells, the induction of a triphasic toxicity curve appeared to be Cu-specific.

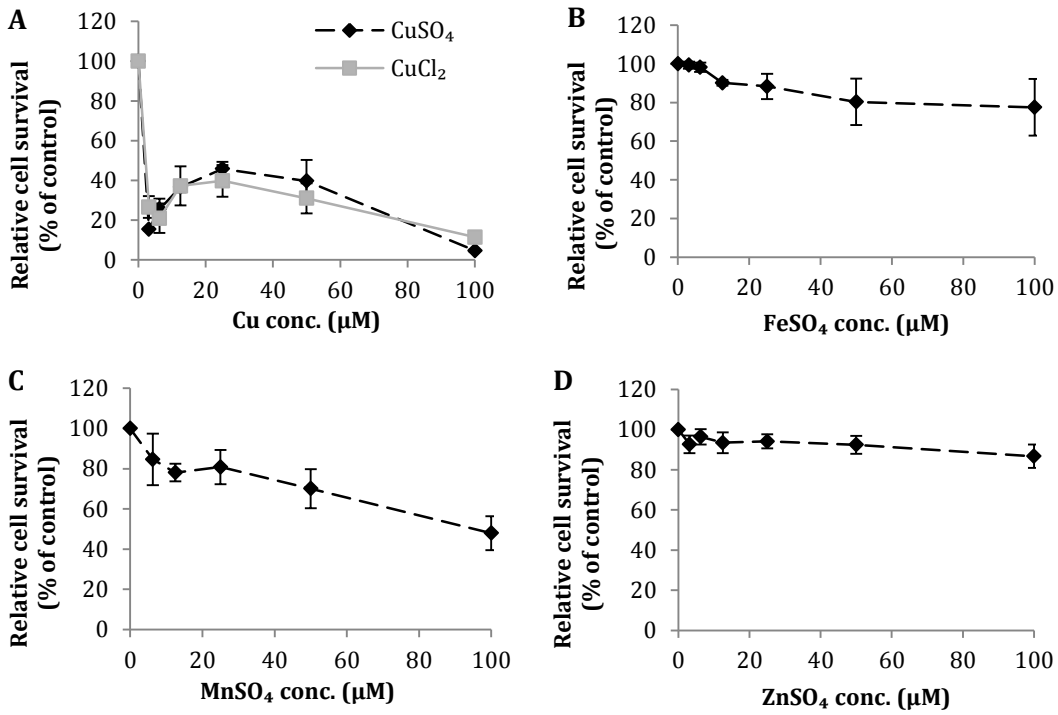

Figure 2.3.3: Caco-2 cell survival following exposure to a) increasing $CuSO_4$ and $CuCl_2$ in 9.5cm^{2}wells and b, c, d) iron sulfate, manganese sulfate and zinc sulfate in 96-well plates. Cells were subjected to continuous exposure after 24 h attachment for 120 h and analysed by acid phosphatase (AP) assay. Results are presented as relative to untreated control (n=3).

Conolly & Lutz 2004 established kinetic models which covered multiple mechanisms for NMDR responses in biological systems. They outlined mechanisms originating from fundamental biochemistry and others postulated on biological processes. The models are based on; (*a*) opposing regulatory effects by membrane receptor subtypes, (*b*) modulation of gene-expression by homodimers but not mixed dimers in increasing xenobiotic concentration (*c*) DNA damage repair induced by xenobiotic in a saturable manner and (*d*) concentration dependant DNA damage leading to two opposing monotonic responses (cell cycle delay/cell cycle acceleration) which generate NMDR

curves when superimposed. The recent publication by Keenan et al. identified that variation in levels of copper between different batches of media had a significant impact on autophagy and apoptosis related proteins. Without this knowledge we would not have been in a position to measure effects at such low levels, as the discrepancy between batches was observed at such a low level thus prompting this investigation.

This study focussed on identifying a triphasic NMDR profile induced by copper in Caco-2 cells, with demonstration of metal and cell type specificity. The observed NMDR profile demonstrates that lower concentrations of Cu result in greater toxicity than higher concentrations and has important practical implications in the modelling of Cu response with Caco-2 cells.

It is possible that this phenomenon represents a physiological response of some intestinal cells *in vivo* to copper deprivation, and that such cells "delay" switching on particular mechanisms such as Cu efflux or sequestration, until copper levels in the cells reach a critical level in order to replenish the bodies stores of copper. More detailed studies will be required to determine the effect, if any, played by protein/DNA repair mechanisms and Cu-related oxidative stress induced pathways in generating the Cu-specific NMDR profile.

Highlights:

- A triphasic non-monotonic dose response was identified, induced by multiple sources of copper in Caco-2 cells and may represent an *in vivo* response of specific intestinal cells to copper exposure.
- NMDRs are increasingly used to improve public-health protection and the identification of copper-induced NMDRs in intestinal niches may be useful in future modelling of optimal intake ranges for humans and animals
- Further proteomic analysis is required to determine the mechanism(s) responsible for the appearance of the Cu-induced NMDR.

2.4 Funding information

This work was funded by a joint Enterprise Ireland Innovative Partnership programme (IP/2015/0375) with Alltech Ireland Ltd.

3 Characterisation and proteomic profiling of continuously exposed Cu-resistant variants of the Caco-2 cell line

Authors: Charles O'Doherty[1], Joanne Keenan[1], Michael Henry[1], Paula Meleady[1], Indre Sinkunaite[2], Martin Clynes[1], Finbarr O'Sullivan[1], Karina Horgan[2] and Richard Murphy[2]

[1] National Institute for Cellular Biotechnology and SSPC-SFI. Centre for Pharmaceuticals, Dublin City University, Glasnevin, Dublin D09 W6Y4, Ireland

[2] Alltech Ireland, European Bioscience Centre, Summerhill Rd, Sarney, Dunboyne, Co. Meath, Ireland

Journal: Toxicology In Vitro

Status: Accepted January 2020

DOI: 10.1016/j.tiv.2020.104773

I participated in all stages of this manuscript from design of study, development of Cu-resistant Caco-2 lines, acquisition of data, analysis and interpretation of data, to drafting, revising and submitting the manuscript. Alongside myself, JK, MC, FOS, PM, KH and RM participated in experimental design and revisions of the manuscript. Additionally, MH ran the samples on LC-MS/MS, JK performed glutathione analysis, IS performed ICPMS and JK acquired and preformed preliminary processing of differential expression data.

Abstract

Studies in hepatic systems identify multiple factors involved in the generation of copper resistance. As the intestine is the route of exposure to dietary copper, we wanted to understand how intestinal cells overcome the toxic effects of high copper and what mechanisms of resistance develop. Using the human intestinal cell line Caco-2, resistance was developed by serial subculture in 50 μM copper in inorganic ($CuSO_4$) or organic (Cu proteinate) forms.

Caco-2 variants exhibited resistance to copper and retained the non-monotonic dose response while displaying stable phenotypes following repeated subculture in the absence of copper. Phenotypic changes on exposure to copper in parental Caco-2 cells included significantly increased total protein yield, ROS, SOD, metallothionein expression, GSH and total glutathione. These phenotypic changes were not replicated in resistant variants on a per cell basis.

Quantitative label-free LC-MS/MS proteomic analysis identified 1,113 differentially expressed proteins (DEPs) between parental Caco-2 and resistant cells. With some exceptions, most of the DEPs were overexpressed to a low level around 2-fold suggesting resistance was supported by multiple small changes in protein expression. These variants may be a useful tool in studying the toxicity of stress responses in further Cu-related studies.

3.1 Introduction

Copper (Cu) is an essential cofactor in several metalloenzymes including Cu, Zn superoxide dismutase (SOD1) and cytochrome C oxidase (CCO). The redox potential of Cu, while essential for co-factor activity can be toxic to cells by causing the formation of excess reactive oxygen species (ROS) which results in cell damage (DNA, lipids, membranes) and eventually cell death (Barceloux and Barceloux, 1999; Nishito and Kambe, 2018). Gupta et al. (1993) identified correlation between serum copper concentration and stage of colorectal cancer. The relationship between copper homeostasis, cancer carcinogenesis and resistance has been extensively studied (Majumder *et al.*, 2009; Denoyer *et al.*, 2015). Currently, robust biomarkers sensitive to early damage from excess Cu are lacking (Gaetke, Chow-Johnson and Chow, 2014).

Factors identified as reducing copper toxicity in eukaryotic cells include metallothionein expression and ATP7B (Schilsky *et al.*, 1998; Adamo *et al.*, 2012). Metallothioneins (MTs) are low molecular weight cysteine-rich proteins (<14 kDa) which exhibit cytoprotective properties by sequestering metal ions (such as cadmium, copper, lead, mercury and zinc), rendering them biologically inactive (Valko, Morris and Cronin, 2005; Ruttkay-Nedecky *et al.*, 2013). ATP7B is an ATPase protein involved in the export of Cu from cells, where the mutated ATP7B was identified as the cause of severe copper overload in the genetic condition Wilson's (Waggoner, Bartnikas and Gitlin, 1999).

To understand Cu homeostasis and toxicity, metal resistant cell line variants have been produced by cloning, continuous selection in high metal concentrations (Freedman, Weiner and Peisachst, 1986; Chimienti et al., 2001) and targeted mutagenicity (Schilsky

et al., 1998). Metallothionein expression was found to confer resistance in rat hepatoma (Freedman et al., 1986) and HeLa cells (Chimienti et al., 2001).

Caco-2 is an epithelial cell line derived from a human colon adenocarcinoma which represents an *in vitro* model of the intestinal route of exposure to ingested micronutrients (Leblondel and Allain, 1999; Sauer *et al.*, 2017). This cell line can spontaneously differentiate into enterocyte-like cells and is often used in toxicity, transport and uptake studies (Fogh and Trempe, 1975; Zerounian *et al.*, 2003). Caco-2 cells have maintained a dominant position as a model for intestinal studies due to the fact they are well-established, versatile and easily maintained (Hidalgo, Raub and Borchardt, 1989; Angelis and Turco, 2011).

As organic forms of copper are becoming important to animal production industries - offering advantages in uptake and copper negative interactions with other metals, the comparison of both forms is of utmost concern (Du *et al.*, 1996; Guo *et al.*, 2001; Ao *et al.*, 2009). In this work, we describe the development of Caco-2 cells resistant to an inorganic and organic form of copper, evaluating mechanisms to protect against ROS-induced toxicity and explore via proteomic analysis further strategies that may protect cells from Cu-induced toxicity.

3.2 Materials and methods

3.2.1 Materials

Irradiated $CuSO_4$ and Cu proteinate (a product resulting from the chelation of soluble Cu with soy hydrolysate, Byrne, 2010) were supplied by Alltech Ireland Ltd. Copper concentrations were validated by ICP-MS.

3.2.2 Cell culture conditions

Exponentially growing Caco-2 cells (HTB-37 ™; American Type Culture Collection) were cultivated at 37 °C under 5% CO_2, in MEM (Gibco, 21090022) supplemented with 10% fetal bovine serum (FBS, Gibco, 10270-106), 10mM HEPES (Sigma Aldrich, H3537) and 2mM L-glutamine (Sigma Aldrich, G7513). Cells were passaged approximately every 4 days, not allowing cells to reach confluence (Natoli *et al.*, 2011). Cells were routinely tested and found to be negative for *Mycoplasma* contamination.

3.2.3 Establishment of Caco-2 cell lines resistant to copper

Caco-2 cells seeded at 3125 cells/cm^2 were continuously exposed to 50 µM $CuSO_4$ or 50 µM Cu proteinate and surviving cells were maintained in this concentration (except to allow 24 hours after subculture before re-exposing). Parental Caco-2 and Cu-resistant cells were maintained for a minimum of 10 subcultures in their respective conditions. Three passages in non-copper supplemented growth media was allowed before testing for out-of-exposure conditions.

3.2.4 Cell survival determination

Cells were seeded at 3125 cells/cm^2 and exposed after 24 hours for up to 120 hours before assaying by (A) acid phosphatase activity in 96-well microtiter plates (adapted from Martin and Clynes, 1993, 1991) and (B) in 6-well tissue culture plates by viable cell count using haemocytometer and trypan blue exclusion method. Acid phosphatase measurements following copper exposure were found to correlate to cell number in the same assay systems (O'Doherty *et al.*, 2019).

3.2.5 Cell imaging and size determination

To calculate cell radius, images of trypsinised Caco-2 cells during exponential growth were captured using an EVOS™ XL Core Cell Imaging System (Thermo Fisher Scientific) and imported into MetaMorph image Software® (Molecular Devices, version 7.7) for integrated morphometry analysis. As Caco-2 cells are irregular in shape when grown adhered to a tissue culture surface, and borders are challenging to discern from the background leading to noise in adherent size analysis, trypsinisation was used to ensure minimum volume per cell and consistent cell size. Other methods such as flow cytometry or image J software were available; however Metamorph software provided more options for setting thresholds and parameters in morphometry analysis and allowed for additional outputs of interest such as elliptical form factor to determine irregularities in cell shape. A minimum of 75 cells in four independent images were used to determine mean radius.

3.2.6 Intracellular copper determination

Cells were washed twice in PBS and lysed in protein 2D lysis buffer (7 M urea, 2 M thiourea, 4% CHAPS and 30 mM tris, pH 8.0). Cell lysates were diluted in trace-analysis grade nitric acid (Sigma, USA), heated at 85–95 ◦C for 1 h and subjected to inductively coupled plasma mass spectrometry (ICP-MS; 7700X, Agilent, USA).

3.2.7 Detection of reactive oxygen species

Caco-2 and Cu-resistant cells were seeded at 3125 cells/cm^2 in 24-well plates and allowed 24 hours before exposure to control media, 50 µM $CuSO_4$ or 50 µM Cu Pro for 72 hours. Cells were washed with HBSS and incubated in 5 µM carboxy-DCFDA (Sigma Aldrich, 21884) at 37°C for 30 minutes. Cells were then washed twice with HBSS and conversion of carboxy-DCFDA into DCF was measured at an excitation of 485 nm and emission of 528 nm on a Biotek plate reader (Synergy HT, version 2.05.5) before measuring viable cell number to determine relative ROS/cell.

3.2.8 Superoxide dismutase activity

Superoxide dismutase (SOD) activity was assayed using SOD activity kit (Sigma-Aldrich, 19160), based on Dojindo's highly water-soluble tetrazolium salt (WST-1). Inhibition curve was generated using bovine erythrocyte SOD (Sigma-Aldrich, S2515). This kit measures the total activity of intracellular SOD by detecting both Cu, Zn SOD activity (comprising approximately 90% of intracellular SOD) and Mn SOD activity (comprising approximately 10% of intracellular SOD)(Weydert and Cullen, 2010).

3.2.9 Glutathione assay

Cells seeded in 25 cm^2 flasks at 1 x 10^6 cells per flask were exposed after 24 hours to basal media, 50 µM $CuSO_4$ or 50 µM Cu Pro for 72 hours and trypsinised. Glutathione level (GSH, GSSG and total) was assessed and normalised to cell counts using a Glutathione Assay Kit (Sigma-Aldrich, CS0260) according to the manufacturer's instructions.

3.2.10 Western blotting

Cell lysates were prepared by solubilising cells in protein 2D lysis buffer, supplemented with nuclease mix (GE Healthcare, 80-6501-42) and protease inhibitor (Thermo Scientific™, A32963). Protein was quantified by modified BioRad assay (BioRad, 5000006). Lysates in Laemmli buffer were separated by SDS-polyacrylamide gel electrophoresis on a 4-12% SDS gel. Transferred blots were blocked in NET buffer (1.5 M NaCl, 0.05 M EDTA, 0.5 M tris pH 7.8, 0.5% Triton X-100) and incubated overnight at 4°C with primary ubiquitin (CST, 3933) CTR1 (Abcam, ad129067), metallothionein (Abcam, ab12228) or GAPDH antibodies (CST, 5174). Secondary antibodies conjugated to horse-radish peroxidase (Sigma Aldrich) were incubated for 1 hour and detected by enhanced chemiluminesence (Luminol, Santa Cruz). Densitometry was performed using Epson Perfection 4990 scanner and TotalLab Quant software version 13.2. Additional Western blots for glutathione peroxidase (GPx) and Microtubule-associated proteins 1A/1B light chain 3 (LC3) are supplied in Appendix Fig. 2.

3.2.11 Proteomic profiling and associated bioinformatics analysis

Exponentially growing parental Caco-2 and Cu-resistant cells (unexposed control, 50 µM $CuSO_4$-resistant and 50 µM Cu proteinate-resistant, out-of-exposure and in-exposure) were harvested by trypsinization. Cell pellets were washed with ice cold PBS, snap frozen and stored at -80 ℃. Cell lysates were solubilised in 2D lysis buffer and mixed for 1 hour at room temperature (RT). Lysates were then centrifuged at 18,800 x g for 15 min at 4 ℃. The supernatants were transferred to a new microcentrifuge tube and protein concentration was determined using the Biorad protein assay. A homogenised lysate of 100 µg protein from each sample was prepared for MS by FASP (Coleman *et al.*, 2017).

Quantitative label-free LC-MS/MS proteomic analysis was performed using a Dionex Ultimate 3000 RSLCnano system coupled to an Orbitrap Fusion Tribrid mass spectrometer (both Thermo Scientific) (Coleman *et al.*, 2019). Peptides were identified in Proteome Discoverer 2.2 and exported to Progenesis QI (NonLinear Dynamics, Waters) for relative quantitative analysis between experimental groups as previously described (Coleman *et al.*, 2018, 2019). A threshold of 5% sequence coverage was set for LC-MS/MS identified proteins, unless the molecular weight of the protein was less than 20 kDa or had greater than 2 unique identified peptide sequences. An additional threshold was set for fold changes > 1.5 with Analysis of Variance (ANOVA) *P* value of < 0.05 and fold changes from 1.2 - 1.5 with *P* value of < 0.01. The proteomic data has been made publicly available online via Mendeley Data, V.2 (O'Doherty, 2019, doi: 10.17632/rm6sjwv2ms.1).

3.2.12 DAVID functional annotation, KEGG pathway and STRING analysis

Upregulated and downregulated DEPs designated as stable, in-exposure only (transient) and out-of-exposure only were collated and uploaded into DAVID v6.8 (https://david.ncifcrf.gov/tools.jsp), which was used to group the biological functions and perform KEGG pathway analysis of the differentially expressed proteins. Similar related terms provided by functional annotation were excluded where these results did not contribute additional information. A *P v*alue of < 0.05 was set as threshold for inclusion of both functional annotation terms and KEGG pathway analysis.

3.2.13 Statistical analysis

To evaluate statistical significance between any two populations, *P*-values were calculated by two-tailed Students' t-test with 2-tailed distribution and two-sample heteroscedastic unequal variance (Microsoft Excel®). Figures 3.3.5 and 3.3.10 were both assessed using one-way ANOVA. Significance was set at *P*-values less than 0.05. Error bars in all figures indicate standard error of the arithmetic mean. Relative values in all figures are expressed as percentage of untreated controls, unless otherwise noted. All experiments were repeated at least three times.

3.3 Results

3.3.1 Cu toxicity in parental and Cu-resistant Caco-2 cells

A recent publication by our group identified 50 μM Cu as sufficient to induce approximately 80% toxicity in parental Caco-2 cells (O'Doherty et al., 2019). In the present study, continuous exposure to 50 μM $CuSO_4$ or Cu Pro was used to generate two copper resistant Caco-2 cell lines ($CuSO_4$-R and Cu Pro-R) in tandem over 30 subcultures. Selective pressure (50 μM $CuSO_4$ or Cu Pro) was maintained for in-exposure (IE) experiments and 3 passages out of Cu supplement for out-of-exposure experiments. Variants generated by exposure to higher Cu concentrations (100 – 200 μM) were not viable over extended subcultures (data not published).

$CuSO_4$-R and Cu Pro-R lines exhibited tolerance (P <0.05) with less impact to Cu exposure than in parental Caco-2 (Fig. 3.3.1). $CuSO_4$-R, Cu Pro-R and parental Caco-2 cells showed a rapid decrease in cell survival with increasing Cu exposure up to 6.25 μM (11% and 45%, respectively), consistent with the Cu-induced non-monotonic dose response recently observed in Caco-2 cells (O'Doherty et al., 2019). $CuSO_4$-R and Cu Pro-R cells demonstrated cross-resistance to either form of Cu tested, with Cu Pro-R exhibiting a slightly reduced toxicity to both forms of copper.

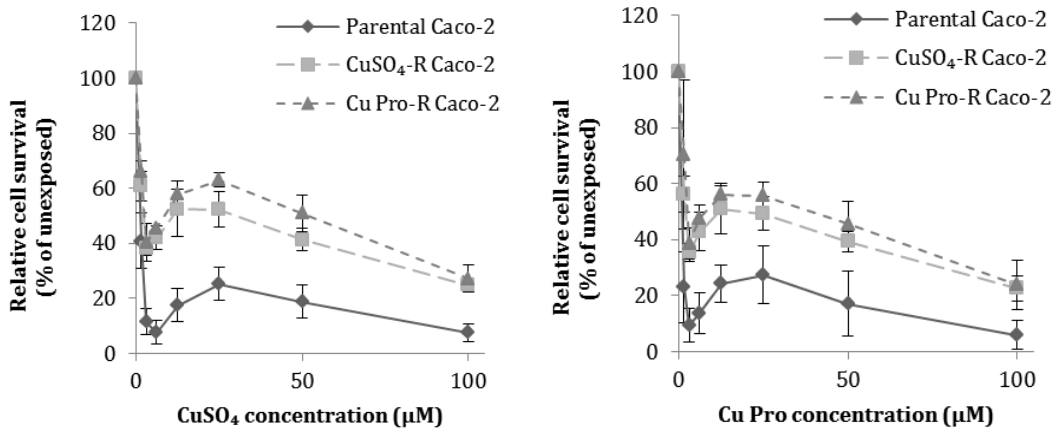

Figure 3.3.1. Relative cell survival of control Caco-2, $CuSO_4$-R and Cu Pro-R cells exposed to increasing $CuSO_4$ or Cu Pro for 96 hours, cultured in 96-well plates, and assayed by acid phosphatase (N>3)

3.3.2 Stability of resistance in the Cu-resistant lines

$CuSO_4$-R and Cu Pro-R Caco-2 cells were subcultured for up to 12 passages out-of-selection pressure to establish whether Cu resistance was stable. Copper tolerance in both copper-resistant variants was comparable to levels observed during selection pressure in $CuSO_4$-R and Cu Pro-R cells versus parental control, indicating that Cu resistance was conserved without selection pressure over extended periods of culture (Fig. 3.3.2).

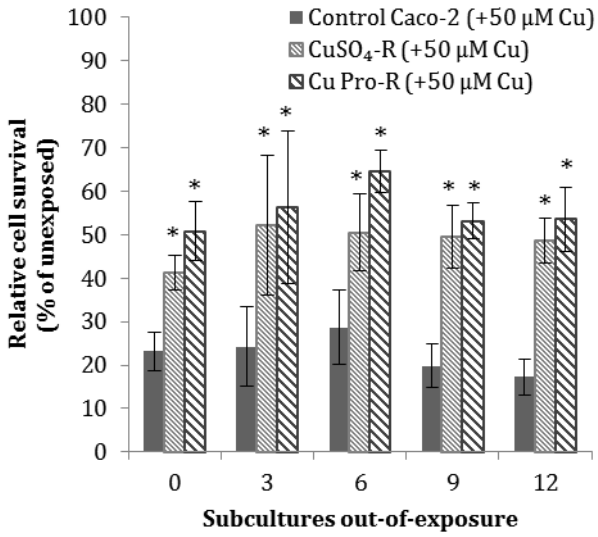

Figure 3.3.2. Stability of Cu-resistance after 0, 3, 6, 9 and 12 passages out-of-exposure. Relative cell survival of control Caco-2 and CuSO4-R and Cu Pro-R Caco-2 cells exposed to 50 µM $CuSO_4$ and 50 µM Cu Pro, cultured in 96-well plates, assayed by acid phosphatase (N=3). Asterisk indicates significant difference from control ($p < 0.05$)

3.3.3 Population growth of parental and Cu-resistant Caco-2 cells

Parental, $CuSO_4$-R and Cu Pro-R Caco-2 cells cultured out-of-exposure for 3 passages were analysed for cell growth and displayed similar total cell yield between 24-72 hours (Fig. 3.3.3), however total cell yield of both $CuSO_4$-R and Cu Pro-R Caco-2 variants was significantly increased versus parental Caco-2 after 96 and 120 hours culture.

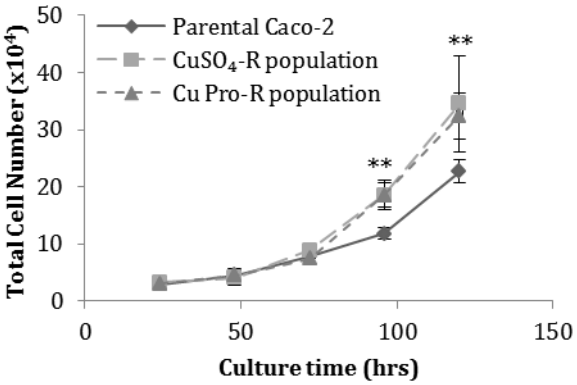

Figure 3.3.3. Total daily viable cell number for unexposed control Caco-2 and Cu-resistant Caco-2 cells seeded at 3 x 10^4 cells per well in 6 well plates (N=3). Asterisk indicates significant difference from control (P <0.05)

3.3.4 Morphological analysis of Cu-resistant Caco-2 cells

Images taken during exponential cell growth for parental Caco-2, $CuSO_4$-R and Cu Pro-R lines revealed comparable global cell morphology (Fig. 3.3.4 A, B and C). Following exposure of parental Caco-2 cells to Cu (50 µM $CuSO_4$ / Cu Pro) cell shrinking was observed however; with rounding and lifting as well as decreased cell yield (Fig. 3.3.4D). In Cu exposed $CuSO_4$-R and Cu Pro-R cells, discrete clusters of smaller colonies were noted with an increased presence of cytoplasmic vesicles. A similar morphology was demonstrated in $CuSO_4$-R and Cu Pro-R Caco-2 cells both out-of-exposure (Fig. 3.3.4B and C) and in the presence of selection pressure (Fig. 3.3.4E and F). Notably, average mean cell radius for parental Caco-2 cells exposed to 50 µM $CuSO_4$ and Cu Pro increased from 11.32 µm to 12.66 µm (P <0.005). No significant change was observed during Cu exposure to $CuSO_4$-R cells ranging from 11.1 µm to

10.65 µm (*P* =0.879), whereas Cu exposure to Cu Pro-R Caco-2 cell radius reduced cell size from 10.11 µm to 9.06 µm (*P* <0.001) (Fig. 3.3.4G).

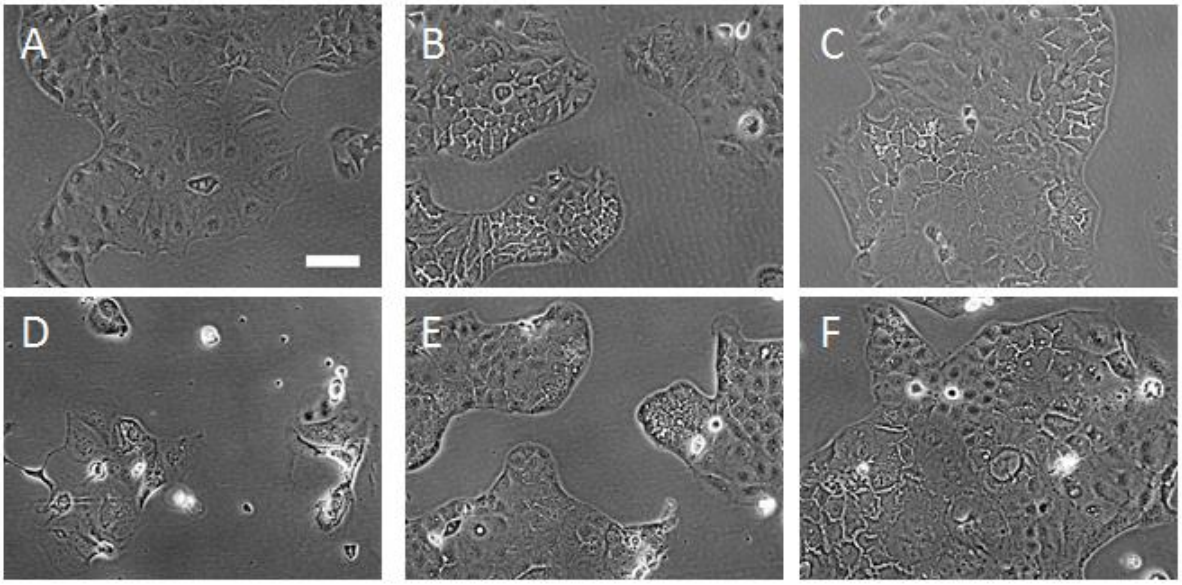

G

	Unexposed			50µM Cu exposed		
	Control Caco-2	**$CuSO_4$-R Caco-2**	**Cu Pro-R Caco-2**	**Control Caco-2**	**$CuSO_4$-R Caco-2**	**Cu Pro-R Caco-2**
Mean Radius (µm)	11.32 ± 0.77	11.1 ± 1.17	10.11 ± 0.73*	12.8 ± 0.67*	10.65 ± 0.15	9.06 ± 0.3*

Figure 3.3.4. Representative phase contrast images of parental Caco-2 unexposed (A) and in 50 µM Cu proteinate (D); $CuSO_4$-R Cells unexposed (B) and in 50 µM $CuSO_4$ (E); Cu Pro-R cells unexposed (C) and in 50 µM Cu proteinate (F). Cells were cultured in the presence of copper compound for 72 hours. Scale bar shown in unexposed control (A) represents 100 µm. (G) Mean radius for parental and Cu-resistant Caco-2 cells, exposed to basal growth media or 50 µM Cu Pro after 72 hours exposure. Asterisk indicates significantly different versus control (P ≤0.05)

3.3.5 Intracellular Cu levels in parental and Cu-resistant Caco-2 cells

Using ICP-MS the intracellular Cu level was assessed in the parental Caco-2, $CuSO_4$-R and Cu Pro-R cells (Fig. 3.3.5). Cu content in unexposed cells was below detectable levels per 1 x 10^6 cells. Interestingly The $CuSO_4$-R and Cu Pro-R cells showed a trend towards reduced Cu accumulation relative to $CuSO_4$-exposed (P <0.05) but not Cu Pro-exposed parental cells.

Studies frequently express Cu accumulation relative to mg protein, however we noted a significant increase in protein yield per cell in parental Caco-2 cells treated with 50 µM $CuSO_4$ and Cu Pro (P <0.05), with no significant change observed during Cu exposure to $CuSO_4$-R and Cu Pro-R Caco-2 cells (Fig. 3.3.6). For this reason, Cu concentration was expressed relative to cell number to assess accumulation in parental Caco-2 and variant cells.

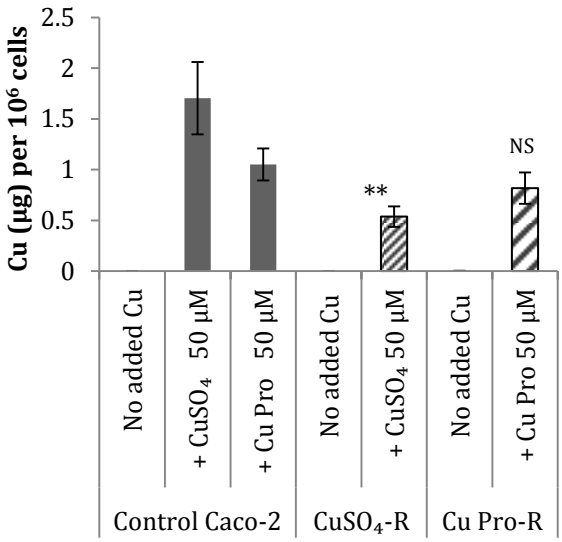

Figure 3.3.5. Copper content per 10^6 cells after 72 hr for control Caco-2, $CuSO_4$-R and Cu Pro-R cells in the presence and absence of added Cu (50 µM $CuSO_4$ or 50 µM Cu Pro) (N>3). Asterisk indicates that there are significant differences (** $P < 0.01$) between the Cu-treated control group and the Cu-treated resistant Caco-2 cell populations. NS = not significant.

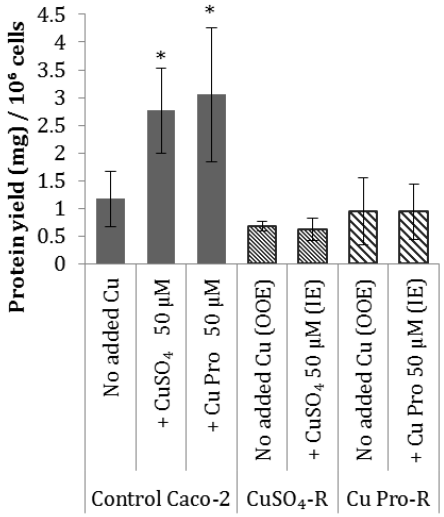

Figure 3.3.6. Yield of protein relative to 10^6 cells after 72 hr for control Caco-2 vs $CuSO_4$-R and Cu Pro-R cells in the presence and absence of added Cu (50 µM $CuSO_4$ or 50 µM Cu Pro) (N=4). Asterisk indicates significant difference from all (P <0.05)

3.3.6 Cu-resistant Caco-2 response to cellular oxidative stress

As cellular oxidative stress can be generated by copper exposure especially at higher concentrations, ROS generation, SOD activity and GSH levels were monitored. The intracellular reactive oxygen species (ROS) generated during exposure to basal media, 50 µM $CuSO_4$ or 50 µM Cu Pro was assessed to determine oxidative stress in $CuSO_4$-R and Cu Pro-R cells (Fig. 3.3.7). In parental control cells treated with 50 µM $CuSO_4$ or 50 µM Cu Pro, an increase in ROS per cell versus unexposed control cells was observed (P <0.05). This increased ROS response was attenuated in the $CuSO_4$-R and Cu Pro-R Caco-2 cells, though not significantly.

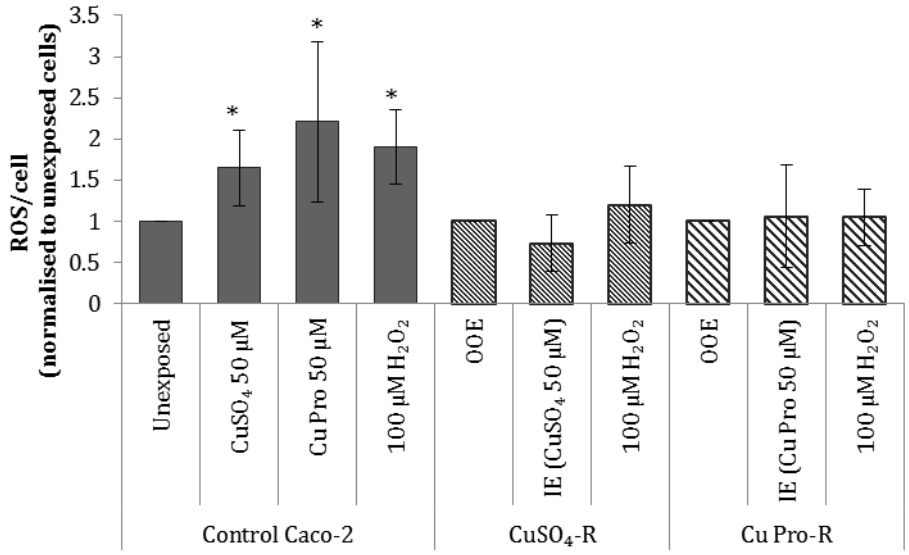

Figure 3.3.7. Relative ROS generated per cell for parental Caco-2 and Cu-resistant variant cells, exposed to basal growth media and 50 µM $CuSO_4$ or 50 µM Cu Pro. H_2O_2 at 100 µM was used as a positive control for inducing cellular ROS. IE: In-exposure, OOE: out-of-exposure. Asterisk indicates significant difference from control (P <0.05) (N>5)

To further investigate the ROS response, the levels of superoxide dismutase (SOD) which functions to convert the superoxide radical to less harmful hydrogen peroxide and molecular oxygen was investigated (Ighodaro and Akinloye, 2018). As with ROS, the increase in SOD activity for parental Caco-2 cells exposed to copper (50 µM $CuSO_4$ and 50 µM Cu Pro) was not reflected in the resistant cell lines (Fig 3.3.8).

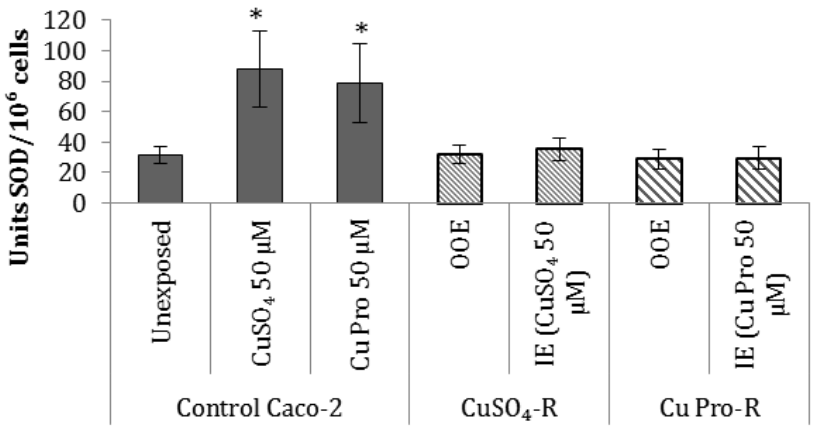

Figure 3.3.8. Equivalent superoxide dismutase units generated per $1x10^6$ cells for parental Caco-2 and Cu-resistant variant cells, exposed to basal growth media "out-of-exposure" (OOE) or "in-exposure" (IE) 50 µM $CuSO_4$ or 50 µM Cu Pro. Asterisk indicates significant difference from control (P <0.05) (N>3)

GSH contributes to cell protection by acting as an antioxidant and free radical scavenger of ROS through oxidation of its sulphur atom to form GS-OH, which in turn may interact with the thiol group of another glutathione thus forming oxidised glutathione disulphide (GSSG) (Benedetto *et al.*, 2014). Glutathione (GSH), glutathione disulphide

(GSSG) and total combined levels were measured in Caco-2 and Cu-resistant cells in- and out-of-exposure to examine the involvement of GSH in Cu toxicity and resistance. In contrast to parental Caco-2 cells, the total glutathione levels in both the $CuSO_4$-R and Cu Pro-R variants appeared to be unchanged upon exposure to 50µM Cu (Fig. 3.3.9 A). The levels of GSSG elevated in the $CuSO_4$-R and Cu Pro-R variants when exposed to 50µM Cu (P <0.05). However, this increase was less than that observed in control parental Caco-2 cells exposed to 50µM Cu (Fig. 3.3.9 B). The levels of GSH were unaltered or decreased in the $CuSO_4$-R and Cu Pro-R variants in comparison to the control parental Caco-2 cells, which showed elevated levels of GSH after Cu exposure (Fig. 3.3.9 C).

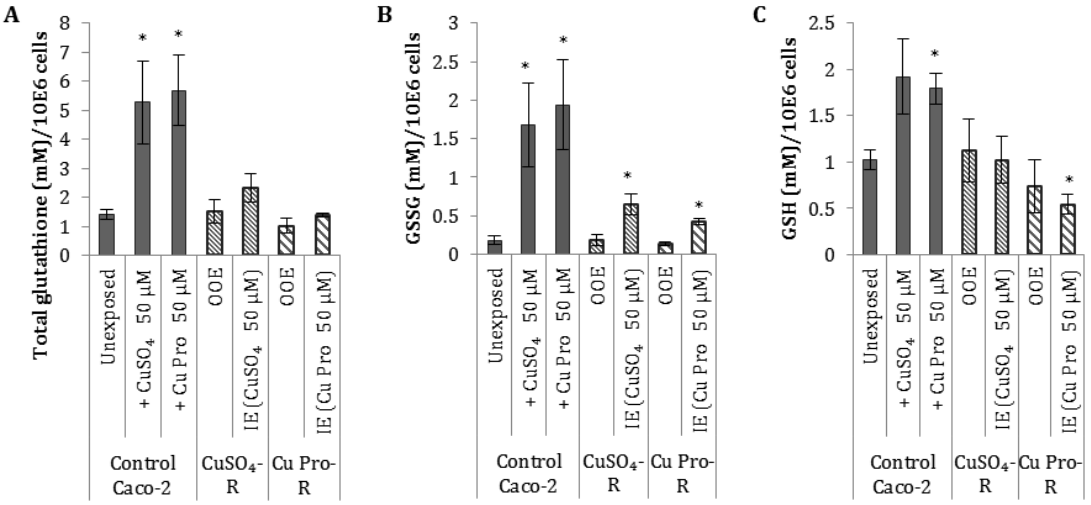

Figure 3.3.9. Glutathione levels measured as (A) total glutathione, (B) GSSG and (C) GSH, normalised per $1x10^6$ cells, for parental Caco-2 and Cu-resistant variant cells exposed to basal growth media only "out-of-exposure" (OOE) or "in-exposure" (IE) 50 µM $CuSO_4$ or 50 µM Cu Pro (N=3). Asterisk indicates significant difference from control (P <0.05)

3.3.7 Western blotting for target proteins in Cu-resistant Caco-2

We looked at protein expression of metallothionein (MT), as it has been reported as a mechanism of resistance as well as changes in expression of the primary Cu transporter in mammalian cells, copper transporter 1 (CTR1). In addition, as the increased resistance to oxidative stress was shown with ROS, GSH and SOD activity, we looked at ubiquitination of proteins which indicate the effect of oxidative stress on cellular protein.

Expression of ubiquitin revealed higher ubiquitination of proteins in Cu exposed parental Caco-2 cells relative to unexposed parental Caco-2 and both copper resistant variants in- and out-of-exposure (Fig. 10A). The mature (35 kDa) and precursor (28kDa) forms of CTR1 were not significantly changed ($P > 0.05$) (Fig. 10B). Expression of metallothionein was highly upregulated in Cu exposed parental cells ($P < 0.05$) and slightly up in Cu Pro-R cells during Cu exposure (Fig. 10C).

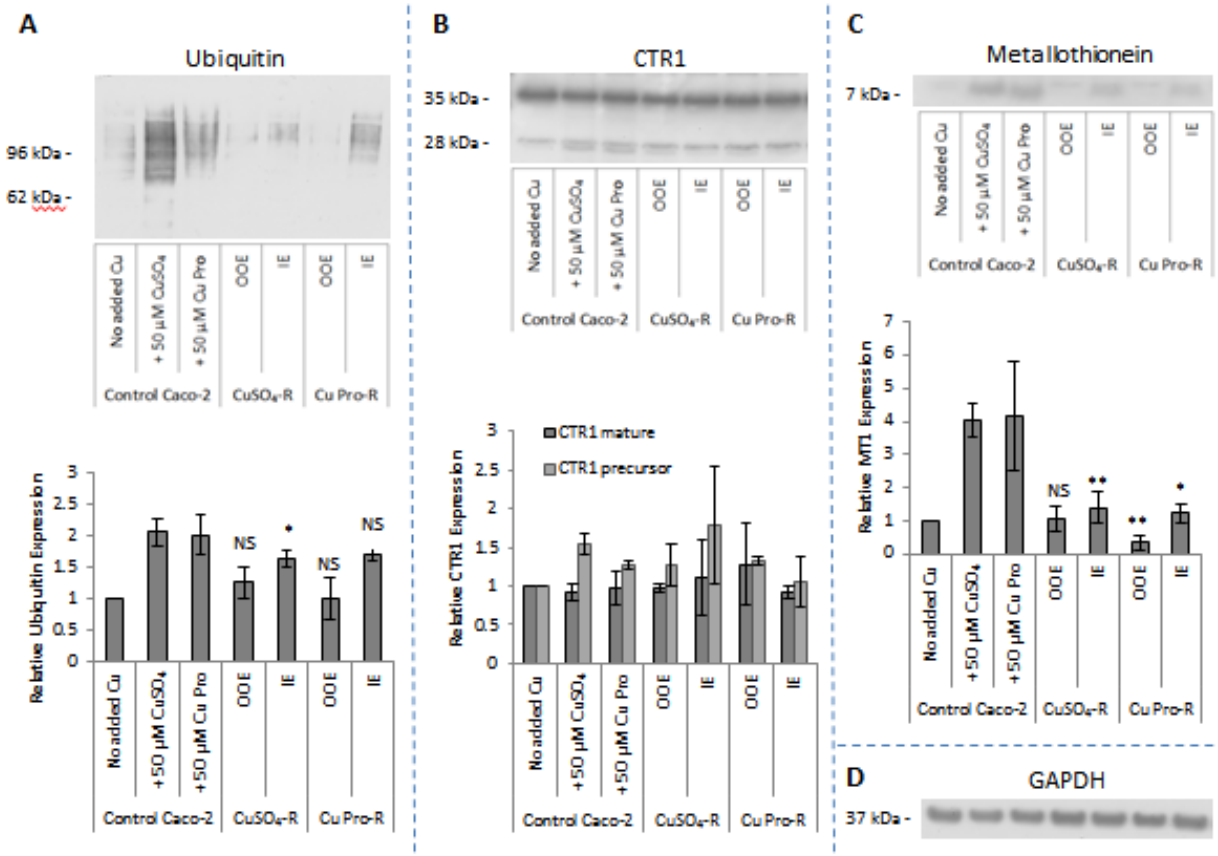

Figure 3.3.10. Representative Western blots for A: Ubiquitinated proteins, B: Copper transporter 1 (CTR1), C: metallothionein (MT1) and D: endogenous control - GAPDH in parental Caco-2, $CuSO_4$-R and Cu Pro-R cells exposed to basal growth media "out-of-exposure" (OOE) and during exposure to 50 µM $CuSO_4$ or 50 µM Cu Pro "in-exposure" (IE) for 96 hours. Densitometry expressed relative to unexposed control and normalised to GAPDH (N=3). Asterisk indicates that there are significant differences (* $P < 0.05$ or ** $P < 0.01$) between the Cu-treated resistant cells and the Cu-treated control group at the same concentration. NS = not significant.

3.3.8 Identification of differentially expressed proteins between parental and Cu-resistant Caco-2 cells

To gain further insight into the factors involved in the resistance of $CuSO_4$-R and Cu Pro-R Caco-2 cells, differentially expressed proteins (DEPs) were examined between parental Caco-2 cells, $CuSO_4$-R and Cu Pro-R cells out-of-exposure and variant cells in selection pressure by quantitative label-free LC-MS/MS. Subsequent bioinformatic analysis was performed on four generated DEP lists; 'out-of-exposure' (OOE) expression changes in $CuSO_4$-R / Cu Pro-R cells versus unexposed parental Caco-2 (google drive file tables S1/S3) and transiently changed $CuSO_4$-R / Cu Pro-R cells 'in-exposure' (IE) relative to the 'out-of-exposure' condition (google drive file tables S2/S4) (Fig. 3.3.11).

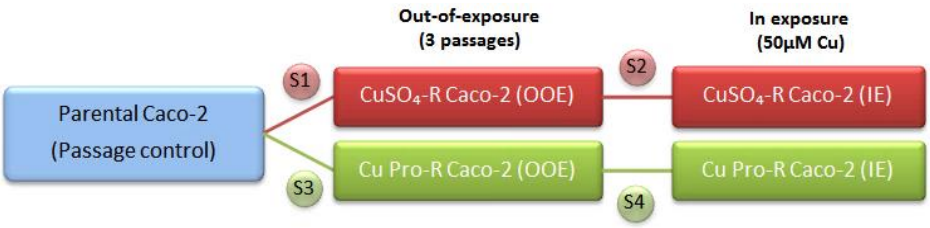

Figure 3.3.11. Schematic for quantitative label-free LC-MS/MS proteomic analysis with corresponding DEP Tables S1-4 (available via google drive file)

Common stable DEPs in both CuSO4-R and Cu Pro-R cells

A Venn diagram between all identified proteins from the DEP lists (S1- S4) was generated (Fig. 3.3.12). A total of 88 proteins were identified as being differentially expressed in common between both $CuSO_4$-R and Cu Pro-R out-of-exposure versus parental Caco-2 cells, with all but 1 protein, voltage-dependent anion-selective channel protein 2 (VDAC2), in the same direction (78 upregulated, 9 downregulated). VDAC2

was downregulated in $CuSO_4$-R Caco-2 versus control and upregulated in Cu Pro-R Caco-2 versus control.

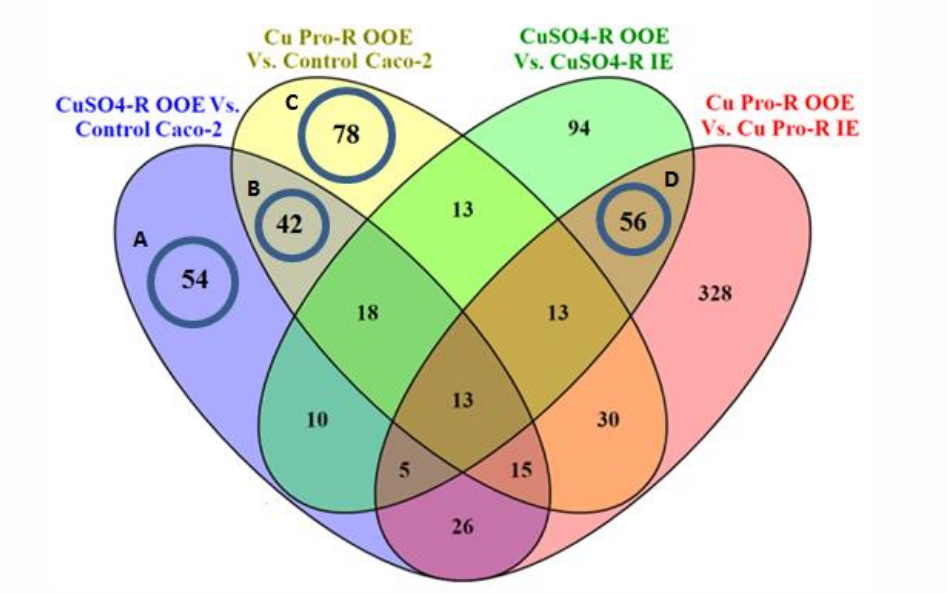

Figure 3.3.12. Venn diagram summary showing overlap of all proteins identified in the differentially expressed protein lists. Circled overlapping areas of interest: A: stable proteins unique to $CuSO_4$-R Caco-2; B: stable proteins common to both copper resistant lines; C: stable proteins unique to Cu Pro-R Caco-2; D: common proteins induced only during Cu exposure and common to both resistant cell lines. Generated using Venny version 2.1, available at http://bioinfogp.cnb.csic.es/tools/venny/index.html

In the group of commonly expressed proteins (Fig. 3.3.12 B) 42 (37 upregulated, 5 downregulated) were unchanged on copper supplementation, suggesting 'stable' expression independent of exposure to Cu compound. Only one stable downregulated protein > 2-fold was observed; CLDN3 (tight junction associated claudin-3) was downregulated (3.32- and 5.19-fold, respectively) in both $CuSO_4$-R and Cu Pro-R cells,

while 16 stably upregulated proteins > 2-fold were found including multiple DEPs with functions associated with mitochondria (mitochondrial ribosomal proteins and ATP5F1B) and protective functions; DNA damage / cell cycle (CHEK1); RNA regulation (NUFIP2 and RBM14) as well as ER homeostasis (UFM1, SIGMAR1) (Table 3.3.1).

	Downregulated		$CuSO_4$-R		Cu Pro-R	
Protein Name	Description	Sequence coverage (%)	Fold change	*P* value	Fold change	*P* value
CLDN3	Claudin-3	7	3.32	0.018	5.19	0.006

	Upregulated		$CuSO_4$-R		Cu Pro-R	
Protein Name	Description	Sequence coverage (%)	Fold change	*P* value	Fold change	*P* value
MRPS22	28S ribosomal protein S22, mitochondrial	6	4.82	0.028	2.85	0.030
CHEK1	Serine/threonine-protein kinase Chk1	7	3.83	0.011	3.86	0.037
PITX1	Pituitary homeobox 1	10	3.69	0.033	3.59	0.004
NAXD	ATP-dependent (S)-NAD(P)H-hydrate dehydratase	7	3.22	0.011	4.11	0.002
PNPO	Pyridoxine-5'-phosphate oxidase	8	3.11	0.024	3.12	0.012
NUFIP2	Nuclear fragile X mental retardation-interacting protein 2	5	2.73	0.012	2.97	0.006
MRPS18C	28S ribosomal protein S18c, mitochondrial	13	2.69	0.013	2.37	0.048
RBM14	RNA-binding protein 14	6	2.32	0.024	2.44	0.001
ATP5F1B	ATP synthase subunit beta, mitochondrial	≥5	2.29	0.027	2.23	0.011
MRPS28	28S ribosomal protein S28, mitochondrial	13	2.23	0.024	1.98	0.009
UXS1	UDP-glucuronic acid decarboxylase 1	6	2.20	0.027	1.75	0.007
NIPSNAP3A	Protein NipSnap homolog 3A	9	2.19	0.024	1.86	0.008
SIGMAR1	Sigma non-opioid intracellular receptor 1	23	2.17	0.020	2.36	0.003
MRPL28	39S ribosomal protein L28, mitochondrial	7	2.06	0.007	2.18	0.010
TKFC	Triokinase/FMN cyclase	≥7	1.86	0.026	2.12	0.010
UFM1	Ubiquitin-fold modifier 1	41	1.71	0.024	2.58	0.028

Table 3.3.1. Overlap of DEPs in Cu-resistant Caco-2 cells identified as stably changed OOE relative to unexposed parental Caco-2 by quantitative label-free LC-MS/MS. Only DEPs where > 2-fold in at least one condition are shown, < 2-fold are presented in supplementary table S5 (available via google drive file)

KEGG pathway analysis of the 42 common stable up- or down-regulated proteins in Cu-resistant Caco-2 cells identified four over-represented pathways including amino sugar and nucleotide sugar metabolism due to the common upregulation of GALT, GMDS and UXS1 (Table 3.3.2) and ribosome due to common upregulated expression of MRPL28, MRPS18C, RPS15 and RPS5. Functional annotation analysis of stable

common DEPs using DAVID (version 6.8) indicated clustering of UniProt keywords including ribosomal protein and mitochondrion (Fig. 3.6.S1).

#term ID	Term description[a]	Observed/background gene count[b]	FDR[c]	Matching proteins in network
Stable DEPs (42 total)				
hsa03010	Ribosome	4/130	0.0081	MRPL28, MRPS18C, RPS15, RPS5
hsa00520	Amino sugar and nucleotide sugar metabolism	3/48	0.0081	GALT, GMDS, UXS1
hsa01100	Metabolic pathways	9/1250	0.0179	ALDH1B1, ATP5B, TKFC, GALT, GMDS, NME1, PAFAH1B3, PNPO, UXS1
hsa00051	Fructose and mannose metabolism	2/33	0.0293	TKFC, GMDS
Transient DEPs (IE vs OOE, 56 total)				
hsa03040	Spliceosome	7/130	3.26E-06	BCAS2,DDX42,PRPF40A,SF3B5,SF3B6,SNRPC ,ZMAT2
hsa04144	Endocytosis	5/242	0.0093	MVB12A,SH3GL1,SNF8,SNX3,VPS28
Unique CuSO4-R stable DEPs (OOE vs control, 54 total)				
hsa04110	Cell cycle	5/123	0.0029	BUB3,MAD2L1,MCM2,MCM4,YWHAQ
hsa03030	DNA replication	3/36	0.0092	FEN1,MCM2,MCM4
hsa03010	Ribosome	4/130	0.0183	MRPL10,RPL3,RPS17,RPS24
Unique Cu Pro-R stable DEPs (OOE vs control, 78 total)				
hsa03010	Ribosome	5/130	0.0197	MRPL21,MRPL4,MRPS9,RPS19,RPS7
hsa03050	Proteasome	3/43	0.0396	PSMC3,PSMC5,PSMC6
hsa05014	Amyotrophic lateral sclerosis (ALS)	3/50	0.04	BID,CYCS,PPP3R1

[a] Enriched terms corresponding to the protein list entered

[b] Number of proteins from the list uploaded that are involved with the term and total number of proteins associated with the term

[c] FDR = False Discovery Rate

Table 3.3.2. Over-represented Kyoto Encyclopaedia of Genes and Genomes (KEGG) pathways associated with stable, transient, $CuSO_4$-R specific and Cu Pro-R specific DEPs

Common copper-exposure induced changes in Cu-resistant Caco-2 cells

Fifty-six (52 upregulated, 4 downregulated) differentially expressed proteins were detected in both $CuSO_4$-R and Cu Pro-R cells during copper exposure (Fig. 3.3.12 D) which were undetected OOE versus control (Table 3.3.3), signifying expression changes in Cu-resistant Caco-2 cells during re-exposure to copper only. Multiple proteins

reported to localise to the mitochondrial intermembrane space were downregulated including GFER, which functions to regenerate the redox-active disulfide bonds in CHCHD4, which was also downregulated. Transient common DEPs revealed two KEGG pathways during exposure: spliceosome (BCAS2, DDX42, PRPF40A, SF3B5, SF3B6, SNRPC, and ZMAT2) and endocytosis (MVB12A, SH3GL1, SNF8, SNX3 and VPS28) (Table 2). UniProt keyword annotations associated with exposure induced $CuSO_4$-R and Cu Pro-R cells included endosome, mRNA splicing and protein biosynthesis (Fig. S3).

Upregulated IE relative to OOE			$CuSO_4$-R		Cu Pro-R	
Gene Name	Description	Sequence coverage (%)	Fold change	*P* value	Fold change	*P* value
DYNC1H1	Cytoplasmic dynein 1 heavy chain 1	2	1.90	0.017	2.42	0.025
HACD3	Very-long-chain (3R)-3-hydroxyacyl-CoA dehydratase 3	6	2.10	0.008	2.34	0.032
UGDH	UDP-glucose 6-dehydrogenase	9	2.23	0.026	1.94	0.031

Downregulated IE relative to OOE			$CuSO_4$-R		Cu Pro-R	
Gene Name	Description	Sequence coverage (%)	Fold change	*P* value	Fold change	*P* value
CHCHD4	Mitochondrial intermembrane space import and assembly protein 40	10	3.68	0.048	4.57	0.004
VPS28	Vacuolar protein sorting-associated protein 28 homolog	6	3.58	0.031	4.03	0.008
C11orf68	UPF0696 protein C11orf68	5	3.33	0.010	3.36	0.018
SRI	Sorcin	10	2.33	0.035	2.71	0.039
DENR	Density-regulated protein	11	1.63	0.009	2.56	0.011
ZMAT2	Zinc finger matrin-type protein 2	10	2.39	0.035	2.55	0.039
PIH1D1	PIH1 domain-containing protein 1	≥8	2.63	0.024	2.49	0.014
EIF1B	Eukaryotic translation initiation factor 1b	21	1.64	0.020	2.37	0.014
SNRPC	U1 small nuclear ribonucleoprotein C	11	1.91	0.016	2.36	0.014
CHCHD3	MIC complex subunit MIC19	≥6	2.05	0.039	2.35	0.009
GFER	FAD-linked sulfhydryl oxidase ALR	6	3.00	0.041	2.30	0.041
TXNDC5	Thioredoxin domain-containing protein 5	7	1.84	0.016	2.27	0.002
FKBP4	Peptidyl-prolyl cis-trans isomerase FKBP4	≥5	1.42	0.008	2.12	0.007
TIMM8B	Mitochondrial import inner membrane translocase subunit Tim8 B	13	2.47	0.000	2.11	0.024
NECAP2	Adaptin ear-binding coat-associated protein 2	8	1.58	0.049	2.02	0.008
ARHGDIB	Rho GDP-dissociation inhibitor 2	13	2.20	0.009	1.93	0.031
SNF8	Vacuolar-sorting protein SNF8	7	2.08	0.023	1.87	0.033
PSMD10	26S proteasome non-ATPase regulatory subunit 10	8	2.87	0.036	1.79	0.003
NAP1L4	Nucleosome assembly protein 1-like 4	≥7	3.34	0.025	1.68	0.000

Table 3.3.3. Common transient DEPs identified by quantitative label-free LC-MS/MS in Cu-resistant Caco-2 cells identified as changed during Cu exposure only. Only DEPs

where > 2-fold in at least one condition are shown, < 2-fold are presented in supplementary Table S6 (available via google drive file)

Stable DEPs unique to $CuSO_4$-R Caco-2 cells

Fifty-four (45 upregulated, 9 downregulated) proteins specific to $CuSO_4$-R Caco-2 cells (Fig. 3.3.12 A) were differentially expressed (Table 3.3.4), including upregulated PSMB3, a subunit of the 20S core proteasome complex which is essential for proteolytic degradation of intracellular proteins. KEGG analysis of stable $CuSO_4$-R DEPs indicated cell cycle and DNA replication were pathways uniquely over-represented by $CuSO_4$-R cells (Table 3.3.2). In both $CuSO_4$-R and Cu Pro-R cells the ribosome was an over-represented KEGG pathway due to upregulation of several ribosomal and mitochondrial ribosomal proteins. UniProt keywords highlighted nucleotide binding and ATP-binding as specific annotations for $CuSO_4$-R cells (Fig. 3.6.3A).

Downregulated IE relative to OOE			$CuSO_4$-R	
Gene Name	Description	Sequence coverage (%)	Fold change	*P* value
SCAMP1	Secretory carrier-associated membrane protein 1	7	Infinity	0.002
HSP90AA1	Heat shock protein HSP 90-alpha	5	3.22	0.021

Upregulated IE relative to OOE			$CuSO_4$-R	
Gene Name	Description	Sequence coverage (%)	Fold change	*P* value
PSMB3	Proteasome subunit beta type-3	9	3.90	0.030
PRKAB1	5'-AMP-activated protein kinase subunit beta-1	11	3.54	0.029
IRF2BP1	Interferon regulatory factor 2-binding protein 1	6	3.21	0.015
PGD	6-phosphogluconate dehydrogenase, decarboxylating	5	2.65	0.036
NPM1	Nucleophosmin	7	2.46	0.046
BANF1	Barrier-to-autointegration factor	13	2.46	0.025
SRSF10	Serine/arginine-rich splicing factor 10	6	2.43	0.049
OSTF1	Osteoclast-stimulating factor 1	6	2.39	0.009
UHRF1	E3 ubiquitin-protein ligase UHRF1	4	2.34	0.008
EEF1A2	Elongation factor 1-alpha 2	6	2.34	0.036
NME2	Nucleoside diphosphate kinase B	13	2.29	0.020
ECHDC1	Ethylmalonyl-CoA decarboxylase	7	2.28	0.046
MAD2L1	Mitotic spindle assembly checkpoint protein MAD2A	8	2.26	0.038
RPS24	40S ribosomal protein S24	9	2.07	0.043
SARS2	Serine--tRNA ligase, mitochondrial	6	2.01	0.025

Table 3.3.4. DEPs identified by label-free LC-MS as stably up- or down-regulated in $CuSO_4$-R Caco-2 cells. Only DEPs where > 2-fold are shown, < 2-fold are presented in supplementary Table S7 (available via google drive file)

Stable DEPs unique to Cu Pro-R Caco-2 cells

Seventy-eight (66 upregulated, 12 downregulated) proteins specific to Cu Pro-R Caco-2 cells (Fig. 3.3.12 C) were differentially expressed (Table 3.3.5). Multiple mitochondrial ribosomal proteins were noted as significantly upregulated including MRPS9, MRPS18B, MRPL4 and MRPL21. Specific DEPs for Cu Pro-R Caco-2 variants revealed proteasome and amyotrophic lateral sclerosis (ALS) as pathways uniquely over-represented during KEGG analysis (Table 3.3.2). UniProt analysis highlighted proteasome and methylation as annotations related to Cu Pro-R cells (Fig. 3.6.3B). Analysis of UniProt keywords for both $CuSO_4$-R and Cu Pro-R stable DEPs revealed four common annotations; mitochondrion, ribonucleoprotein, ribosomal protein and transit peptide (Fig. 3.6.3).

Downregulated IE relative to OOE			Cu Pro-R	
Gene Name	Description	Sequence coverage (%)	Fold change	*P* value
ITM2C	Integral membrane protein 2C	7	3.94	0.037
TMCO1	Calcium load-activated calcium channel	8	3.10	0.041
H1F0	Histone H1.0	7	3.03	0.038

Upregulated IE relative to OOE			Cu Pro-R	
Gene Name	Description	Sequence coverage (%)	Fold change	*P* value
MRPS9	28S ribosomal protein S9, mitochondrial	5	Infinity	0.002
GDA	Guanine deaminase	6	6.13	0.001
RPS19	40S ribosomal protein S19	10	4.46	0.012
MACROD1	O-acetyl-ADP-ribose deacetylase MACROD1	8	3.48	0.020
POLR2E	DNA-directed RNA polymerases I, II, and III subunit RPABC1	13	3.43	0.030
NPM3	Nucleoplasmin-3	12	3.31	0.030
MRPS18B	28S ribosomal protein S18b, mitochondrial	13	3.16	0.031
TXNL1	Thioredoxin-like protein 1	7	3.09	0.036
NDUFA6	NADH dehydrogenase [ubiquinone] 1 alpha subcomplex subunit 6	13	3.01	0.043
TDP2	Tyrosyl-DNA phosphodiesterase 2	5	2.88	0.032
VPS37B	Vacuolar protein sorting-associated protein 37B	7	2.85	0.031
SAMD4B	Protein Smaug homolog 2	4	2.73	0.017
PRMT3	Protein arginine N-methyltransferase 3	10	2.71	0.048
HSPBP1	Hsp70-binding protein 1	5	2.61	0.031
BID	BH3-interacting domain death agonist	14	2.53	0.031
EIF3F	Eukaryotic translation initiation factor 3 subunit F	8	2.44	0.033
IGBP1	Immunoglobulin-binding protein 1	6	2.43	0.010
MRPL4	39S ribosomal protein L4, mitochondrial	5	2.39	0.003
STARD7	StAR-related lipid transfer protein 7, mitochondrial	6	2.24	0.024
HNRNPA2 B1	Heterogeneous nuclear ribonucleoproteins A2/B1	12	2.10	0.028
GLUD1	Glutamate dehydrogenase 1, mitochondrial	7	2.10	0.031
SERPINB1	Leukocyte elastase inhibitor	6	2.08	0.029
H2AFX	Histone H2AX	16	2.07	0.026
NUDT15	Nucleotide triphosphate diphosphatase NUDT15	16	2.04	0.029
MRPL21	39S ribosomal protein L21, mitochondrial	19	2.01	0.013

Table 3.3.5. DEPs identified by quantitative label-free LC-MS/MS as stably up- or down-regulated in Cu Pro-R Caco-2 cells. Only DEPs where > 2-fold are shown, < 2-fold are presented in supplementary Table S8 (available via google drive file)

Further investigation identified additional differentially expressed targets of interest (Table 3.3.6) which did not separate into the categories generated by Venn, including DEPs associated with; mitochondria, oxidative stress, unfolded protein response, metallothioneins and endosome.

		CuSO4-R		Cu Pro-R	
Protein name	Description	Fold Change OOE relative to control	Fold Change IE relative to OOE	Fold Change OOE relative to control	Fold Change IE relative to OOE
Mitochondrial					
NDUFV1	NADH dehydrogenase [ubiquinone] flavoprotein 1, mitochondrial	4.72 ↑			1.64 ↓
Oxidative stress					
COMMD1	COMM domain-containing protein 1	2.08 ↑	2.08 ↓	2.49 ↑	
GCLM	Glutamate--cysteine ligase regulatory subunit	1.94 ↓		2.02 ↓	2.07 ↑
GLRX	Glutaredoxin-1	2.09 ↑	1.83 ↓	1.77 ↑	1.88 ↓
GLRX3	Glutaredoxin-3				1.34 ↓
GLRX5	Glutaredoxin-related protein 5, mitochondrial				1.89 ↓
GPX1	Glutathione peroxidase 1				33.12 ↓
GPX4	Phospholipid hydroperoxide glutathione peroxidase				2.73 ↓
GSR	Glutathione reductase, mitochondrial				1.6 ↑
GSTP1	Glutathione S-transferase P			1.54 ↓	4.24 ↑
TXN	Thioredoxin				1.55 ↓
TXNDC12	Thioredoxin domain-containing protein 12				1.31 ↓
TXNDC17	Thioredoxin domain-containing protein 17				1.98 ↓
TXNL1	Thioredoxin-like protein 1			3.09 ↑	
Unfolded protein response					
DNAJA1	DnaJ homolog subfamily A member 1	1.61 ↑	1.64 ↓	1.57 ↑	
DNAJA2	DnaJ homolog subfamily A member 2		1.52 ↓		
DNAJA3	DnaJ homolog subfamily A member 3, mitochondrial			2.44 ↑	1.57 ↓
DNAJB1	DnaJ homolog subfamily B member 1				1.29 ↓
DNAJB11	DnaJ homolog subfamily B member 11		1.45 ↓		
DNAJC2	DnaJ homolog subfamily C member 2			2.72 ↑	5.8 ↓
DNAJC7	DnaJ homolog subfamily C member 7				1.86 ↓
DNAJC9	DnaJ homolog subfamily C member 9				2 ↓
HSP90B1	Endoplasmin		1.54 ↓		
HSPA1B	Heat shock 70 kDa protein 1B				1.67 ↑
HSPA4L	Heat shock 70 kDa protein 4L			4.13 ↑	
HSPA5	Endoplasmic reticulum chaperone BiP		1.33 ↓		
HSPBP1	Hsp70-binding protein 1			2.61 ↑	
HSPD1	60 kDa heat shock protein, mitochondrial	1.52 ↑	1.7 ↓	1.36 ↑	1.52 ↓
HSPH1	Heat shock protein 105 kDa				1.58 ↑
TRAP1	Heat shock protein 75 kDa, mitochondrial	1.44 ↑			
Metallothioneins					
MT1F	Metallothionein-1F	9.14 ↓		15.38 ↓	18.82 ↑
MT1G	Metallothionein-1G	8.22 ↓	7.81 ↑	10.35 ↓	13.33 ↑
Endosome					
MVB12A	Multivesicular body subunit 12A		1.92 ↓		1.81 ↓
VPS37A	Vacuolar protein sorting-associated protein 37A				8.65 ↓

Table 3.3.6. Summary of fold-changes for differentially expressed proteins of interest in Cu-resistant Caco-2 cells identified by quantitative label-free LC-MS/MS. Direction of expression for out-of-exposure (OOE) and (in-exposure) cells indicated by arrows

3.4 Discussion

In this study, analysis of copper-resistant Caco-2 cells was used to gain insights into how intestinal cells may survive the toxic effects of high copper (Cu) through development of resistance mechanisms. Inorganic copper sulfate and organic copper proteinate, an animal feed supplement to boost performance and health (Alltech Ireland Ltd.), were used to establish the resistant populations to examine differences between their effects on the cells.

Compared to parental Caco-2 cells, both $CuSO_4$-resistant and Cu Pro-resistant cells displayed differences in growth, morphology and intracellular Cu. Changes in doubling time (both increased and decreased) were a feature of Cu-resistant hepatoblastoma (HUH7) cells cultured in 50 µM Cu-supplemented media (Schilsky et al., 1998). In our resistant cell lines however, no change in growth was observed compared to the control al lower time points, but at later time points (96 and 120 hr) there were higher cell yields. This could possibly be due to a smaller cell size of the resistant variants not becoming contact inhibited unlike the parent. While Cu Pro-R cells were consistently less sensitive than $CuSO_4$-R cells, both forms of Cu displayed similar changes in oxidative stress response (ROS and SOD) and sequestration (MT and GSH). Proteomic analysis revealed proteins associated with reduced oxidative stress and the involvement of other pathways including DNA repair, unfolded protein response, mitochondria and endocytosis.

In order to understand any mechanism of resistance, the first step relates to levels of accumulation; sometimes there are decreases in importers (Bertino *et al.*, 1996), in other instances there are increases in exporters (Heenan *et al.*, 1997; Joyce *et al.*, 2015), both of which lead to a lower accumulation in the resistant cells. In this study both parent and

resistant variants out of Cu had negligible Cu levels, while measurement of intracellular Cu levels during exposure to 50 µM $CuSO_4$ showed higher accumulation in parental Caco-2 than resistant variants. These results suggest that resistance to Cu in $CuSO_4$-R cells was assisted by either decreased Cu uptake, increased Cu export or a combination of both (Fig. 3.3.5). In intestinal-like cells such as Caco-2, copper transporter 1 (CTR1) is the major membrane bound Cu transporter (Klomp *et al.*, 2002). No significant change in protein expression during Western blotting of mature or precursor CTR1 was found in Cu-resistant cells during exposure (Fig 3.3.10B). However, it is possible that CTR1 may be endocytosed, thereby reducing uptake without affecting total cellular CTR1 levels, as seen in HEK293 cells (Molloy and Kaplan, 2009). Additionally, while the involvement of endocytosis in uptake of organic metal complexes such as Cu Pro remains to be fully elucidated (Puckett, Ernst and Barton, 2010), organic cation transporters (OCT1/2/3) and peptide transporters (PEPTs) were not detected as differentially expressed by our proteomic analysis. ATP7B is the main exporter of Cu in hepatic cells and Schilsky *et al.* (1998) reported increased ATP7B expression in Cu resistant HuH7 cells to facilitate extracellular Cu export; however, ATP7B did not appear in our proteomic differential list.

To gain further understanding of the resistance to Cu toxicity, global proteome analysis was employed using quantitative label-free LC-MS/MS. Mechanisms previously reported to be associated with metal resistance were found including sequestration with metallothioneins (Freedman, Ciriolo and Peisach, 1989), the unfolded protein response (Rousselet et al., 2008) and antioxidant response (Hayes and McLellan, 1999). In addition, our analysis suggests other processes to be implicated in Cu resistance included DNA repair, mitochondrial changes and endocytosis.

Expression of Cu-sequestering proteins

Enterocytes produce cysteine-rich metallothionein (MT) in response to elevated Cu levels as a backup detoxification during elevated Cu exposure or during dysfunction of normal Cu efflux (Erdman Jr. *et al.*, 2014). Freedman and Peisach, (1989) and Chimienti et al. (2001) identified metallothioneins (MTs) as playing a critical role in the observed metal resistance in rat hepatoma (H4AzC2) and HeLa cells, respectively, due to their high affinity for divalent metal ions. Western blots identified a significant induction of metallothionein expression during Cu-exposure parental Caco-2 (Fig. 3.3.10C). However, MT induction was not increased to the same extent in Cu exposed resistant variants. These results suggest that although MTs may contribute to tolerance of Cu toxicity, other factors must also be involved.

Unfolded protein response in Cu-resistant Caco-2 cells

Disturbance in endoplasmic reticulum (ER) homeostasis can cause activation of the unfolded protein response (UPR); thus increased protein accumulation in parental Caco-2 cells exposed to Cu suggests increased stress in the ER (Zhang *et al.*, 2012). This accumulation was not observed in Cu-resistant cells (Fig. 3.3.6) and would suggest either an increased capacity for Cu-resistant cells to handle misfolded proteins or increased efficiency of vesicle trafficking associated with alleviation of ER stress or both. We noted upregulated expression for both mitochondrial and cytosolic heat shock proteins (HSPs), alongside proteins associated with 26S proteasome and ufmylation in Cu-resistant Caco-2 cells during proteomic analysis. Moreover, Cu exposed parental Caco-2 cells demonstrated an increase in ubiquitination of proteins during Western blot analysis, while a reduced response was seen in Cu-resistant variants during Cu exposure (Fig. 3.3.10A). Expression of microtubule-associated proteins 1A/1B light chain 3B (LC3) was analysed by Western blot as autophagy increases conversion of LC3-I to LC3-II indicating indicate autophagosome formation (Wang *et al.*, 2017). Increased

expression of the upper LC3-I band in Cu-exposed parental but not resistant populations suggesting autophagy was not induced in the resistant populations relative to parental (Appendix Fig. 2).

In both Cu-resistant Caco-2 variants, mitochondrial HSPD1, a chaperonin required for correct folding of stress-denatured mitochondrial proteins (Levy-Rimler *et al.*, 2001), was upregulated out-of-exposure versus control. Furthermore, 26S proteasome non-ATPase regulatory subunit 14 (PSMD14) was stably upregulated in both Cu-resistant lines (>1.6- fold) while increased expression of multiple regulatory subunits was observed in the individual $CuSO_4$-R and Cu Pro-R cells. $CuSO_4$-R specific DEPs included upregulated ER chaperone BiP (HSPA5), mitochondrial heat shock protein 75 kDa (TRAP1), and endoplasmin (HSP90B1). For Cu Pro-R cells, Hsp70-binding protein 1 (HSPBP1), a nucleotide exchange factor for Hsp70-mediated protein folding *in vivo* (Shomura *et al.*, 2005), was stably upregulated (2.61-fold); heat shock 70 kDa protein 4L (HSPA4L), inhibitor of citrate synthase aggregation, was upregulated out-of-exposure relative to control (4.13-fold); and HSP 70 kDa protein (HSPA1B), conferring resistance to stress-induced apoptosis (Radons, 2016) alongside heat shock protein 105 kDa (HSPH1), nucleotide-exchange factor for HSPA1B, were upregulated during selection pressure (1.67- and 1.58-fold, respectively).

DNAK/J proteins protect cells from protein misfolding before damage occurs (Santra, Dill and de Graff, 2018). Multiple members of the DNAJ family were upregulated out-of-exposure relative to control. DNAJA1, implicated in the prevention of nitric oxide- and CHOP-induced apoptosis (Gotoh *et al.*, 2004), was upregulated in both resistant variant lines. Additionally, there were upregulated $CuSO_4$-R specific (DNAJA2 and DNAJB11) and Cu Pro-R specific DNAJs (DNAJA3, DNAJB1, DNAJC2, DNAJC7

and DNAJC9). Upregulation of DNAJ proteins supports a contribution towards protection against Cu-exposure in Cu-resistant Caco-2 cells.

UFM1 (Ubiquitin-fold modifier 1), a protein responsible for the post translational modification ufmylation and recently identified as a key regulator in ER stress response (Zhang *et al.*, 2012; Sutherland and Barrio, 2018), was stably upregulated in both Cu-resistant lines. Coordinated upregulation of HSPs, proteasomal components and UFM1 possibly contribute a cytoprotective role in Cu resistant Caco-2 cells against Cu mediated toxicity by reducing protein misfolding/aggregation, facilitating increased degradation of misfolded proteins and decreased ER stress.

Cu-resistant variants response to oxidative stress

Oxidative stress is activated upon exposure to Cu and our biochemical studies (ROS, SOD and GSH) showed ablation or attenuation of oxidative stress response. Examining the evolution of Cu resistance in yeast cells, Adamo *et al.* (2012) identified reduced Cu uptake, altered antioxidant and ROS response and changes in the Cu binding proteome as contributing to Cu tolerance. Other markers of oxidative stress not seen in our proteomic analysis, such as heme oxygenase and sulfiredoxin, may only be associated with early acute response (Keenan, O'Sullivan, *et al.*, 2018).

Antioxidant proteins involved in glutathione metabolism alongside reducing agents were found to be differentially expressed in Cu-resistant Caco-2. Glutaredoxins and thioredoxins are small ubiquitous proteins (9-16 kDa) which reduce protein-glutathione and protein-protein disulfides, respectively (Lillig and Berndt, 2009). Glutaredoxin-1 (GLRX) plays a role in protection against oxidative stress-induced apoptosis in endothelial (Li *et al.*, 2017) and epithelial cells (Liu *et al.*, 2015) and was upregulated out-of-exposure relative to control for both Cu-resistant lines (1.77- and 2.09- fold).

Additional thioredoxin/glutaredoxin domain containing proteins (TXNL1, TXN, TXNDC-12, TXNDC-17 GLRX3, and GLRX5) were specifically upregulated in Cu Pro-R cells. Taken together, the modified expression of thioredoxins and glutaredoxins may act as redox regulators of signalling molecules and transcription factors by controlling the redox state of protein thiols (Lillig and Berndt, 2009), thereby enhancing stress tolerance and functioning to maintain a reduced environment intracellularly.

Copper metabolism MURR1-domain-containing 1 (COMMD1) plays a crucial role in Cu ion homeostasis through binding to copper-transporting P(1B)-type ATPases (ATP7A and ATP7B) and has also been shown to play a role in the maturation and activation of SOD1 (Osredkar and Sustar, 2011; Materia *et al.*, 2012). More recently, the mechanism by which COMMD1 facilitates Cu transport via ATP7A was established (Phillips-Krawczak *et al.*, 2015) and knockout of COMMD1 resulted in intracellular Cu accumulation. Proteomic analysis showed higher levels of COMMD1 in both Cu-resistant Caco-2 variants out-of-exposure relative to control (>2.08 fold). However, for $CuSO_4$-R Caco-2, COMMD1 levels reduced to a level comparable to the control, while no change was seen in Cu Pro-R Caco-2 on exposure.

Glutathione peroxidase (GPX1) is a first line defence antioxidant breaking down hydrogen peroxides to water and molecular oxygen (Ighodaro and Akinloye, 2018). In Cu Pro-R cells, GPX1 expression was identified as highly decreased (33.12- fold) during proteomic analysis and a decrease was confirmed by Western expression of the protein (Appendix Fig. 2). Phospholipid hydroperoxide glutathione peroxidase (GPX4) was moderately decreased in-exposure relative to out-of-exposure levels (2.73- fold). Expression of glutathione S-transferase P (GSTP), shown previously to protect against hydroperoxides *in vivo* (Hayes and McLellan, 1999), was upregulated during Cu exposure to Cu Pro-R cells (4.24- fold). Furthermore, proteomic analysis of copper

chaperone to Cu/Zn superoxide dismutase (CCS), responsible for cytosolic delivery of Cu to SOD1, showed decreased expression (6.33- fold) during Cu exposure in Cu Pro-R Caco-2 cells. CCS was shown previously to degrade via 26S proteasome under conditions of excess Cu exposure (Bertinato and L'Abbé, 2003; Huppke *et al.*, 2012), resulting in a decrease in overall Cu,Zn superoxide dismutase (SOD1) activity, consistent with our findings in Cu-resistant Caco-2 cells. In addition, increased SOD1 activity in parental Caco-2 cells is consistent with Cu-induced SOD1 activity in yeast (Schmidt, Kunst and Culotta, 2000).

Glutamate-cysteine ligase (GCL), a component of the antioxidant response element (Brown *et al.*, 2002) was remarkably lower out-of-exposure relative to control in $CuSO_4$-R and Cu Pro-R cells (1.94- and 2.02- fold, respectively) and was upregulated during re-exposure to Cu Pro-R cells only. Similarly, glutathione reductase (GSR), responsible for maintaining a high level of GSH in the cytosol, was upregulated when Cu Pro-R cells were re-exposed to Cu (1.6- fold). (Armendariz *et al.*, 2004) saw no change in gene expression of either GCL or GPx for two ATP7A-mutated mouse fibroblast lines during chronic Cu exposure (25 µM Cu-His), with upregulated metallothionein expression reported as the only indicator of oxidative stress in their system. In Cu-resistant Caco-2 variants, oxidative stress proteins appear to coordinate in a fashion which allows for the attenuation of normal stress responses to elevated Cu.

DNA Repair and protection of cell cycle regulation

Proteins associated with DNA repair and cell cycle protection (Table 1), include checkpoint kinase 1 (CHEK1), a serine/threonine kinase required for genomic stability regulation and activation of DNA repair in response to DNA damage (Huang et al., 2008). CHEK1 was upregulated in both Cu-resistant lines (3.8- fold). Additionally,

mitotic spindle assembly checkpoint protein (MAD2L1), which plays important roles in chromosome segregation and maintaining spindle assembly checkpoint function (Cahill *et al.*, 1999), was stably upregulated in $CuSO_4$-R Caco-2 cells only (2.3- fold).

Mitochondrial associated protein upregulation in Cu-resistant cells:

A large proportion of proteins were stably upregulated relative to downregulated proteins, and "metabolic pathways" was highlighted in KEGG analysis, suggesting increased impact on metabolic processes are a stable alteration in Cu-resistant Caco-2 lines. (Gioria *et al.*, 2018) found upregulation of mitochondrial ATP synthase subunit α (ATP5A1) in Caco-2 cells following exposure to silver nanoparticles (1- 10 µg/ml) at 24 and 72 hours. Our analysis identified stable increased expression of subunit β (ATP5F1B) in $CuSO_4$-R and Cu Pro-R cells (2.29- and 2.23- fold, respectively). Mitochondrial NADH dehydrogenase [ubiquinone] flavoprotein 1 (NDUFV1) was also upregulated out-of-exposure relative to control in $CuSO_4$-R cells and downregulated in-exposure relative to out-of-exposure in Cu Pro-R cells. We noted the expression of multiple mitochondrial ribosomal proteins was stably increased for both Cu-resistant lines (Table 1), suggesting increased demand for mitochondrial protein translation. During Cu-exposure to $CuSO_4$-R and Cu Pro-R cells, CHCHD4 (mitochondrial intermembrane space import and assembly protein 40) was downregulated (3.68- and 4.57- fold, respectively). Substrates of CHCHD4 include Cox17, a chaperone of Cu essential for the assembly of complex IV in the electron transport chain (ETC) (Hofmann *et al.*, 2005). Differential expression of ETC and other mitochondrial associated proteins indicated increased cellular metabolic demand in $CuSO_4$-R and Cu Pro-R cells (Herst *et al.*, 2017).

Components of endocytosis pathway identified in Cu-resistant Caco-2 cells

Endocytosis was identified as a KEGG pathway common to both Cu-resistant variants during exposure (Table S8). The endosomal sorting complex required for transport (ESCRT) plays an essential role in sorting and degradation of ubiquitinated membrane proteins by mediating their processing between the plasma membrane and the endosomal vesicle (Tsunematsu et al., 2010). The hetrotetramer ESCRT-I recognizes ubiquitinated proteins and delivers them into the ESCRT pathway for lysosomal degradation (Katzmann, Babst and Emr, 2001; Wollert *et al.*, 2009). Proteomic analysis showed ESCRT-I components; MVB12A, VPS28 and an additional component of the ESCRT-II complex, SNF8, were downregulated when both Cu-resistant lines were exposed to Cu. Likewise, VPS37A was downregulated during Cu exposure to Cu Pro-R cells (8.65- fold). Taken together, we suspect reduced protein ubiquitination and downregulation of ESCRT components in Cu exposed $CuSO_4$-R and Cu Pro-R cells relative to parental Caco-2 may play a role in the increased protection against excess Cu exposure.

Suggested model of primary mechanisms of resistance in Cu-resistant Caco-2 cells

As opposed to conventional models where Cu resistance is suggested to be conferred through a single upregulated protein, such as metallothionein or ATP7B, our analysis suggests a cohort of multiple small changes in Cu-resistant Caco-2 cells contribute towards Cu resistance (Fig. 3.4.1). Our biochemical analysis indicated the involvement of MT and attenuation of oxidative stress (GSH, SOD activity), while proteomic analysis revealed Cu-resistance mechanisms occur at multiple levels: (1) protection at the DNA level by DNA damage and cell cycle proteins e.g. CHEK1 (2) protection at the RNA level by increased RNA turnover and degradation, ensuring less stress was placed on the endoplasmic reticulum e.g. UFM1 (3) increased expression of protein chaperones and UPR related proteins e.g. DNAJA1, PSMD14 and decreased ubiquitinated proteins

(4) increased handling of oxidative stress by regulation of components of mitochondrial transport e.g. ATP5F1B, CHCHD4 and (5) decreased expression of components required for ESCRT formation related to endosomal sorting e.g. MVB12A, VPS28 and SNF8.

Copper is elevated in many cancers (breast, leukemia and colorectal) and copper transporters have been linked with acquired resistance especially to platinum-based drugs. Copper thus provides a targeted approach to reduce tumour levels through the use of chelation therapy (Lu *et al.*, 2010; Chan *et al.*, 2017) or in novel DNA targeting copper (II)-complexes (Jany *et al.*, 2015; McGivern *et al.*, 2018). The models of Cu-resistant cells developed in this work demonstrate resistant mechanisms similar to those observed in some platinum-resistant cancers such as DNA repair and GSH modulation (Damia and Broggini, 2019), suggesting that these platinum-resistant cells may be less sensitive to increased copper therapy.

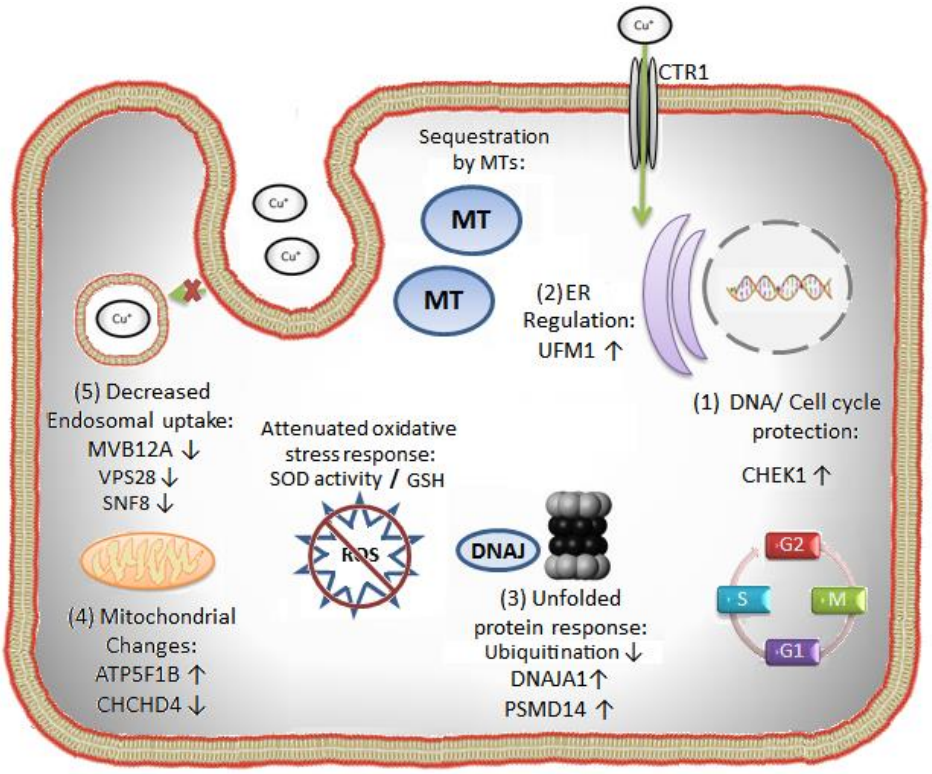

Figure 3.4.1. Summary diagram of primary proposed mechanisms of resistance in Cu-resistant Caco-2 cells: proteomic analysis indicated multiple resistance mechanisms including: (1) increased DNA damage and cell cycle proteins (2) increased RNA turnover and degradation and ER homeostasis (3) increased UPR related protein expression (4) increased handling of oxidative stress and (5) decreased endocytosis. CTR1: Copper transporter 1, MT: metallothionein, SOD: superoxide dismutase, GSH: glutathione, ROS: reactive oxygen species

3.5 Conclusions

This study demonstrated that stable resistance to toxicity of high copper levels can be induced in the enterocyte-like cell line Caco-2. Furthermore, this resistance is not dependent on the copper species and appears to be the consequence of a number of different mechanisms. These mechanisms potentially include; the improved ability to deal with oxidative stress, changes in proteins related to DNA damage and cell cycle,

and a reduction in ER stress and RNA turnover. However, while both the $CuSO_4$-R and Cu Pro-R Caco-2 variants show similar levels of resistance and while the broad pathways responsible for this resistance are similar, specific protein changes were identified as associated with the specific resistant variant. The significance of these variations in the resistant profile needs to be further assessed.

Further studies are required to determine which of these potential mechanisms has the largest role to play in the development of resistance to high copper levels and how these might relate *in vivo*. The combination of characterisation and proteomic profiles generated in this study have contributed toward the understanding of the evolution of copper resistance in Caco-2 cells and the role played by cell stress response in cytoprotection and cell survival during copper toxicity. Finally, the differentially expressed proteomic profiles provided in this work may prove useful in further investigations.

Highlights

- Continuous exposure of Caco-2 cells to copper resulted in Cu-resistance generation
- Copper toxicity, growth and phenotypic profiles were altered in Cu-resistant Caco-2
- ROS, SOD and GSSG increased in Cu-exposed parent but not Cu-resistant Caco-2 cells
- Quantitative proteomic profiling identified 1,113 differentially expressed proteins

3.6 Funding information

This work was funded by a joint Enterprise Ireland Innovative Partnership programme (IP/2015/0375) and Science Foundation Ireland cofunded by ERDF, Grant no: 12/RC/2275_P2. The Orbitrap Fusion Tribrid mass spectrometer was funded by an SFI Infrastructure Award (grant no. 16/RI/3701).

3.7 Supplementary Material

All supplementary information (including Tables S1-S8) is available on Google Drive:

https://drive.google.com/open?id=178OLcClU5I90jfKqny9vYUFMr6TBwlsn

Raw and filtered proteomic data sets are published in mendeley's online repository:

http://dx.doi.org/10.17632/rm6sjwv2ms.1

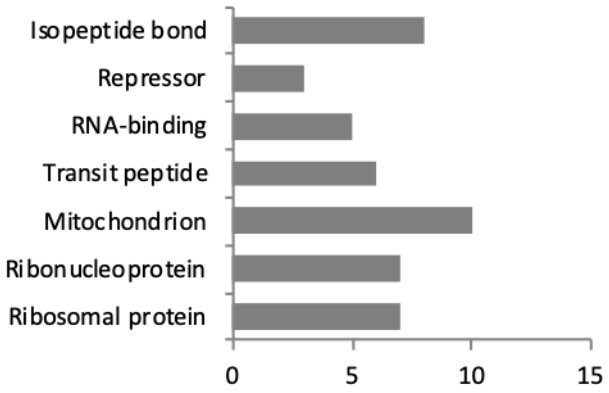

Figure 3.6.1. UniProtKB entries classified by DAVID functional annotation tool for proteins identified as stably expressed in both $CuSO_4$-R and Cu Pro-R cells out-of-exposure versus unexposed control (P <0.05)

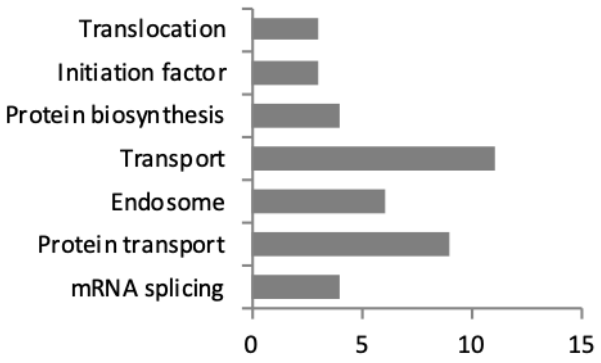

Figure 3.6.2. UniProtKB entries classified by DAVID functional annotation tool for differentially expressed proteins (DEPs) identified as transiently changed in common between $CuSO_4$-R and Cu Pro-R cells in-exposure versus out-of-exposure (P<0.05)

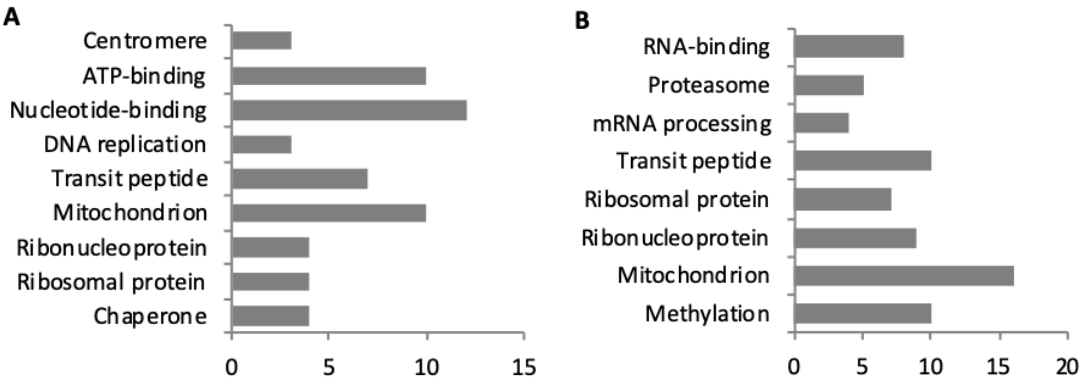

Figure 3.6.3. UniProtKB entries classified by DAVID functional annotation tool for stable differentially expressed proteins (DEPs) identified as specific to (A): $CuSO_4$-R and (B): Cu Pro-R cells out-of-exposure versus control (P <0.05)

4 Gene expression profiling of copper-resistant Caco-2 clones

Authors: Charles O'Doherty[1], Joanne Keenan[1], Fiona O'Neill[1], Martin Clynes[1], Indre Sinkunaite[2], Karina Horgan[2], Richard Murphy[2] and Finbarr O'Sullivan[1]

[1] National Institute for Cellular Biotechnology and SSPC-SFI. Centre for Pharmaceuticals, Dublin City University, Glasnevin, Dublin D09 W6Y4, Ireland

[2] Alltech Ireland, European Bioscience Centre, Summerhill Rd, Sarney, Dunboyne, Co. Meath, Ireland

Journal: Metallomics

Status: Accepted July 2020

DOI: DOI: 10.1039/D0MT00126K

I participated with RM, KH, MC, FOS and JK in all stages of this manuscript from conception and design of the study, interpretation of data, to drafting and revising the manuscript. I was responsible for isolation of Caco-2 clones, acquisition of data, analysis and interpretation of data and submitting the manuscript. I completed all steps of microarray sample processing assisting FON, including RNA extraction, bioanalyser quality control, mRNA and miRNA preparation and hybridization onto the genechip arrays. . Alongside myself, JK and IS carried out the other experiments. COD, JK, MC and FOS wrote the manuscript.

Abstract

The Caco-2 cell line is comprised of a heterogenous mix of cells; isolation of individual clonal populations from this mix allows for specific mechanisms and phenotypes to be further explored. Previously, we exposed Caco-2 cells to inorganic copper sulfate or organic copper proteinate to generate resistant variant populations. Here, we describe the isolation and characterisation of clonal subpopulations from these resistant variants to organic (clone Or1, Or2, Or3) or inorganic (clone In1 and In2) copper. The clones show considerable homogeneity in response to Cu-induced toxicity and heterogeneity in morphology with variations in level of cross-resistance to other metals and doxorubicin. Population growth of Cu-resistant clones in selective pressure was comparable to parental Caco-2 cells for clone In1, Or1 and Or2 and reduced for clone In2 and Or3.

Microarray analysis identified 4,026 total (2,102 unique and 1,924 shared) differentially expressed genes including those involved in the MAP Kinase and Rap 1 signalling pathways, and in the focal adhesion and ECM-receptor contact pathways. Gene expression changes common to all clones included upregulation of ANXA13 and GPx2. Our analysis additionally identified differential expression of multiple genes specific to two forms of copper; UPK1B was overexpressed in Cu proteinate-isolated clones Or1, Or2 and Or3 and AIFM2 was decreased in $CuSO_4$-isolated clones In1 and In2. The adaptive transcriptional responses established in this study indicate a cohort of genes, which are involved in copper resistance regulation and chronic copper exposure.

4.1 Introduction

The transition metal copper is an essential dietary micronutrient acting as a cofactor for several metalloenzymes involved in biological functions including iron mobilization, antioxidant defence and electron transport (Barceloux and Barceloux, 1999; Harvey and McArdle, 2008). The redox cycling of Cu oxidation states via Fenton reactions is capable of generating hydroxyl radicals, important for co-factor function but when in excess, reactive oxygen species (ROS) cause subsequent oxidative damage to surrounding cells and tissues (Valko, Morris and Cronin, 2005). This is apparent in Wilson's disease, a potentially fatal genetic disorder resulting from dysfunction of Cu homeostasis (Cu-transporting ATP7B) and manifests as severe systemic Cu overload (Waggoner, Bartnikas and Gitlin, 1999). For this reason, studies that examine molecular mechanisms of Cu resistance are of particular interest.

To gain a better understanding of Cu homeostasis in mammalian cells, multiple studies have generated Cu resistant cell lines, predominantly focussing on liver hepatocytes (Freedman and Peisach, 1989; Schilsky *et al.*, 1998; Groba *et al.*, 2017). Known regulatory mechanisms invoked to handle excess Cu such as increased cellular sequestration (metallothionein) (Freedman and Peisach, 1989) and export (ATP7B) (Schilsky *et al.*, 1998) have been reported, however, research has yet to examine global mRNA expression changes that contribute to Cu resistance in intestinal-like cells.

The parental Caco-2 cell line has been studied extensively as a model of intestinal permeability and transport as well as in gene regulation during transport of drugs and metal micronutrients (Natoli *et al.*, 2009; Angelis and Turco, 2011), while clonal populations of Caco-2 cells exhibiting particular traits have allowed for studies on

taurocholic acid transport (Woodcock *et al.*, 1991) and Caco-2 BBE, for distinct brush borders upon differentiation (Peterson and Mooseker, 1992).

In this study, we generated clones of the parental Caco-2 line, which exhibited Cu-resistance and cross-resistances to other stressors, alongside altered cell morphology and Cu accumulation. We then used these Cu-resistant clones to dissect changes in resistance and through microarray analysis determined: a) common transcriptomic factors involved in Cu-resistance and b) changes which distinguish differences between clones established using inorganic $CuSO_4$ versus organic Cu proteinate.

4.2 Materials and Methods

4.2.1 Materials

Irradiated $CuSO_4$ and Cu proteinate were supplied by Alltech Ireland Ltd, validated by ICP-MS.

4.2.2 Cell culture conditions

Exponentially growing Caco-2 cells (HTB-37 ™; American Type Culture Collection) were cultivated at 37 °C under 5% CO_2, in MEM (Gibco, 21090022) supplemented with 10% Fetal bovine serum (FBS, Gibco, 10270-106), 10mM HEPES (Sigma Aldrich, H3537) and 2mM L-glutamine (Sigma Aldrich, G7513). Cells were passaged approximately every 4 days, not allowing cells to reach confluence (Natoli *et al.*, 2011). Cells were routinely tested and found to be negative for *Mycoplasma* contamination.

4.2.3 Isolation of Cu-resistant Caco-2 clones

Cu-resistant clones were isolated from Cu-resistant Caco-2 mixed populations, (O'Doherty et al 2020) by limited dilution in selective pressure (50 µM $CuSO_4$ or 50 µM Cu proteinate). Individual colonies presenting homogeneous morphology were selected and lifted off the tissue culture surface using sterile glass picking tool under EVOS™ XL Core Cell Imaging System (Thermo Fisher Scientific). Clones were then trypsinised and reseeded in 96 well tissue culture plates to scale the population size for a minimum of 10 subcultures before experiments were performed.

4.2.4 Cell survival determination

Cells were seeded at 3125 cells/cm^2 and exposed after 24 hours for up to 120 hours before assaying by (A) acid phosphatase activity in 96-well microtiter plates using serial dilutions (Martin and Clynes, 1991, 1993) and (B) in 6-well tissue culture plates by viable cell count using haemocytometer and trypan blue exclusion method.

4.2.5 Cell imaging and size determination

Images of cells were captured using an EVOS™ XL Microscope. Images of trypsinised cells were imported into MetaMorph image Software® (Molecular Devices, version 7.7) for integrated morphometry analysis. A minimum of six independent images were used to determine mean radius, calculated as average distance from the centroid to all points along the cell's edge.

4.2.6 Intracellular copper determination

Intracellular Cu was measured following incubation with or without supplemented Cu using inductively coupled plasma mass spectrometry (ICP-MS; 7700X, Agilent, USA). Cells were washed twice in PBS, and lysed in protein lysis buffer (7 M urea, 2 M thiourea, 4% CHAPS and 30 mM tris, pH 8.0). Cell lysates were diluted in trace-analysis grade nitric acid (Sigma, USA), heated at 85–95 ◦C for 1 h and subjected to ICP-MS analysis.

4.2.7 Microarray mRNA analysis

Total RNA was extracted from triplicate biological samples using the Qiagen miRNeasy kit according to the manufacturer's instructions. RNA quantity was assessed using the

NanoDrop ND-1000 spectrophotometer (Labtech International, Uckfield, East Sussex, UK) and RNA quality assayed using the Agilent RNA 6000 NANO KIT and Agilent Bioanalyzer (Agilent, Santa Clara, CA, United States). The RNA purity and quality is indicated by 260/280 and 260/230 absorbance ratios and the RNA integrity numbers supplied in Appendix Fig. 3.

Microarray profiling and associated bioinformatics analysis was carried out on the Affymetrix GeneChip Human Gene 2.0 ST array according to the manufacturer's instructions (Affymetrix, Santa Clara, CA, United States). The methodology and criteria used for total RNA purification, ssDNA sample processing and hybridisation to human microarrays have been previously described (Gallagher *et al.*, 2014). Prior to data analysis, probesets that did not reach the detection threshold (fluorescence level ≥ log2 (100) for at least 1 sample) were identified and designated undetected. Remaining probesets were considered differentially expressed between the two cell types if a fold change ≥ 1.5 in either direction along with a BH adjusted *P* value ≤ 0.01 was observed.

Upregulated and downregulated differentially expressed genes (DEGs) were collated and uploaded into DAVID (version 6.8, https://david.ncifcrf.gov/tools.jsp) and used to annotate and group the UniProt keywords and to perform KEGG pathway analysis on the DEGs. A *P v*alue of <0.05 was set as the threshold for inclusion of both functional annotation terms and KEGG pathway analysis.

4.2.8 qRT-PCR validation of microarray results

Reverse transcription of RNA to cDNA was carried out using the High Capacity cDNA reverse transcription kit (Applied Biosystems, Cat 4368814). Real-time qPCR was performed using the Applied BioSystems™ PowerUp SYBR® Green Master Mix

(Applied BioSystems™, Cat A25778) in accordance with the manufacturers' specifications (7500 Fast System software version 1.3.1.21). Data analysis was based on the relative quantitation ($2^{-\Delta\Delta Ct}$) where relative expression of the target gene is compared to the expression of endogenous β-actin (Livak and Schmittgen, 2001). Primers used for qRT-PCR are listed in Table 4.5.1.

4.2.9 Statistical Analysis

To evaluate statistical significance between any two populations, *P*-values were calculated by two-tailed Students' t-test with 2-tailed distribution and two-sample heteroscedastic unequal variance (Microsoft Excel®). Some figures were assessed using two-way analysis of variance (ANOVA) (4.3.1 and 4.3.3A) or one-way ANOVA (4.3.3B). Significance was set at *P*-values less than 0.05. Error bars in all figures indicate standard error of the arithmetic mean. Relative values in all figures are expressed as percentage of untreated controls, unless otherwise noted. All experiments were repeated at least three times.

4.3 Results

4.3.1 Cu-tolerant Caco-2 clone isolation and analysis of resistance

Five Caco-2 clones were generated from Cu-resistant Caco-2 cells. Clone In1 and In2 were isolated from $CuSO_4$-resistant Caco-2 cells and clone Or1, Or2 and Or3 were isolated from Cu proteinate-resistant Caco-2 cells. All five Cu-resistant clones exhibited increased tolerance to Cu exposure (Fig. 4.3.1 A, B and Fig. 4.5.1 A, B), particularly at lower concentrations (up to 100 µM $CuSO_4$ or Cu Pro,) relative to parental Caco-2 and

Cu-resistant variant populations ($CuSO_4$-R and Cu Pro-R Caco-2, P <0.05). Although a small decrease in cell yield was observed for each of the clones at 3.125 µM Cu, the non-monotonic dose response between 3 µM and 25 µM Cu was only maintained in parental Caco-2 cells, Cu-resistant variants and clone In2 (Fig. 4.3.1 A, B).

To determine the presence of cross-resistance in Cu-resistant Caco-2 clones, exposure to other metals and chemotherapeutic agents was assessed. Elevated cross-resistance of specific clones was observed during manganese (Mn) exposure (In2 and Or3, Fig. 4.3.1 C, *P* <0.01) and during iron (Fe) exposure (In2, Or1 and Or3, Fig. 4.3.1 D, *P* <0.01). Exposure to the anthracycline doxorubicin resulted in reduced toxicity in clones In2, Or2 and Or3 (Fig. 4.3.1 E, *P* <0.01). However, exposure to docetaxel, a taxane that inhibits cell cycle progression by targeting microtubule formation, elicited no significant changes in clone cell survival relative to parental Caco-2 (Fig. 4.3.1 F).

Two main mechanisms of action are proposed for doxorubicin-induced toxicity: (i) free radical generation and subsequent DNA damage resulting in cell death and (ii) DNA intercalation and inhibition of topoisomerase II leading to structural changes in chromatin (Thorn *et al.*, 2011; Taymaz-nikerel *et al.*, 2018). Cu resistant Caco-2 clone cross-resistance to doxorubicin was attributed to increased protection against the generation of free radicals by reducing oxidative stress.

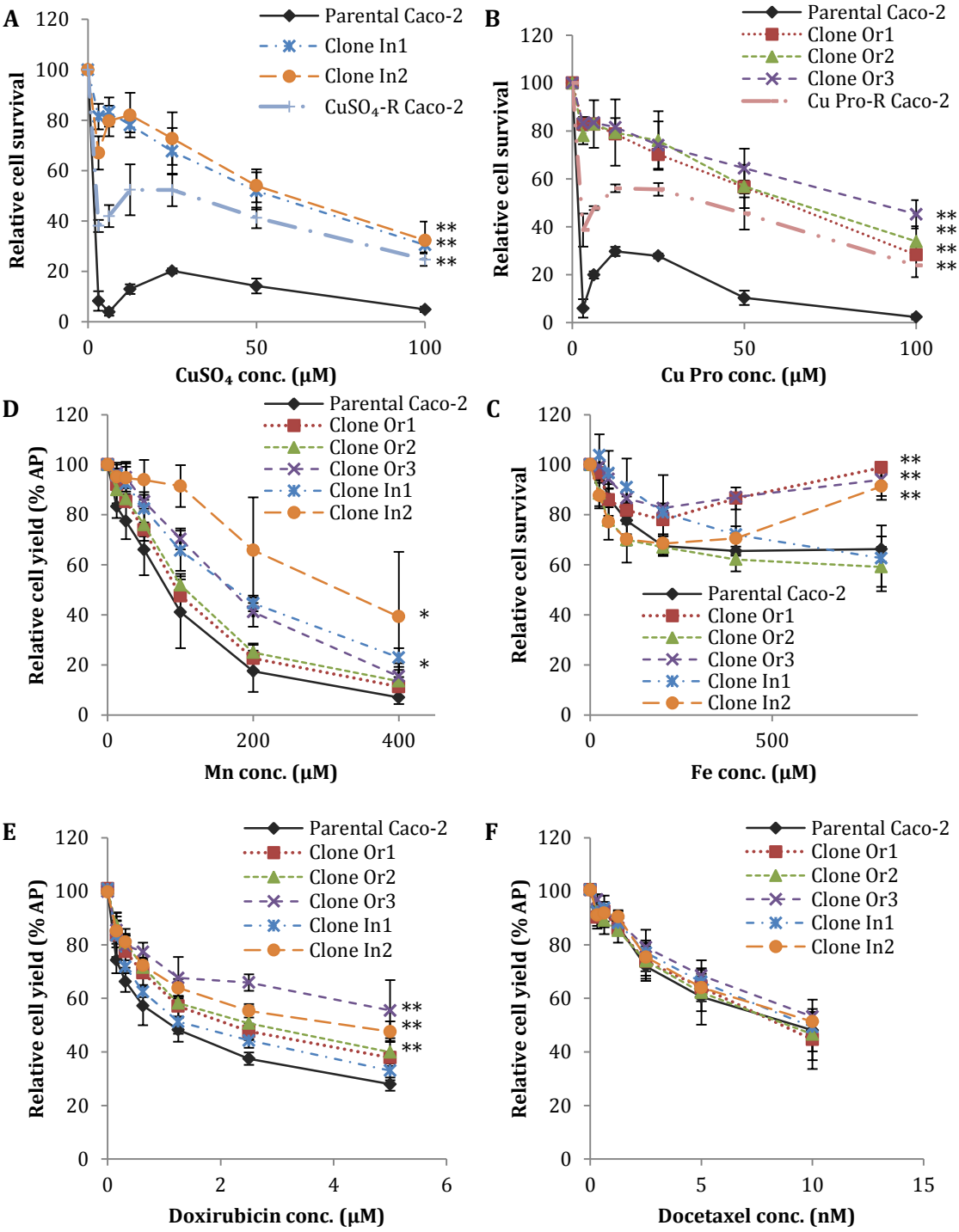

Figure 4.3.1. Toxicity and cross-resistance profiles of parental and copper resistant Caco-2 clones In1, In2, Or1, Or2 and Or3. Relative cell survival of Caco-2 clones during exposure to increasing concentrations of A: $CuSO_4$, B: Cu proteinate, C: manganese, D: iron, E: doxorubicin and F: docetaxel (N=3). Asterisk indicates significant difference from parental Caco-2 (* = $P < 0.05$, ** = $P < 0.01$)

4.3.2 Morphological analysis of Cu-resistant Caco-2 cell clones

Phase contrast images were taken of exponentially growing parental Caco-2 and Cu-resistant clone populations to compare colony structure and cell morphology (Fig. 4.3.2A and B, indicated by arrows). Parental Caco-2 cells exposed to $CuSO_4$ or Cu Pro (50 μM) were subject to extensive membrane blebbing, cell nuclear condensation, cell rounding and lifting. In the clonal populations, the same concentration permitted cell growth with distinct phenotypic differences: clone In1 displayed clusters of small colonies with prominant borders between cells; clone In2 cell morphology was larger with fewer clusters; clone Or1 grew in small clustered colonies and displayed small uniform tight borders between cells; clone Or2 presented pronounced cytosolic vesicles ubiquitously; and clone Or3 was characterised by large, well spread out cells which reached confluence faster than parental Caco-2 (Fig. 4.3.2B). When trypsinised, cells isolated from inorganic $CuSO_4$-resistant Caco-2 only (clones In1 and In2) were significantly smaller than the parental population (Fig. 4.3.2C, $P < 0.05$).

A

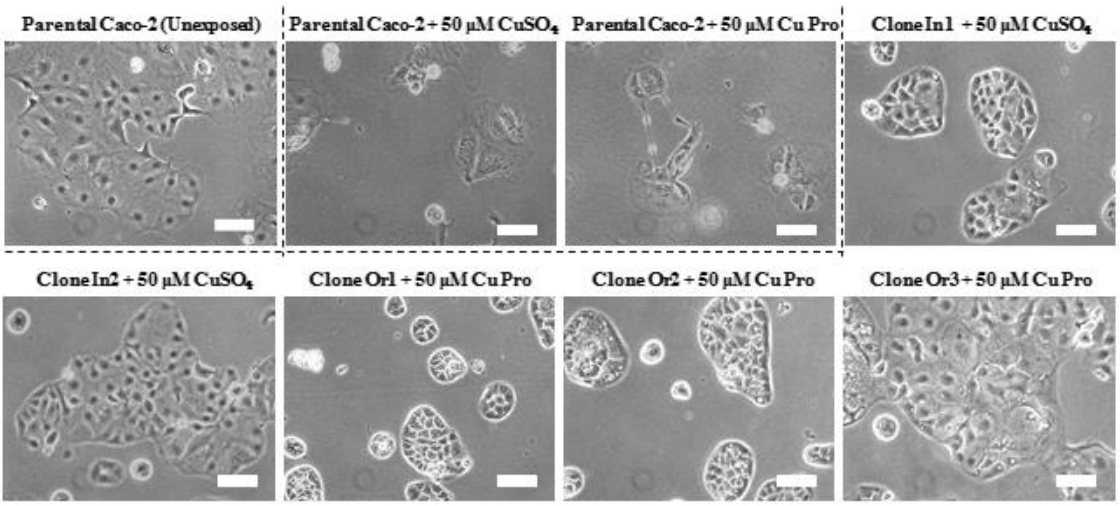

B

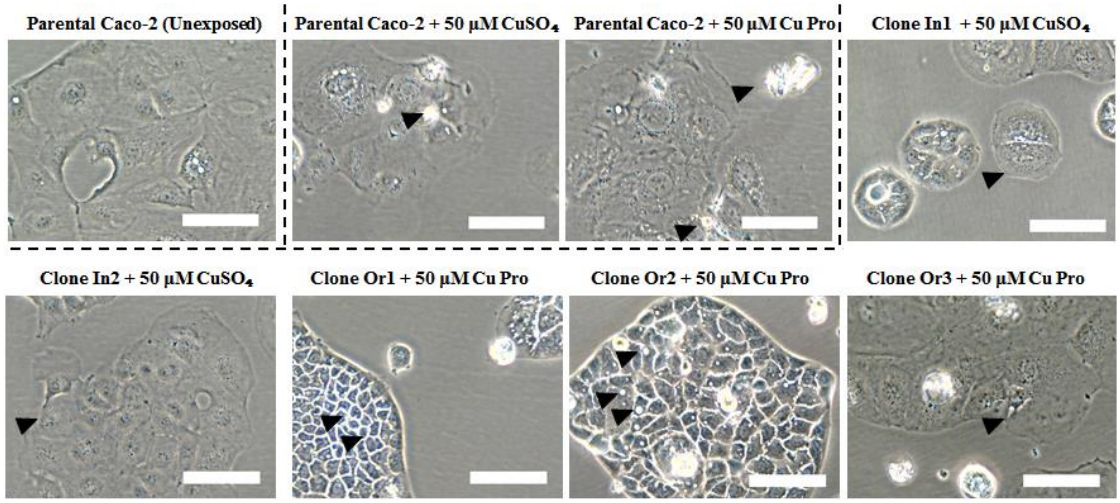

C

	Control Caco-2	Clone In1	Clone In2	Clone Or1	Clone Or2	Clone Or3
Mean radius (µm)	10.5 ± 1.14	8.8 ± 1.34*	8.75 ± 1.51*	9.7 ± 1.13	10.01 ± 0.58	11.32 ± 0.91

Figure 4.3.2. A: Representative phase contrast images for control Caco-2 and in the presence of added Cu (50 µM $CuSO_4$ or 50 µM Cu Pro) and Cu-resistant clones (In1, In2, Or1, Or2 and Or3) demonstrating growth profiles. B: Higher magnification images demonstrating cell morphological differences between clones and parental Caco-2 cells. Scale bar represents 100 µm, C: Average mean radius for control Caco-2 cells and Cu-resistant clones. '±' denotes standard deviation. Asterisk indicates significant difference from control ($P < 0.05$) ($N > 3$)

4.3.3 Cell growth and Cu levels in parental and Cu-resistant Caco-2 clones

Unexposed parental Caco-2 cells and all Cu-resistant Caco-2 clones in selection pressure displayed exponential growth from 48 - 144 hours in culture (Fig. 4.3.3A). Cell yield of Cu-exposed parental Caco-2 (50 µM $CuSO_4$ and Cu Pro) did not increase throughout the duration of exposure (Fig. 4.3.3A). Two of the clones (In2 and Or3) had significantly reduced cell yield relative to the parental population after 144 hours in culture (P <0.05). Intracellular Cu in unexposed parental Caco-2 cells was below detectable levels per 10^6 cells (Fig. 4.3.3B). Cu accumulation in parental Caco-2 cells exposed to 50 µM Cu was increased relative to the Cu-resistant clones (all except clone In2, P <0.05).

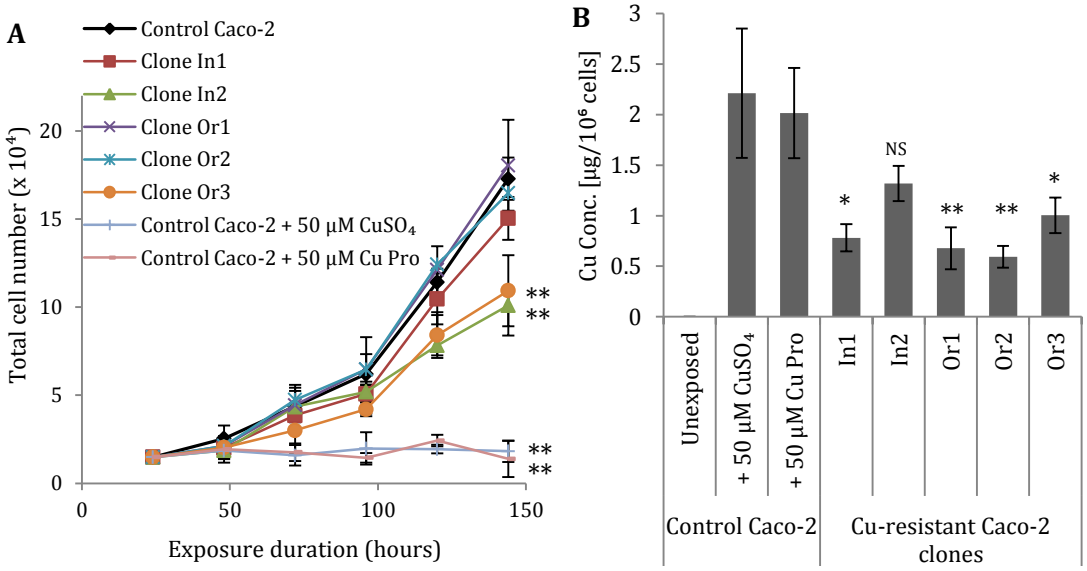

Figure 4.3.3. A: Viable cell yield during culture for unexposed control Caco-2 and control Caco-2 and Cu-resistant clones (In1, In2, Or1, Or2 and Or3) in the presence of added Cu (50 µM $CuSO_4$ or Cu proteinate) (N=3). Asterisk indicates significant differences (** P < 0.01) relative to untreated control Caco-2; B: Copper content per 10^6 cells after 96 hours for unexposed parental Caco-2 cells and control Caco-2 and Cu-resistant clones in the presence of added Cu (50 µM $CuSO_4$ or Cu proteinate) (N=3). Asterisk indicates significant differences (* P < 0.05 or ** P < 0.01) between the Cu-treated resistant clones and the Cu-treated control group. NS = not significant.

4.3.4 Differentially regulated gene expression between parental Caco-2 cells and copper resistant clones

To investigate differentially expressed genes (DEGs) between parental Caco-2 and the five Cu-resistant clones, all clones were individually compared to the parent using microarray analysis (Fig. 4.3.4A). Overlap between all discovered DEGs (4,026 total genes) revealed 1,924 genes to be shared across the clones (Fig. 4.3.4B). In spite of similar levels of Cu resistance, only 6% (245 DEGs) were identified as overlapping between all clones and large transcriptomic changes unique to each clone were discovered (2,102 total unique DEGs), illustrating their diversity. The complete raw and filtered data sets are published in mendeley's online repository, available via: http://dx.doi.org/10.17632/p976x9rk6w.2.

As the clones shared comparable resistance levels to Cu exposure, we were firstly interested in differentially expressed genes that were common to the clones. To increase reliability, an average threshold of two-fold change was applied and DEGs shared between all clones were combined with DEGs shared in four out of five clones (588 total, Fig. 4.3.4B, circled in black), resulting in 331 'common' target genes after threshold. All 331 common DEGs were co-expressed in the same direction except Calpain 6 (CAPN6); CAPN6 was upregulated 3.91- fold in clone Or3, downregulated in clones In1, In2, Or1 and Or2. Interestingly, there was no common differential expression for genes associated with Cu transport and trafficking such as copper transporter 1 (CTR1), divalent metal transporter 1 (DMT1), antioxidant protein 1 (ATOX1), and P-type ATPase / Menkes disease protein (ATP7A). This suggested other factors were involved in Cu-resistance in the clones.

DAVID (v6.8) analysis of the 331 common DEGs clustered into five over-represented KEGG pathways: MAPK signalling pathway, Rap1 signalling pathway, toxoplasmosis, focal adhesion and ECM-receptor interaction (Table 4.5.2) and fourteen UniProt keyword annotations (Table 4.5.3), suggesting cell adhesion, cell-cell interaction and cell cycle may play important roles in conferring Cu-resistance in the clones. We noted predominant downregulation for genes associated with MAPK signalling (9/13 DEGs) and Rap1 signalling pathways (6/9 DEGs).

Annexin A13 (ANXA13 or intestine specific annexin), was the highest common upregulated gene between all clones (average 18.7- fold) (Fig. 4.3.4C). ANXA13 is continually transcribed throughout differentiation and villus migration in intestinal epithelial cells, with localisation focussed at the apical membrane of polarised enterocytes (Wice and Gordon, 1992) and plays a direct role in apical transport via budding from trans-golgi network (Lafont *et al.*, 1998). Clones In1, Or1 and Or2 displayed the highest upregulation of intestine specific annexin (ANXA13) and closest resembled semi-differentiated Caco-2 cell morphology during exponential growth, suggesting Caco-2 clones selected for Cu resistance may be characterised by enhanced cell polarity and differentiation.

Common downregulated genes included LOC105372013 (69.8- fold downregulated), predicted as a locus for basic salivary proline-rich protein 2-like transcript in the human genome (https://www.ncbi.nlm.nih.gov/gene/105372013), although has since been withdrawn from NCBI's database because the model on which it was based was not predicted in a later annotation. ABCA9 antisense RNA 1 (ABCA9-AS1) and inter-alpha-trypsin inhibitor heavy chain 2 were also downregulated (ITIH2) (13.9- and 10.5-fold downregulated, respectively).

Our analysis identified differential expression of multiple genes specific to two forms of Cu in the Cu-resistant clones. Thirty-one genes were differentially expressed in common between the Cu proteinate-isolated clones Or1, Or2 and Or3 (Fig. 4.3.4B, circled in red) including highly expressed uroplakin 1B (UPK1B) and a slight increase in Cu^{2+} transporting ATPase (ATP7B), while thirty-eight genes were differentially expressed in common between $CuSO_4$-isolated clones In1 and In2 (Fig. 4.3.4B, circled in grey) including downregulated mitochondrion-associated apoptosis-inducing factor 2 (AIFM2) and increased ephrin-B2 (EFNB2). For validation of the genes identified by microarray analysis, a cohort of targets was selected (ANXA13, ATP7B, GPX2, AIFM2 and UPK1B) representing highly overexpressed and Cu specific targets of interest. Corresponding quantitative RT-PCR analysis of these targets demonstrated good correlation with the microarray transcriptomic data, validating expression of these genes and overall confirmed the microarray analysis (Fig. 4.5.2 and 4.5.3).

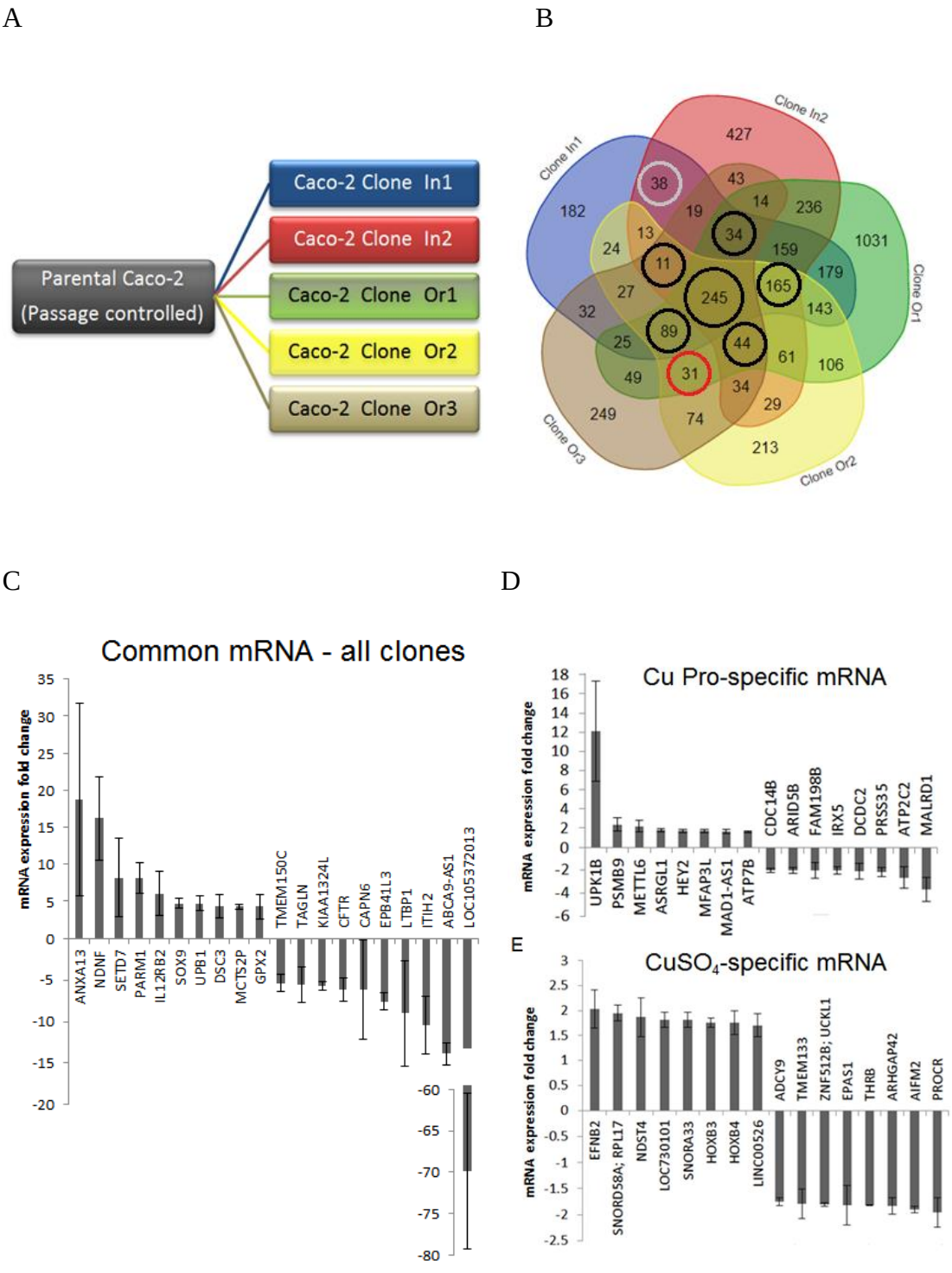

Figure 4.3.4: A: Design schematic for microarray analysis, B: 5-set Venn diagram showing overlap of DEGs identified between Cu-resistant clones and parental Caco-2 cells (http://bioinformatics.psb.ugent.be/webtools/Venn/), C: Bar chart of top ten upregulated and downregulated genes in common between all Cu-resistant Caco-2 clones, D/E: Bar chart of top eight upregulated and downregulated genes specific to Cu-proteinate isolated clones (Or1, Or2, Or3) and $CuSO_4$ isolated clones (In1, In2)

4.4 Discussion

Characterisation of Cu-resistant Caco-2 clones

In this study, a range of clones were isolated from the Caco-2 cell line (In1, In2, Or1, Or2 and Or3) exhibiting resistance to both inorganic $CuSO_4$ and organic Cu proteinate (Cu Pro). These clones presented different morphologies compared to parental Caco-2 cells and to each other. Select clones also demonstrated cross-resistance to iron (clones In2, Or1 and Or3) and manganese (clones In2 and Or3). To provide insight into the physiological state of the clonal populations, changes on the gene level were investigated using microarray profiling and revealed shared and unique transcriptomic changes resulting from Cu resistance generation.

Cross-resistance to chemotherapeutic drugs

Toxicity resulting from docetaxel exposure was not altered in Cu-resistant Caco-2 clones (Fig. 4.3.1 F), indicating that mechanisms involved in Cu-resistance did not confer protection against chemotherapeutic drugs targeting cell cycle progression. Three clones exhibited increased cross-resistance ($P < 0.01$) to doxorubicin exposure (Fig 4.3.1 E) – normally associated with drug efflux (e.g. multidrug resistance-associated protein) and increased resistance to oxidative stress (e.g. glutathione S-transferase) (Hayes and McLellan, 1999). However, the lack of cross-resistance to docetaxel in Cu-resistant clones suggest the overall resistance is supported by a base-line increase in oxidative stress genes and not drug efflux. Additionally, genes associated with drug efflux were not detected as differentially expressed during transcriptomic analysis. This agrees with previous observations of upregulated antioxidant proteins in Cu-resistant Caco-2 mixed populations (O'Doherty et. al, 2020).

Cellular copper uptake

Parental Caco-2 cells demonstrated greater Cu accumulation when exposed to 50 µM $CuSO_4$ or Cu Pro, suggesting resistance to Cu in Caco-2 clones was to some extent mediated by decreased Cu uptake or increased Cu export. No differential expression for the main Cu importer CTR1 was found in our microarray analysis, however transport via CTR1 is often perturbed via translocation from the membrane into the cell rather than via decreased translation (Molloy and Kaplan, 2009). Interestingly, of the Cu-resistant clones, Cu accumulation was highest in clones In2 and Or3, correlating with lowest cell yields during selection pressure.

Established mechanisms of Cu-resistance

Cytosolic storage protein metallothionein (MT), which protects against metal-induced toxicity through sequestration of intracellular metal ions, was previously identified in Cu-resistant hepatoma cells (Freedman and Peisach, 1989). In specific Cu-resistant Caco-2 clones, several isoforms of metallothionein mRNA were upregulated (MT1B, MT1CP, MT1X and MT2A), however moderate MT expression (between 1.63- and 2.97- fold) was detected in clones In1, In2 and Or1 only.

Increased expression of Cu-transporting ATP7B was previously identified as a mechanism conferring Cu resistance in hepatoblastoma cells (5- fold increased mRNA) by enhancing extracellular Cu export (Schilsky *et al.*, 1998). Our microarray analysis determined slight overexpression of ATP7B in clones isolated from organic Cu proteinate only (average 1.63- fold), however ATP7B expression in clone In1 may also be increased as indicated by qRT-PCR (Fig. 4.5.2).

Oxidative stress related gene expression

Microarray analysis identified several differentially expressed genes related to oxidative stress commonly expressed between the clones. Gastrointestinal glutathione peroxidase (GI-GPx, GPX2), which protects cells against hydroperoxide-induced toxicity (Wingler *et al.*, 2000), was upregulated (average 4.26- fold). NAD(P)H dehydrogenase [quinone] 1 (NQO1), which is induced by oxidative stress and protects against cellular damage through direct scavenging of superoxide (Ross and Siegel, 2018)**,** was likewise upregulated (average 2.03- fold) and sulfiredoxin 1 (SRXN1), a sulfinic reductase recently implicated in acute Cu-induced response to HT29 cells (Keenan, O'Sullivan, *et al.*, 2018), was also upregulated (1.9- fold). Furthermore, expression of two isoforms of the major 70 kDa heat shock protein (HSPA1B/A, 2.6- fold average) were both increased, signifying HSP70 may serve in detoxification or as chaperones to coordinate misfolded proteins for proteasomal degradation in Cu-resistant clones (Santra, Dill and de Graff, 2018). Taken together, this suggests that resistance to Cu in Cu-resistant Caco-2 clones was aided by increased constitutive expression of genes that ameliorate the effects of excess oxidative stress.

$CuSO_4$ and Cu Proteinate specific gene changes

Finally, specific DEGs were identified as associated to either $CuSO_4$-isolated clones (clone In1 and In2) or Cu proteinate-isolated clones (clone Or1, Or2 and Or3). For $CuSO_4$-isolated clones these included downregulation of apoptosis-inducing factor 2 (AIFM2 / AMID, average 1.9- fold), which is induced by tumor suppressor protein p53 in colon cancer cells (Marshall *et al.*, 2005) and upregulation of ephrin-B2 (EFNB2, average 2.03- fold), a transmembrane ligand for Eph receptors facilitating cell-cell interactions. Interestingly, uroplakin 1B (UPK1B), a member of the transpannin family

with a critical role in urothelial plaque stability, maturation and differentiation (Carpenter *et al.*, 2016) was the highest upregulated gene common to Cu proteinate resistant Caco-2 clones (average 12.1- fold). Future studies will be required to determine the functional role played by AIFM2, EFNB2 and UPK1B in Cu resistant Caco-2 cells.

The transcriptomic data from Cu-resistant Caco-2 clones was compared to previous proteomic analysis of the parental resistant populations to determine whether correlation exists between the two data sets. Common expression of several overlapping gene/proteins between the data sets were observed including overexpression of the previously highlighted chaperone HSPA1B, alongside increased ACTL8, which is associated with epithelial differentiation. Decreased correlating expressions included prosaposin (PSAP) involved in lysosomal lipid degradation, and actin cross-linking transgelin (TAGLN) which has been observed to decrease in differentiating Caco-2 previously (Buhrke, Lengler and Lampen, 2011). Interestingly, few of the KEGG pathways shared commonality between the studies, likely owing to the mixed resistant populations in the proteomic study (O Doherty *et al.*, 2020), whereas the current study focussed on isolated homogenous clones which also presented increased resistance to Cu and lacked the non-monotonic dose response.

In this study, multiple $CuSO_4$-resistant and Cu proteinate-resistant Caco-2 clones were isolated which exhibited similar response to Cu exposure while simultaneously demonstrating differences in morphological features and cross resistances to other metals and doxorubicin. Microarray profiling applied to each Cu-resistant clone identified a cohort of common differentially expressed genes and subsets of dysregulated genes resulting from changes specific to $CuSO_4$-isolated and Cu proteinate-isolated clones. In summary, this research provided insight into adaptive

transcriptional responses in mammalian cell clones selected for Cu-resistance and contributed to the knowledgebase surrounding regulation of Cu resistance and the effects of chronic exposure of two different forms of Cu to intestinal-like cells.

Highlights:

- Multiple Cu-resistant Caco-2 clones and their phenotypes were characterised
- Cross resistance to Fe, Mn and doxorubicin was identified in select clones
- ICP-MS analysis revealed reduced Cu accumulation in Cu-resistant clones
- Microarray profiling identified 4,026 differentially expressed genes
- Constitutively upregulated expression of oxidative stress genes included GPx2

4.5 Funding information

This work was funded by a joint Enterprise Ireland/Alltech Innovative Partnership programme (IP/2015/0375) and Science Foundation Ireland cofunded by ERDF, Grant no: 12/RC/2275_P2.

4.6 Supplementary Material

Raw and filtered transcriptomic data sets are published in mendeley's online repository:

http://dx.doi.org/10.17632/p976x9rk6w.2

Figure 4.5.1: Relative cell survival of parental control Caco-2 and Cu-resistant clones Or1, Or2, Or3, In1 and In2 exposed to increasing A: Cu proteinate, B: $CuSO_4$. Asterisk indicates significant difference from parental Caco-2 (** = P < 0.01), N=3.

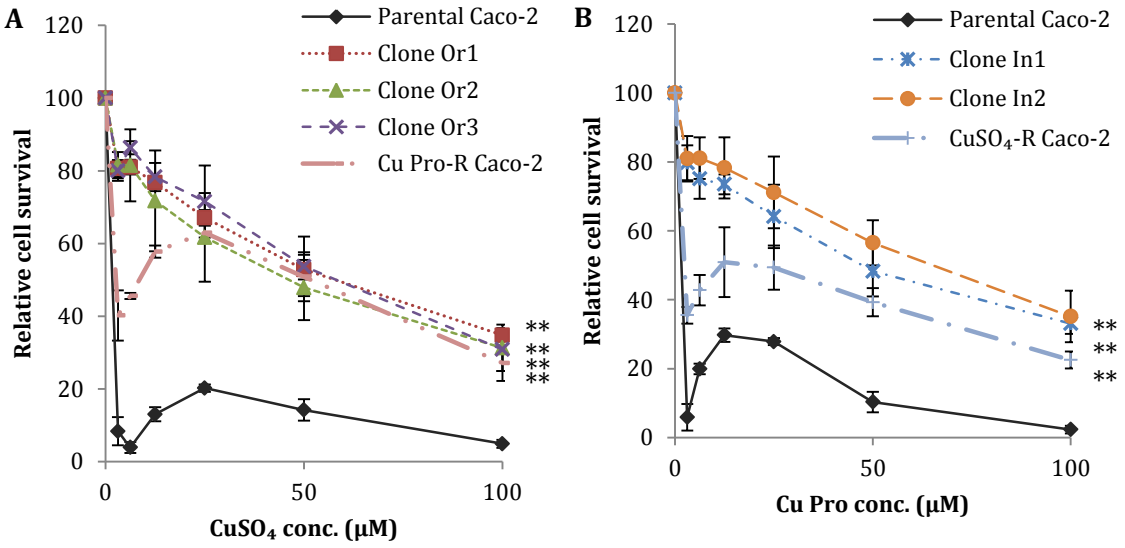

Figure 4.5.2: Relative mRNA expression determined by qRT-PCR for: ANXA13, GPx2, AIFM2, ATP7B and UPK1B in Caco-2 and Cu-resistant clones In1, In2, Or1, Or2 and Or3. Control Caco-2 exposed to 50 μM $CuSO_4$ and Cu proteinate also shown. β-actin used as endogenous control. Logarithmic scale used for ANXA13 and UPK1B for clarity. Asterisk indicates significant difference from parental ($P < 0.05$). N=3

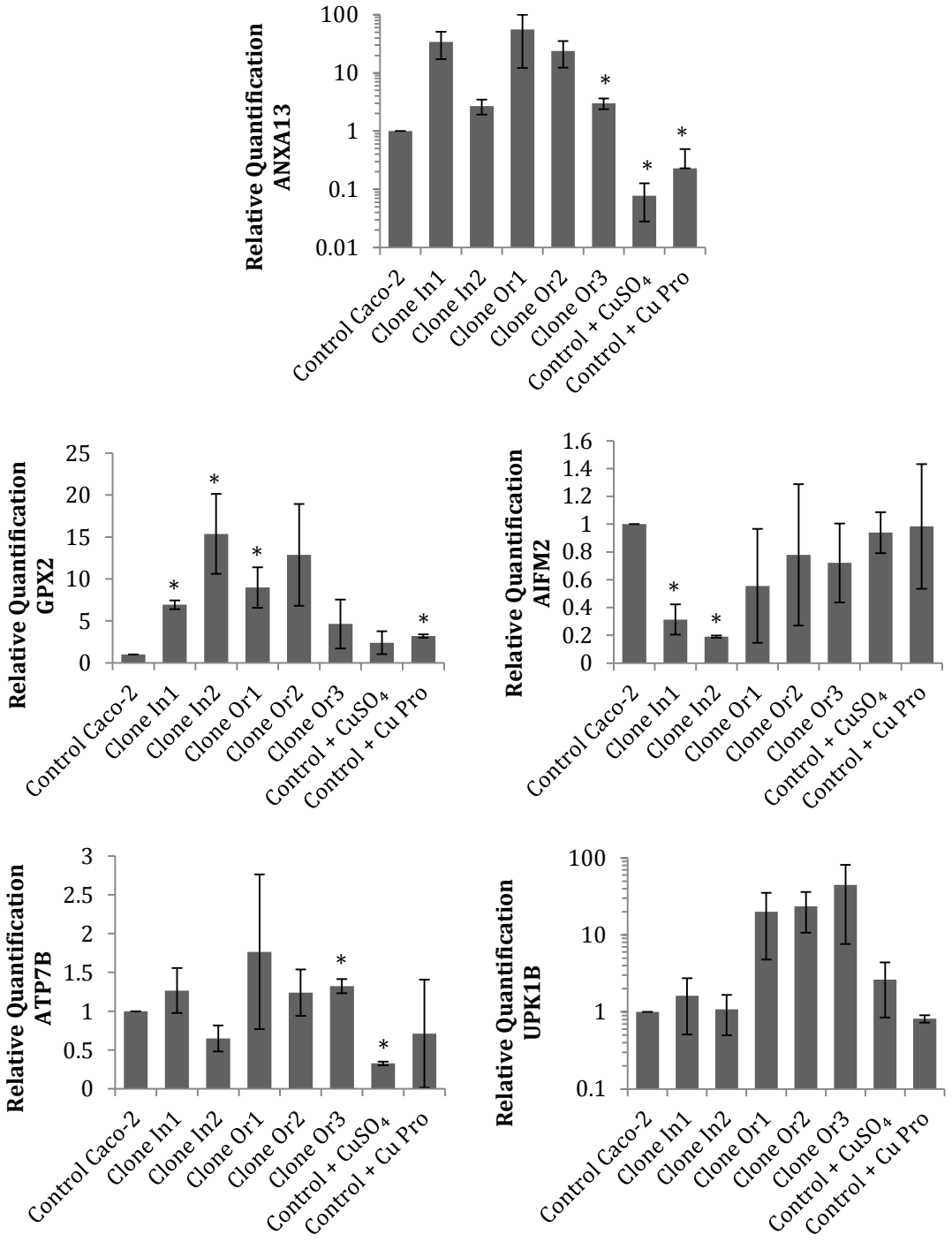

Figure S3: mRNA fold-change determined by microarray analysis for: ANXA13, GPx2, AIFM2, ATP7B and UPK1B in Caco-2 and Cu-resistant clones In1, In2, Or1, Or2 and Or3. Only targets detected as differentially expressed are shown (N=3)

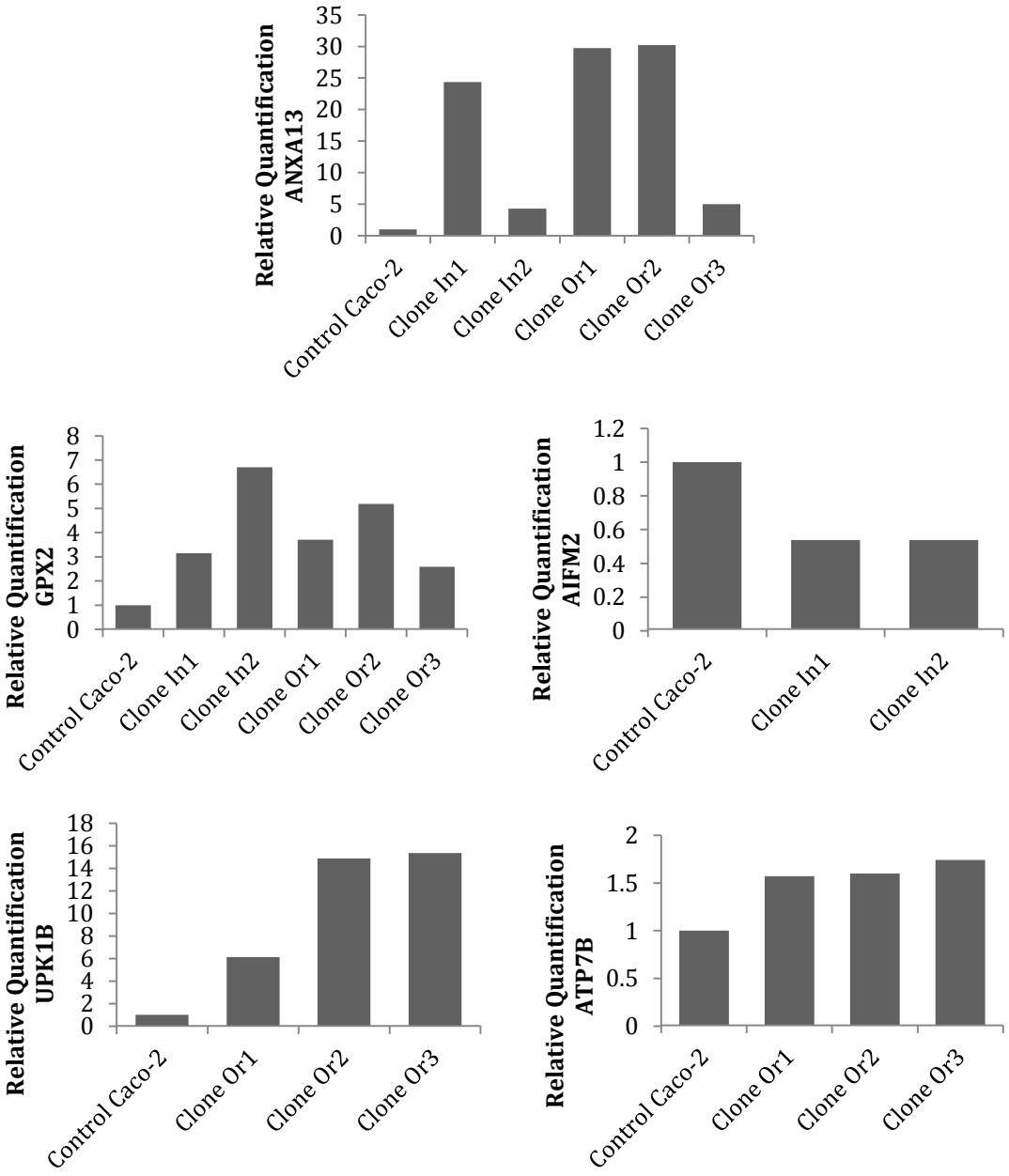

Table 4.5.1: List of primers for qRT-PCR, supplied by Invitrogen™ Custom DNA Oligos (Thermo Fischer)

Gene name	Forward	Reverse
ANXA13	5'-GGTTCGCTCAGATACCTCCG-3'	5'-TTCCTATTGCCCTGGCTTGG-3'
ATP7B	5'-GTGGGCAATGACACCACTTT-3'	5'-TGGGTGCCTTTGACATCTGA-3'
GPX2	5'-AGCTCATCATTTGGAGCCCT-3'	5'-TTGATGGTTGGGAAGGTGCG-3'
AIFM2	5'-ATGGTTCGGCTGACCAAGAG-3'	5'-GCCACCACATCATTGGCATC-3'
UROPLAKIN 1B	5'-GGCGTAAATGGTCCATCAGA-3'	5'-AGGCGTGTCGGTTCATTGGA-3'
β-actin	5'-TGGACATCCGCAAAGACCTGTA-3'	5'-TCAGGAGGAGCAATGATCTTGA-3'

Table 4.5.2: KEGG analysis of common genes >2 fold differentially expressed in at least 4/5 clones (331 total input into DAVID version 6.8). Only pathways with ANOVA P value less than 0.05 shown. Arrows indicate direction of expression relative to parental Caco-2

Term	Genes	P-Value
MAPK signalling pathway	EGF ↑, FGFR4 ↑, HSPA1A ↑, HSPA1B ↑, ARRB1 ↓, DUSP10 ↓, HSPA2 ↓, FGFR2 ↓, RASGRP1 ↓, RASGRP3 ↓, MAP2K6 ↓, MAP3K5 ↓, RPS6KA5 ↓	5.20E-04
Rap1 signalling pathway	RASGRP3 ↓, ADORA2B ↑, ADCY7 ↓, EGF ↑, FGFR2 ↓, FGFR4 ↑, MAGI3 ↓, MAP2K6 ↓, THBS1 ↓	1.60E-02
Toxoplasmosis	BIRC2 ↑, BIRC3 ↑, HSPA1A ↑, HSPA1B ↑, HSPA2 ↓, MAP2K6 ↓	2.80E-02
Focal adhesion	BIRC2 ↑, BIRC3 ↑, EGF ↑, COL2A1 ↓, COL5A2 ↓, ITGA1 ↓, MYL9 ↓, THBS1 ↓	4.10E-02
ECM-receptor interaction	CD44 ↑, COL2A1 ↓, COL5A2 ↓, ITGA1 ↓, THBS1 ↓	4.60E-02

Table 4.5.3: DAVID UniProt keywords associated with common DEGs >2 fold differentially expressed in at least 4/5 clones (331 total input into DAVID version 6.8). Only annotations with P value less than 0.05 shown.

	Gene Count	*P* value
Signal	89	0.000025
Glycoprotein	95	0.00003
Membrane	135	0.00036
Secreted	47	0.00042
Stress response	8	0.00054
Annexin	4	0.0009
Calcium/phospholipid-binding	4	0.0011
Transmembrane helix	101	0.0044
Chloride channel	5	0.0057
Disulfide bond	64	0.015
EGF-like domain	9	0.02
Chloride	5	0.02
SH3 domain	8	0.033
Pyrrolidone carboxylic acid	5	0.043

5 LC-MS proteomic profiling of Caco-2 human intestinal cells exposed to the copper-chelating agent, triethylenetetramine : A preliminary study

Authors: Charles O'Doherty[1], Finbarr O'Sullivan[1], Michael Henry[1], Paula Meleady[1], Martin Clynes[1], Karina Horgan[2], Joanne Keenan[1] and Richard Murphy[2]

[1] National Institute for Cellular Biotechnology and SSPC-SFI. Centre for Pharmaceuticals, Dublin City University, Glasnevin, Dublin D09 NR58, Ireland

[2] Alltech Ireland, European Bioscience Centre, Summerhill Rd, Sarney, Dunboyne, Co. Meath, Ireland

Journal: Biochemical and Biophysical Research Communications

Status: Accepted January 2020

DOI: 10.1016/j.bbrc.2020.01.138

I participated in all stages of this manuscript from conception and design of study, acquisition of data, analysis and interpretation of data, to drafting and revising the manuscript. MH ran the samples on LC-MS/MS, JK and FOS acquired and preformed preliminary processing of differential expression data. Alongside myself, FOS and JK carried out the experiments; and FOS, JK, MC, KH and RM participated in design concept, interpretation of data and review and revision of the manuscript.

Abstract

Homeostasis of metal micronutrients such as copper (Cu) is tightly regulated to ensure deficiency does not occur while restricting damage resulting from excess accumulation. Using LC-MS the effect on the proteome of intestinal-like Caco-2 cells of exposure to the chelator triethylenetetramine (TETA) was investigated. Continuous exposure of TETA at 25 µM to Caco-2 cells caused decreased cell yields and morphological changes. These effects were reversed when cells were no longer exposed to TETA.

Quantitative proteomic analysis identified 957 mostly low-fold differentially expressed proteins, 41 of these returned towards control Caco-2 expression following recovery. Proteins exhibiting this "reciprocal" behaviour included upregulated deoxyhypusine hydroxylase (DOHH, 15.69- fold), a protein essential for eIF-5A factor hypsuination, a post translational modification responsible for eIF-5A maturation, which in turn is responsible for translation elongation. Exposure to TETA also resulted in 87 proteins, the expression of which was stable and remained differentially expressed following recovery.

This study helps to elucidate the stable and transient proteomic effects of TETA exposure in intestinal-like cells.

5.1 Introduction

Metal micronutrients are essential dietary elements in humans and animals for proper cell function but may cause toxicity when present in excess due to their catalytic roles in redox reactions, thus homeostasis is strictly regulated to ensure adequate supply without causing toxicity. In cases of accidental overexposure or poisoning, chelators have long been employed to reduce absorption and toxicity of metals in the body (Sarkar and Clarke, 1969). Metal chelators are commonly used to treat accidental ingestion of heavy metals and also for the treatment of genetic disorders which result in systemic metal overload such as autosomal recessive Wilson's disease, characterised by potentially fatal Cu accumulation in the liver due to dysregulation of Cu exporter ATP7B (Purchase, 2013). Without adequate therapy, Wilson's disease can manifest in hepatic failure and may cause copper deposits to form in the basal ganglia, leading to Parkinsonian like disorders (Waggoner, Bartnikas and Gitlin, 1999).

To counterbalance the debilitating effects of Wilson's disease, regulation of systemic copper bioavailability may be achieved through chelation with a Cu^{2+} chelator; such as triethylenetetramine (TETA) (Sarkar and Clarke, 1969; Lu, 2010; Lu *et al.*, 2010). TETA is normally administered orally and its bioavailability is low, likely as a result of high charge at physiological pH (Lu, 2010; Tegoni *et al.*, 2014). The therapeutic mode of action for TETA relies on complex formation with dietary copper in the intestine, thus decreasing copper absorption (Purchase, 2013) but following administration of TETA, increased copper excretion in urine is observed (Flora and Pachauri, 2010). Clinical applications of TETA are also being explored for the treatment of cancer (Lu, 2010), diabetes mellitus (Gong *et al.*, 2009; Lu *et al.*, 2010) and Alzheimer's disease (Garth J.S. Cooper, 2011).

TETA is described as an extremely strong copper chelator (Nurchi *et al.*, 2013), capable of removing Cu from albumin-copper complex (Laurie and Sarkar, 1977) and reducing Cu absorption by 80% *in vivo,* restoring physiological Cu levels (Siegemund *et al.*, 1991). TETA also has binding affinity for other dietary metal micronutrients (Co, Fe, Mn, Ni and Zn), stability constants for which have been established (Pettit, Powell and Chemistry., no date; Nurchi *et al.*, 2013; Rakshit *et al.*, 2018).

Following digestion, absorption for most micronutrients takes place via enterocytes of the intestinal epithelium (Powell, Jugdaohsingh and Thompson, 1999). The intestinal-like Caco-2 line is a well characterised human colon adenocarcinoma cell line capable of substantial *in vitro* differentiation and often employed to represent enterocyte-like cells *in vitro*.

Our research has previously examined the effect of Cu toxicity and resistance in intestinal cell lines (O'Doherty *et al.*, 2019; O Doherty *et al.*, 2020), however micronutrient depletion and subclinical deficiency are of growing concern to human health (Bost *et al.*, 2016; DiNicolantonio, Mangan and O'Keefe, 2018) and represent the focus of the current study. To further elucidate the effect(s) of TETA chelator treatment on intestinal-like tissues, we examined exposure of Caco-2 cells to TETA and employed quantitative proteomic analysis to identify proteins which were differentially expressed both during TETA and following removal of the chelator.

5.2 Materials and Methods

5.2.1 Cell culture conditions

Exponentially growing Caco-2 cells (HTB-37 ™; American Type Culture Collection) were cultivated at 37 °C under 5% CO_2, in MEM (Gibco, 21090022) supplemented with 10% fetal bovine serum (FBS, Gibco, 10270-106), 10 mM HEPES (Sigma Aldrich, H3537), 2mM L-glutamine (Sigma Aldrich, G7513), with or without 25 µM added triethylenetetramine (TETA, Sigma Aldrich, 90460). Cells were passaged every 4 days, not allowing cells to reach confluence (Natoli *et al.*, 2011). Cells were routinely tested and found to be negative for *Mycoplasma* contamination.

5.2.2 Cell survival determination

Cells were seeded at 3125 cells/cm^2 and exposed after 24 hours for up to 120 hours before assaying by (A) acid phosphatase activity in 96-well microtiter plates (Martin and Clynes, 1991, 1993) and (B) in 25 cm^2 tissue culture flasks by viable cell count using haemocytometer and trypan blue exclusion method.

5.2.3 Western blotting

Cell lysates were prepared by solubilising cells in protein 2D lysis buffer (7 M Urea, 2 M Thiourea, 4% CHAPS and 30 mM Tris, pH 8.0), supplemented with nuclease mix (GE Healthcare, 80-6501-42) and protease inhibitor (Thermo Scientific™, A32963). Protein was quantified by modified Biorad assay (BioRad, 5000006). Lysates in Laemmli buffer were separated by SDS-polyacrylamide gel electrophoresis on a 4-12% SDS gel, transferred blots were blocked in NET buffer (1.5 M NaCl, 0.05 M EDTA, 0.5 M Tris pH 7.8, 0.5% Triton X-100) and incubated overnight at 4°C with primary

DOHH (SCBT, sc-376929) or GAPDH antibodies (CST, 5174). Secondary antibodies conjugated to horse-radish peroxidase (Sigma Aldrich) were incubated for 1 hour and detected by enhanced chemiluminesence (Luminol, Santa Cruz). Densitometry was performed using Epson Perfection 4990 scanner and TotalLab Quant software version 13.2.

5.2.4 Proteomic profiling and associated bioinformatics analysis

Exponentially growing Caco-2, TETA exposed (25 µM) treated and subsequently growth media recovered cells were harvested by trypsinization. Cell pellets were washed with ice cold PBS, snap frozen and stored at -80 ℃. Cell lysates were solubilised in 2D lysis buffer and mixed for 1 hour at room temperature (RT). Lysates were then centrifuged at 18,800 x g for 15 min at 4 ℃. The supernatants were transferred to a new microcentrifuge tube and protein concentration was determined using the Biorad protein assay. A homogenised lysate of 100 µg protein from each sample was prepared for MS by FASP (Coleman *et al.*, 2017).

Quantitative label-free LC-MS/MS proteomic analysis was performed using a Dionex Ultimate 3000 RSLCnano system coupled to an Orbitrap Fusion Tribrid mass spectrometer (both Thermo Scientific) (Coleman et al. 2019). Peptides were identified in Proteome Discoverer 2.2 and exported to Progenesis QI (NonLinear Dynamics, Waters) for relative quantitative analysis between experimental groups as previously described (Coleman *et al.*, 2018, 2019). A threshold of 5% sequence coverage was set for LC-MS/MS identified proteins, unless the molecular weight of the protein was less than 20 kDa or had greater than 2 unique identified peptide sequences. An additional threshold was set for fold changes > 1.5 with *P* value of < 0.05 and fold changes from 1.2 - 1.5 with *P* value of < 0.01.

Differentially expressed proteins (DEPs) were collated and uploaded into STRINGv11 (https://string-db.org/) to perform KEGG pathway analysis of the targets (Szklarczyk *et al.*, 2019). A *P v*alue of < 0.05 was set as threshold for inclusion of KEGG pathway analysis. The full proteomic data sets have been made publicly available online via Mendeley Data, V.2 (http://dx.doi.org/10.17632/wgh6hbt9kh.1).

5.2.5 Statistical analysis

To evaluate statistical significance between any two populations, *P*-values were calculated by two-tailed Students' t-test with 2-tailed distribution and two-sample heteroscedastic unequal variance (Microsoft Excel®). Significance was set at *P*-values less than 0.05. Error bars in all figures indicate standard error of the arithmetic mean. Relative values in all figures are expressed as percentage of untreated controls, unless otherwise noted. All experiments were repeated at least three times.

5.3 Results

5.3.1 Effect of TETA treatment on Caco-2 cell growth

Caco-2 cells demonstrated reduced cell growth with increasing concentrations of TETA exposure (1.6 µM – 204.8 µM) at 120 hours (Fig. 5.3.1A). Two phases of cell growth inhibition were observed during increasing TETA exposure to Caco-2 cells, with rapid decrease observed up to 25 µM (33% reduction) and thereafter a gradual reduction in cell yield up to 204.8 µM TETA (maximum 37% reduction) after 120 hours exposure. Due to TETA's effect on the Caco-2 phenotype and physiological relevance during treatment in a clinical setting, 25 µM TETA was selected for subsequent experiments (Lu, 2010, Pfeiffenberger *et al.*, 2018).

To examine the effect of sustained TETA treatment on cell yield, Caco-2 cells were continuously exposed to 25 µM TETA for 5 days before passaging and reseeding at the same density allowing surviving cells to attach overnight before re-exposing. Reduced cell yield was obtained following each passage in TETA (Fig. 5.3.1B), demonstrating that a phenotypic effect was achieved with exposure to TETA as low as 25 µM. When Caco-2 cells were subcultured twice in 25 µM TETA, removing TETA in the basal growth media on the third passage restored growth equivalent to untreated control within 72 hours.

The continous culture of of Caco-2 cells in 25 µM TETA over multiple subcultures resulted in several morphological differences compared to control cells (Fig. 5.3.1C). Caco-2 cells in continuous TETA treatment (25 µM) exhibited decreased cell volume and irregular cell borders (Fig. 5.3.1C II). These morphologic effects caused by TETA

exposure were reversed upon removal of the chelator and replacement with basal growth media (Fig. 5.3.1C III).

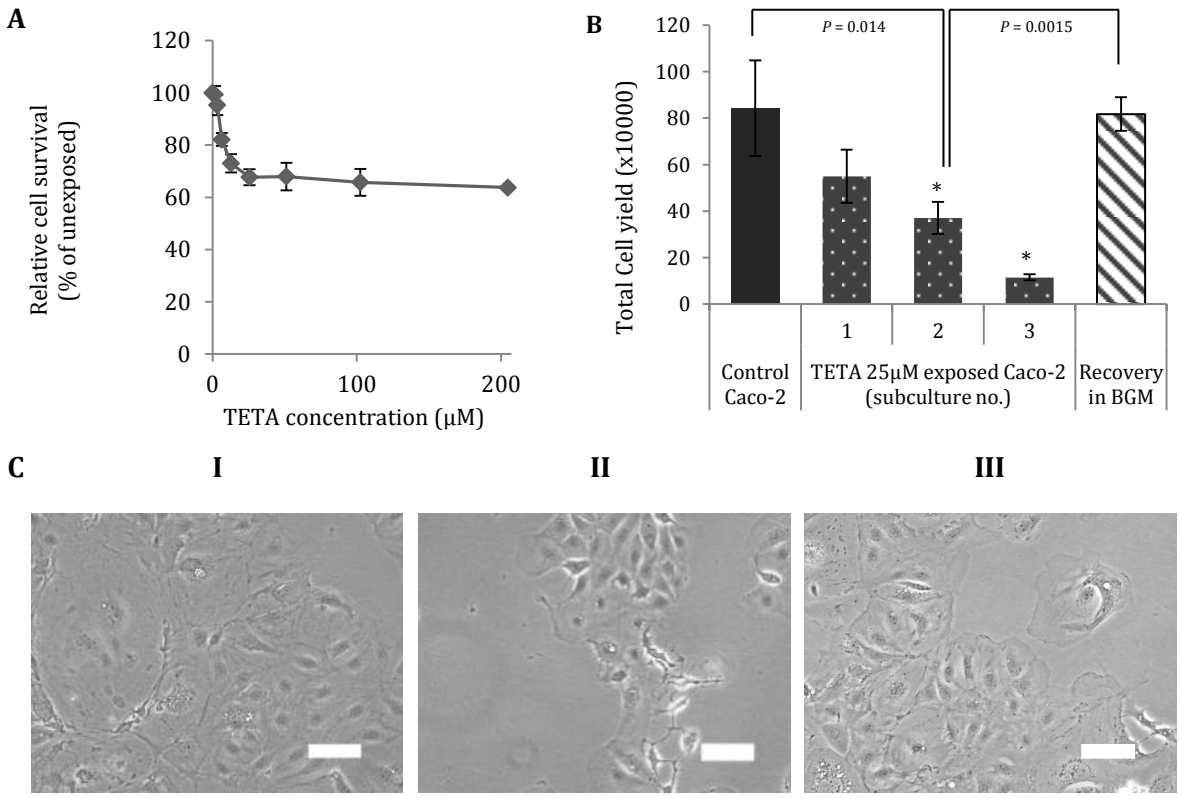

Figure 5.3.1: A: Relative cell survival of Caco-2 cells exposed to increasing TETA for 120 hours, cultured in 96-well plates, assayed by acid phosphatase (N=3). B: Total cell yield for untreated Caco-2 and Caco-2 cells following multiple exposures to 25 µM TETA. The hashed bar shows yield of cells pre-treated with 25 µM TETA for two passages and recovered in basal growth media (BGM) (N>3). Asterisk indicates significant difference from unexposed control ($p < 0.05$). C: Representative phase contrast images of (I) unexposed control Caco-2 cells (II) Caco-2 cells after two subcultures in presence of 25 µM TETA and (III) Caco-2 cells following restoration in basal growth media. Scale bar shown represents 100 µm

5.3.2 Identification of DEPs in Caco-2 cells exposed to TETA

To gain further insight into the proteins transiently and stably altered by TETA treatment to Caco-2 cells, differentially expressed proteins (DEPs) between unexposed control Caco-2, cells after two subcultures in 25 µM TETA treatment and cells recovered in basal growth media were examined by quantitative label-free LC-MS (Fig. 5.3.2A). A combined total of 957 differentially expressed proteins (DEPs) were identified during the three conditions and overlap between all discovered targets is represented by Venn diagram (Fig. 5.3.2B) - note this is an overlap of DE proteins, each circle representing a DE list (Google drive file tables S1-S3) generated by comparison of proteomic profiles between each of these conditions. KEGG pathways corresponding to each list were generated using STRINGv11 (Google drive file tables S4-S6) and included: protein processing in endoplasmic reticulum and cell death mechanisms including apoptosis and ferroptosis during TETA exposure.

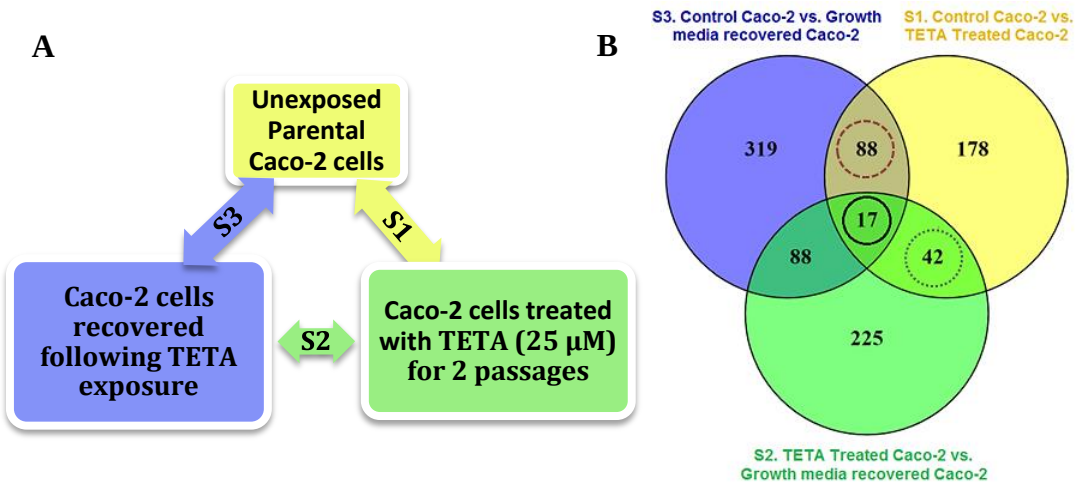

Figure 5.3.2: A: Design schematic for label-free LC-MS analysis with corresponding DEP tables S1-3. B: Venn diagram summary showing overlap of all differentially expressed proteins identified between Caco-2, 25 µM TETA treated Caco-2 and basal media-recovered Caco-2 cells. Oliveros, J.C. (2007-2015) Venny. Version 2.1. http://bioinfogp.cnb.csic.es/tools/venny/index.html

Forty-one of the 42 DEPs in common between 'control Caco-2 versus TETA treated' and 'TETA treated Caco-2 versus recovered' were "reciprocal" in their expression, i.e. proteins differentially expressed during TETA treatment which returned towards unexposed control Caco-2 levels during recovery (Fig. 5.3.2B, circled in grey dots, all except T-complex protein 1 subunit theta, CCT8). These reciprocal targets included proteins with established roles in handling excess oxidative stress: upregulated phospholipid hydroperoxide glutathione peroxidase (GPX4) and glutathione S transferase P (GSTP) and downregulated metallothionein 1G (MT1G) (Table 5.3.1A/B).

Similarly, 87 out of 88 proteins discovered between 'control Caco-2 versus TETA treated' and 'control Caco-2 versus recovered' were differentially expressed in the same direction, indicating protein expression induced by Caco-2 cell exposure to TETA which remained stably up- or downregulated after recovery in basal growth media (Fig. 5.3.2B, circled in red dashes, all except NAD(P)H-hydrate epimerase, NAXE). Stable proteins induced by TETA exposure included upregulated CAD protein, involved in biosynthesis of pyrimidines, and downregulated DNAJB11, co-chaperone for heat shock protein A5 (Table 5.3.1 C/D).

In addition, seventeen proteins were detected as differentially regulated in all three lists (Fig. 5.3.2B, circled in black), but these proteins exhibited predominantly low-fold changes (maximum 2.6- fold) and may be of limited functional significance. This list of 17 included two importins (IPO-4 and IPO-7) and two t-RNA ligases (NARS and EPRS) which increased during TETA treatment, increasing further following removal of TETA.

(A) DEPs reciprocally upregulated during TETA exposure

Protein Name	Description	Fold change up during TETA exposure	*P* Value	Fold change down following removal of TETA	*P* Value
DOHH	Deoxyhypusine hydroxylase	15.69	0.017	1.40	0.007
GSTP1	Glutathione S-transferase P	2.62	0.025	2.70	0.004
LSM14B	Protein LSM14 homolog B	1.64	0.007	2.56	0.014
GPX4	Phospholipid hydroperoxide glutathione peroxidase	1.63	0.007	3.66	0.023

(B) DEPs reciprocally downregulated during TETA exposure

Protein Name	Description	Fold change down during TETA exposure	*P* Value	Fold change up following removal of TETA	*P* Value
ACBD6	Acyl-CoA-binding domain-containing protein 6	4.95	0.035	6.31	0.045
SPINK1	Serine protease inhibitor Kazal-type 1	2.99	0.023	2.35	0.043
NAALAD2	N-acetylated-alpha-linked acidic dipeptidase 2	2.66	0.007	3.29	0.010
MT1G	Metallothionein-1G	2.06	0.019	3.07	0.018

(C) DEPs stably upregulated by TETA exposure

Protein Name	Description	Fold change up during TETA exposure	*P* Value	Fold change up following removal of TETA	*P* Value
CAD	CAD protein	2.77	0.017	3.87	0.005

(D) DEPs stably downregulated by TETA exposure

Gene Name	Description	Fold change down during TETA exposure	*P* Value	Fold change down following removal of TETA	*P* Value
DNAJB11	DnaJ homolog subfamily B member 11	3.68	0.047	1.69	0.005
UBE2E1	Ubiquitin-conjugating enzyme E2 E1	3.03	0.032	1.76	0.028
MRPL50	39S ribosomal protein L50, mitochondrial	2.63	0.039	2.26	0.019
HPGD	15-hydroxyprostaglandin dehydrogenase [NAD(+)]	2.58	0.022	1.68	0.018
UQCR11	Cytochrome b-c1 complex subunit 10	2.05	0.040	3.51	0.047
MARCKSL1	MARCKS-related protein	1.21	0.002	2.56	0.032

Table 5.3.1: Overlap of DEPs identified by quantitative label-free LC-MS/MS as: (A) reciprocally upregulated and (B) reciprocally downregulated during TETA treatment relative to unexposed parental Caco-2; (C) stably upregulated and (D) stably downregulated by TETA exposure to Caco-2 cells. Only DEPs where > 2.5-fold in at least one condition are shown, < 2.5-fold are presented in supplementary table S7 and S8 (available on Google Drive file).

5.3.3 Western blotting validation of DOHH

Expression of deoxyhypusine hydroxylase (DOHH), a hydroxylase required for hypusine modification of the translation factor eukaryotic initiation factor 5A (Frey *et al.*, 2014), was identified by proteomic analysis as highly increased during TETA treatment and subsequently decreased following restoration in basal growth media. Significantly increased DOHH expression was confirmed by Western blotting during TETA exposure (P = 0.009), and appeared to return towards unexposed control Caco-2 upon removal of TETA (Figure 5.3.3).

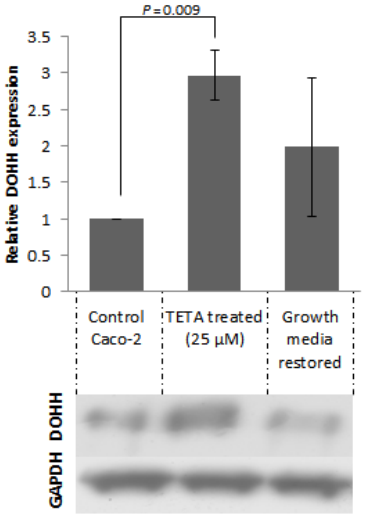

Figure 5.3.3: Representative Western blot for deoxyhypusine hydroxylase expression in Caco-2 cells pretreated with TETA 25 µM and following multiple passsages out of TETA exposure. Densitometry expressed relative to unexposed control and normalised to GAPDH (N=3).

5.4 Discussion

Both overload and deficiency of copper are detrimental to health, as evidenced by the genetic conditions Wilson's disease and Menkes disease (Lutsenko *et al.*, 2007; Purchase, 2013). We here describe the phenotypic and proteomic effects caused by exposure of intestinal-like Caco-2 cells to triethylenetetramine (TETA), a chelator used in the treatment of Wilson's disease. We examined the proteomic profiles generated both during TETA exposure and following recovery in basal growth media. TETA treatment (25 μM) resulted in mostly low-fold changes to the proteomic profile of Caco-2 cells, with 957 total differentially expressed proteins (DEPs) identified by quantitative label-free LC MS/MS as a consequence of exposure and subsequent recovery.

Effect of TETA treatment on copper related protein expression

Though TETA is used to treat copper overload *in vivo*, very few of the key proteins related to copper metabolism were differentially regulated under the conditions of our experiment, despite the extensive range of discovered. Metallothioneins (MT) protect against metal-induced toxicity by scavenging intracellular metal ions and rendering them inactive. Overexpression of MT was observed following BCS exposure to induce Cu depletion in cultured wild type and MT-knockout mouse cells, resulting in protection against copper deficiency by maintaining cuproenzyme function (Ogra, Aoyama and Suzuki, 2006). Only one isoform of metallothionein (MT1G) was detected by proteomic analysis as downregulated during TETA exposure, returning towards control level of ion during recovery.

Decreased cytochrome c oxidase (CCO) and superoxide dismutase (SOD) activities were demonstrated in neurons following exposure of BCS previously (Ogra *et al.*, 2016). During our proteomic analysis cytochrome c oxidase subunit 1 (MT-CO1) was

upregulated during TETA treatment while cytochrome c oxidase subunit 2 (MT-CO2) was stably upregulated after removal of TETA. SOD protein was not detected, although copper chaperone for superoxide dismutase (CCS) was decreased during recovery in basal growth media (1.54- fold), potentially indicating reduced availability of Cu for SOD synthesis following TETA exposure. The contrast in the expression of MT, SOD and CCO with the results obtained by other studies suggests their relative expression may differ depending on the chelator used during exposure or may be cell type specific. In parallel with TETA, BCS has been employed to deplete Cu in cells *in vitro* previously (Zerounian and Linder, 2002; Ramos *et al.*, 2016), both demonstrating decreased intracellular Cu accumulation and comparable increased iron uptake following exposure.

TETA treatment results in upregulated DOHH expression

A major unanticipated and novel discovery from our profiling was that levels of deoxyhypusine hydroxylase (DOHH) protein were significantly increased by exposure of Caco-2 cells to TETA. DOHH is a highly specialized hydroxylase, serving an essential role in the hydroxylation of a critical lysine residue of highly-conserved eukaryotic translation initiation factor 5A (eIF-5A) to complete a process known as hypusination (Chattopadhyay, Myung and Tabor, 2008). eIF5A is involved in multiple cellular processes including actin dynamics and mRNA decay and plays a key role in the regulation of cell proliferation (Vu *et al.*, 2009). Hypusination modification of eIF-5A is essential for translation of several proteins in eukaryotes (Gutierrez *et al.*, 2013; Schuller *et al.*, 2017).

Spermidine is the limiting substrate for hypusination of eIF-5A (Chattopadhyay, Myung and Tabor, 2008) and expression of spermidine synthase; the enzyme responsible for

spermidine synthesis, was increased by TETA exposure in our proteomic analysis (1.58-fold). Moreover, affinity between eIF-5A and the ribosomal components were recently determined to be hypusine-dependent and displacement between the ribosome and endogenous eIF-5A was generated by eukaryotic elongation factor 2 (eEF2) and hypusinated eIF-5A (Rossi *et al.*, 2016), suggesting eEF2 is responsible for maintaining balance of translation elongation. In our analysis expression of eEF2 was stably upregulated by TETA exposure in Caco-2 cells (1.67- and 1.81- fold, respectively).

Further studies will be required to determine the effect TETA exposure has on hypusinated eIF5A in intestinal tissues. It may be useful to examine whether hypusination of eIF5A is specific to TETA or it also follows exposure to other chelators. Isoforms of eIF5A are involved in carcinogenesis, and as DOHH is specifically required for post-translational hypusination of eIF5A, drugs which target DOHH expression are being explored as potential cancer therapies (Mathews and Hershey, 2015).

To the best of our knowledge this is the first report of quantitative proteomic profiling of intestinal-like cells during TETA exposure. TETA treatment resulted in many phenotypic and proteomic changes to Caco-2 cells, only some of which were identified as reversible upon removal of the chelator. In summary, we examined the effect of chelator TETA exposure to intestinal-like cells to examine the proteomic profiles generated. TETA treatment (25 μM) demonstrated decreased total Caco-2 cell yield, which progressively reduced over multiple passages and subsequent restoration of cell yield by recovery in growth media. Quantitative label-free proteomic analysis revealed multiple proteins which were differentially expressed both stably and transiently by TETA exposure including the specific hydroxylase DOHH. The proteomic profiles generated in this study served to increase understanding of the effect of TETA treatment

on the proteome of intestinal-like Caco-2 cells. Further analysis will help to elucidate additional mechanisms which play roles in intestinal metal micronutrient homeostasis and their potential implications *in vivo*.

Highlights:

- Exposure to chelator TETA altered Caco-2 cell phenotype and protein expression
- 957 differentially expressed (DE) proteins were identified following TETA exposure
- Stable and transiently expressed proteins were collated between DE lists
- Deoxyhypusine hydroxylase expression was highly increased following TETA exposure

5.5 Supplementary material

All supplementary information (Tables S1-S8) is available on Google Drive:

https://drive.google.com/open?id=1B-WUKjGXBBalH_CQ3urvx6SjAvUvtxSL

Raw and filtered proteomic data sets are published in mendeley's online repository:

http://dx.doi.org/10.17632/wgh6hbt9kh.1

5.6 Funding information

This work was funded by a joint Enterprise Ireland Innovative Partnership programme (IP/2015/0375) and Science Foundation Ireland cofunded by ERDF, Grant no: SFI SSPC Centre 12/RC/2275_P2

6 Overview, future perspectives and concluding remarks

Many metals (Cu, Fe, Mn, Co, Ni, and Zn) are required as essential micronutrients for healthy physiological function. In animals these metal micronutrients are acquired predominantly through ingestion with uptake via transport pathways present in enterocytes.

The research in this thesis has focussed on the trace micronutrient copper (Cu), whose homeostasis is strictly regulated and highly conserved across species (Festa and Thiele, 2011). Dysfunction of the Cu transport and storage mechanisms can lead to multiple disease states and predominantly due to oxidative damage via uncontrolled redox-reactions (Bleackley *et al.*, 2009; Kozlowski *et al.*, 2009).

The study of intestinal mechanisms involved *in vivo* is complex. To overcome this, the studies presented in this thesis employed the Caco-2 cell line, which has characteristics of enterocytes, and are the cell line of choice when generating *in vitro* models of the intestine (Sambuy *et al.*, 2005; Shah *et al.*, 2006). The use of this cell line allowed for robust and reproducible *in vitro* culture studies.

The studies presented here are linked by their use of the same model to examine micronutrient interactions, specifically focussing on copper exposure in the intestine. The combination of approaches used has resulted in the identification of a previously undiscovered cellular response to copper in intestinal Caco-2 cells: the non-monotonic dose response. This discovery led to the examination of proteomic and transcriptomic profiles in Caco-2 variants and clones resistant to inorganic $CuSO_4$ and Cu proteinate,

which were developed throughout the course of the study. Finally, to complement the overload and resistance studies and also to distinguish from them, micronutrient restriction was examined by exposure to chelator TETA, allowing for the identification of a variety of changes at the protein level.

Importantly, studies are rarely completed without limitations, and this body of work is no exception. Naturally, additional models (ideally *ex vivo* enteroids) would be necessary to verify the targets and pathways identified in the 'OMIC's' chapters. Additionally, to accurately depict the *in vivo* journey of dietary nutrients through the gastrointestinal tract, intestinal exposure studies would ideally mimic the involvement of pH gradient shifts alongside exposure to the gut microbiome and also facilitate digestion prior to exposure (Glahn *et al.*, 1998), as these interactions both play important roles in nutrient acquisition. However, they often also result in increased variability and thus require rigorous optimisation before incorporating in experimental design. These steps would be prudent and advised for subsequent *in vitro* analysis of intestinal exposures.

6.1 Non-monotonic dose response to copper by Caco-2 cells

The discovery of a non-monotonic dose response (NMDR) in parental Caco-2 cells during Cu exposure lead to the paper *"Copper-induced non-monotonic dose response in Caco-2 cells"*. The identification of a non-linear dose-response relationship by two different forms of copper (inorganic $CuSO_4$ and organic Cu Pro) in Caco-2 cells reflects the complexity of response to compounds and interactions that can occur. In recent years there is increasing research focussed on the identification and characterisation of mechanisms associated with NMDRs (Calabrese *et al.*, 2016).

NMDRs are being increasingly considered when revising safe dose ranges for exposure in both animals and humans (Chambers *et al.*, 2010; Hill, Myers and Vandenberg, 2018). To the best of my knowledge, this study was the first to identify such a NMDR of Cu in the Caco-2 intestinal cells. We also know from previous work in our lab that small fluctuations in copper content will cause significant changes in protein expression and can have impacts on cell growth and cell stress (Keenan, O'Sullivan, *et al.*, 2018) and the NMDR concentrations identified in this study are being investigated further in terms of their resulting proteomic profile to examine the mechanism(s) involved.

Future work:

Proteomic, mRNA and miRNA microarray profiling would further our understanding of the biological mechanisms of the observed inflection point

1. Proteomic profiling at early time points (4 hr, 24 hr and 48 hr) has been carried out at the inflection point (3.125 μM $CuSO_4$) and at the higher less toxic copper concentration (25 μM $CuSO_4$). Preliminary results indicate early induction of proteins related to antioxidant and cell stress response at the higher copper concentration (25 μM) lead to a greater protective effect as measured by the reduction in misfolded proteins in Caco-2 exposed to the higher copper concentration (manuscript in preparation).
2. Analysis of mRNA and miRNA microarray profiling will shed more light on the factors controlling the earlier induction of protective effects seen at the higher copper concentration.
3. NMDR in Caco-2 cells should also be examined in a differentiated system such as 21-day co-cultured Caco-2:HT29-MTX.

6.2 The study of resistance to copper in Caco-2 cells

In response to elevated concentration of trace metals, cells may exhibit or generate metal defence/resistance mechanisms to offset negative effects. There is a lack of knowledge about the development of metal resistance in animals. Arising from the concentrations defining NMDR response in the first study, two further studies were conducted to gain insights into the regulation of metal stress responses in Caco-2 cells. This involved the generation of Cu resistant Caco-2 cells with altered toxicity/growth and ROS profiles using exposure to either inorganic ($CuSO_4$) or organic (Cu proteinate) sources of copper. The most powerful proteomic profiling technology available allowed for the identification of different pathways specifically associated with different forms of Cu; organic Cu proteinate resistant Caco-2 revealed the specific upregulation of proteasome while inorganic $CuSO_4$ indicated greater involvement of DNA replication and cell cycle specific proteins.

To further study this Cu resistance, multiple clones from the Cu-resistant Caco-2 variants were isolated. The mRNA expression of these Cu resistant clones was investigated using microarrays. The strength of this study lies in the identification of multiple pathways associated with Cu-resistance and metal homeostasis during overexposure of Cu, by overlapping the differentially expressed genes from all clones to examine commonality between their respective expression patterns. Additionally, novel changes specific to clones derived from organic Cu proteinate and inorganic $CuSO_4$ were identified.

These studies of the proteome of Cu resistant Caco-2 variants and the mRNA expression of resistant clones resulted in two manuscripts, *"Characterisation and*

proteomic profiling of continuously exposed Cu-resistant variants of the Caco-2 cell line" and *"Microarray profiling of copper-resistant Caco-2 clones"*.

In tandem with mRNA microarray profiling, the profiling of micro RNAs (miRNA or miRs) was also completed. Preliminary analysis using of the dysregulated miRs in Cu-resistant Caco-2 clones indicated 181 total miRNA (78 unique and 103 shared) were differentially expressed (Appendix Fig. 4). Threshold responses indicate a cohort of 23 miRNA which were shared in expression between all clones. This group of 23 miRs may be involved in copper resistance regulation and response to chronic copper exposure including highly overexpressed miR-486-5p.

Reduced miR-486-5p expression has been found previously in colorectal cancer patients (Zhang *et al.*, 2018) and its involvement with MAPK and insulin growth factor (IGF) signalling pathways has also been elucidated in hepatocellular carcinoma, via repression of multiple members across the IGF-axis (Youness *et al.*, 2016). Putative targets of miR-486-5p (TargetScan 7.1) include cell adhesion molecule 1 (CADM1) which was found to be downregulated in multiple clones. The connection between specific miRNAs such as miR-486-5p with predicted protein targets and pathways in Cu-resistance is the subject of ongoing investigation.

These investigations on Cu-resistance and overload exploited the heterogeneous property of Caco-2 cells. However, this also represents a limitation, as additional Caco-2 subpopulations may also present with Cu-resistance and generate vastly different profiles than those established and isolated in these studies.

Further analysis is required to generate increased physiologically relevant data and to build a broader picture of the relevance *in vivo* by incorporating the use of differentiated models to further analyse differences associated with inorganic and organic Cu sources

and the role played by miRNA in regulation of protein expression. The following outlines how this and additional future work could be undertaken:

Future work:

1. *In silico* prediction of protein targets for miRNAs using various software packages such as TargetScan is unreliable. To obtain greater clarity on possible miRNA targets a triomic approach is envisaged as has been previously used within the laboratory (O'Sullivan *et al.*, 2017). The output from proteomic profiling of each of the clones will be co-ordinated with the outputs from the existing mRNA and miRNA profiles to identify high value targets for follow up validation.
2. Validation of the involvement of the proteasome in Cu proteinate derived Caco-2 variants using activity-based proteasome probes (Gan *et al.*, 2019). Cell cycle involvement in $CuSO_4$ derived Caco-2 variants may be examined by flow cytometry to determine phases of the cell cycle (G0/G1, S, and G2/M).
3. Further investigations on different mechanisms of resistance.

   Potential future studies on Cu resistance include the focus of individual clones of Caco-2 which display particular phenotypic and expression traits. Validation of phenotypic differences observed in Cu resistant Caco-2 clones by immunofluorescence to stain for specific targets such as zonula occludens (tight junction presence).
4. Functional validation of targets arising from Cu resistant Caco-2 variants and clones (e.g. ANXA13) by knockdown of specific mRNA using RNA interference to selectively inhibit their expression (via transfection with small interfering RNA or short hairpin RNA plasmids). Similarly the induction of

expression in parental cells by transfection with a plasmid containing the target may also be incorporated.

5. Inhibition of miRNAs by sponge technology to determine the effect of specific miRNA on Cu resistance in Caco-2 clones. Alternatively genetic knockout of the gene encoding the target miRNA may be attempted (Ebert and Sharp, 2010).
6. In addition the use of the resistant clones to generate differentiated *in vitro* co-culture models would provide a means to determine the effect of these targets in more physiologically representative conditions. As such models are usually on a transwell system it would also allow for epithelial barrier to be assessed and transport studies to be conducted using ICP-MS. The various mechanisms and targets can be further validated using primary cultures such as intestinal enteroids from human and mouse primary tissues or those derived from iPS cell differentiation.

6.3 Effect of micronutrient restriction on the Caco-2 proteome

The previous method of Cu overload demonstrated a significant shift in both protein and gene expression, however constitutive expression of Cu homeostasis proteins was relatively intact. An alternative to manipulate the balance of the Cu binding proteome was proposed via restriction using a Cu chelator. Thus, the effect of metal chelation by exposure of a chelator used to treat Cu overload in Wilson's disease: triethylenetetramine (TETA) was examined.

This was an exploratory investigation into the effect of TETA exposure to intestinal-like cells, under the hypothesis that depletion of intracellular micronutrients would yield a protective response, as observed by others examining different conditions (Ogra,

Aoyama and Suzuki, 2006). This study was limited by the specificity of TETA; while the chelator is often referred to as Cu^{2+}-selective, it has binding affinity to multiple other metals and this must be kept in consideration when interpreting the proteomic data analysis which resulted following exposure and recovery.

Regardless, this study served as the first to examine the effect on Caco-2 global proteomic expression during exposure to a chelator such as TETA, resulting in a paper entitled *"Response of Caco-2 human intestinal cells to TETA exposure: LC-MS proteomic profile demonstrates multiple changes including greatly increased level of deoxyhypusine hydroxylase"*. The novel finding of highly upregulated expression of deoxyhypusine hydroxylase during TETA exposure may have implications for patients receiving TETA treatment and also in drug development, as DOHH is being explored as a potential cancer therapy.

Future work:

1. Examine the effect on DOHH expression in Caco-2 cells during exposure to additional chelators (as described in section 1.9).
2. Determine the effect of DOHH expression knockdown during exposure to TETA using RNA interference (as described in section 6.2).

6.4 Final conclusions

In this body of work, proliferating Caco-2 cells were chosen since they represent a well characterised model of the small intestine and have been used to examine micronutrient interactions and effects on gene and protein expression *in vitro* previously. The work led to the novel identification of the NMDR in Caco-2 cells in response to copper exposure, the generation and characterisation of Cu-resistant Caco-2 variants and clones as models of Cu resistance and increased our understanding of micronutrient restriction by TETA exposure. Overall, the studies have proven to be useful in assessing toxicity responses and the development of metal resistance in eukaryotic intestinal cells.

In conclusion, the studies presented in this thesis on the response of Caco-2 cells to Cu exposure provide an increase in the knowledge regarding how enterocytes manage their response to Cu uptake. The various findings demonstrated that the response to different forms of copper (inorganic and organic) possessed not only similarities but also differences. In particular, it was noted that in Caco-2 cells exposure to the organic Cu proteinate, while generating vastly different protein, mRNA and miRNA expression profiles, did not generate increased toxicity or markers of cell stress response. In addition, the research identified a novel NMDR response in Caco-2, greatly furthered the understanding regarding protein and mRNA expression during Cu overload by the use of "omics" tools, and during TETA exposure, identified the upregulation of DOHH; an enzyme essential in the maturation of factor eIF-5A. Furthermore, by publishing all raw proteomic and transcriptomic analyses to Mendeley's online repository, the data sets arising from this thesis have added to the knowledge base available to researchers.

Transition metals are becoming increasingly implicated in health and disease, particularly in neurodegenerative, metabolomic and other disorders, thus identification of novel genes and pathways involved in both overload and deficiency is of great importance in the prevention, diagnosis and for the potential treatment of such diseases. Oxidative stress and copper are intrinsically linked to the majority of diseases from diabetes to Alzheimer's to cancer, evidenced by exciting novel treatments involving copper-conjugated drugs and copper chelators. Thus, furthering our understanding of cell responses to oxidative stressors, such as excess copper, via their transcriptomic and proteomic expression patterns and associated pathways brings us a step closer to reducing harm caused by these debilitating and too-often fatal diseases.

7 References

Adamo, G. M. *et al.* (2012) 'Laboratory evolution of copper tolerant yeast strains', *Microbial Cell Factories*. BioMed Central Ltd, 11(1), p. 1. doi: 10.1186/1475-2859-11-1.

Aebersold, R. and Mann, M. (2016) 'Mass-spectrometric exploration of proteome structure and function', *Nature*, 537(7620), pp. 347–355. doi: 10.1038/nature19949.

Aldave, A. J. *et al.* (2006) 'Corneal Copper Deposition Associated With Chronic Lymphocytic Leukemia', *American Journal of Ophthalmology*, 142(1), pp. 174–176. doi: 10.1016/j.ajo.2006.01.078.

Almeqdadi, M. *et al.* (2019) 'Gut organoids: Mini-tissues in culture to study intestinal physiology and disease', *American Journal of Physiology - Cell Physiology*, 317(3), pp. C405–C419. doi: 10.1152/ajpcell.00300.2017.

Andersen, O. and Freeland-Graves, J. (2012) 'Recent developments in trace element research', *Journal of Trace Elements in Medicine and Biology*. Elsevier GmbH., 26(2–3), pp. 59–60. doi: 10.1016/j.jtemb.2012.05.004.

Angelis, I. De and Turco, L. (2011) 'Caco-2 Cells as a Model for Intestinal Absorption', *Current Protocols in Toxicology*, 20.6(February), pp. 1–15. doi: 10.1002/0471140856.tx2006s47.

Antoniades, V. *et al.* (2013) 'Is copper chelation an effective anti-angiogenic strategy for cancer treatment?', *Medical Hypotheses*. Elsevier Ltd, 81(6), pp. 1159–1163. doi: 10.1016/j.mehy.2013.09.035.

Antunes, F. *et al.* (2012) 'Establishment of a triple co-culture in vitro cell models to study intestinal absorption of peptide drugs.', *European journal of pharmaceutics and biopharmaceutics : official journal of Arbeitsgemeinschaft für Pharmazeutische Verfahrenstechnik e.V*, 83(3), pp. 427–35. doi: 10.1016/j.ejpb.2012.10.003.

Ao, T. *et al.* (2009) 'Effects of feeding different forms of zinc and copper on the performance and tissue mineral content of chicks.', *Poultry science*, 88(10), pp. 2171–2175. doi: 10.3382/ps.2009-00117.

Araújo, F. and Sarmento, B. (2013) ‘Towards the characterization of an in vitro triple co-culture intestine cell model for permeability studies.’, *International journal of pharmaceutics*. Elsevier B.V., 458(1), pp. 128–34. doi: 10.1016/j.ijpharm.2013.10.003.

Araya, M. *et al.* (2002) ‘Biological Effects of Chronic Copper Exposure’, in Massaro, E. J. (ed.) *Handbook of Copper Pharmacology and Toxicology*. Totowa, NJ: Humana Press, pp. 385–396. doi: 10.1007/978-1-59259-288-3_23.

Araya, M. *et al.* (2005) ‘Supplementing Copper at the Upper Level of the Adult Dietary Recommended Intake Induces Detectable but Transient Changes in Healthy Adults’, *The journal of Nutrition*, (January), pp. 2367–2371.

Armendariz, A. D. *et al.* (2004) ‘Gene expression profiling in chronic copper overload reveals upregulation of Prnp and App.’, *Physiological genomics*, 20(1), pp. 45–54. doi: 10.1152/physiolgenomics.00196.2003.

Arredondo, M. *et al.* (2006) ‘Inhibition of iron and copper uptake by iron, copper and zinc’, *Biological Research*, 39(1), pp. 95–102. doi: 10.4067/S0716-97602006000100011.

Arredondo, M., Uauy, R. and González, M. (2000) ‘Regulation of copper uptake and transport in intestinal cell monolayers by acute and chronic copper exposure’, *Biochimica et Biophysica Acta - General Subjects*, 1474(2), pp. 169–176. doi: 10.1016/S0304-4165(00)00015-5.

Artursson, P., Palm, K. and Luthman, K. (2001) ‘Caco-2 monolayers in experimental and theoretical predictions of drug transport’, *Advanced Drug Delivery Reviews*, 46(1–3), pp. 27–43. doi: 10.1016/S0169-409X(00)00128-9.

Bajak, E. *et al.* (2015) ‘Changes in Caco-2 cells transcriptome profiles upon exposure to gold nanoparticles’, *Toxicology Letters*. Elsevier Ireland Ltd, 233(2), pp. 187–199. doi: 10.1016/j.toxlet.2014.12.008.

Barceloux, D. G. and Barceloux, D. (1999) ‘Copper’, *Journal of Toxicology: Clinical Toxicology*, 37(2), pp. 217–230. doi: 10.1081/CLT-100102421.

Barker, N. (2014) ‘Adult intestinal stem cells: critical drivers of epithelial homeostasis and regeneration.’, *Nature reviews. Molecular cell biology*. Nature Publishing Group,

15(1), pp. 19–33. doi: 10.1038/nrm3721.

Barresi, V. *et al.* (2016) 'Transcriptome analysis of copper homeostasis genes reveals coordinated upregulation of SLC31A1 , SCO 1, and COX11 in colorectal cancer', *FEBS Open Bio*, 6(8), pp. 794–806. doi: 10.1002/2211-5463.12060.

Bartłomiejczyk, T. *et al.* (2013) 'Silver nanoparticles – allies or adversaries ?', *Annals of Agricultural and Environmental Medicine*, 20(1), pp. 48–54.

Bauer, H. *et al.* (2010) 'The dual role of zonula occludens (ZO) proteins', *Journal of Biomedicine and Biotechnology*, 2010(Figure 1). doi: 10.1155/2010/402593.

Beloqui, A. *et al.* (2017) 'A human intestinal M-cell-like model for investigating particle , antigen and microorganism translocation', 12(7), pp. 1387–1399. doi: 10.1038/nprot.2017.041.

Benedetto, L. M. De *et al.* (2014) 'Glutaredoxin 1 is a major player in copper metabolism in neuroblastoma cells', *Biochimica et Biophysica Acta BBA - General Subjects*. Elsevier B.V., 1840(1), pp. 255–261. doi: 10.1016/j.bbagen.2013.09.008.

Van den Berghe, P. V. E. and Klomp, L. W. J. (2009) 'New developments in the regulation of intestinal copper absorption.', *Nutrition reviews*, 67(11), pp. 658–72. doi: 10.1111/j.1753-4887.2009.00250.x.

Bertinato, J. and L'Abbé, M. R. (2003) 'Copper modulates the degradation of copper chaperone for Cu,Zn superoxide dismutase by the 26 S proteosome', *Journal of Biological Chemistry*, 278(37), pp. 35071–35078. doi: 10.1074/jbc.M302242200.

Bertinato, J., Sherrard, L. and Plouffe, L. J. (2010) 'Decreased erythrocyte CCS content is a biomarker of copper overload in rats', *International Journal of Molecular Sciences*, 11(7), pp. 2624–2635. doi: 10.3390/ijms11072624.

Bertino, J. *et al.* (1996) 'Resistance Mechanisms to Methotrexate in Tumors', *The Oncologist*, 1, pp. 223–226.

Bigagli, E. *et al.* (2010) 'Extremely low copper concentrations affect gene expression profiles of human prostate epithelial cell lines', *Chemico-Biological Interactions*. Elsevier Ireland Ltd, 188(1), pp. 214–219. doi: 10.1016/j.cbi.2010.06.009.

Bleackley, M. R. *et al.* (2009) 'Blood Iron Homeostasis: Newly Discovered Proteins and Iron Imbalance', *Transfusion Medicine Reviews*. Elsevier Inc., 23(2), pp. 103–123. doi: 10.1016/j.tmrv.2008.12.001.

Bost, M. *et al.* (2016) 'Dietary copper and human health: Current evidence and unresolved issues', *Journal of Trace Elements in Medicine and Biology*, 35, pp. 107–115. doi: 10.1016/j.jtemb.2016.02.006.

Braiterman, L. *et al.* (2011) 'Critical roles for the COOH terminus of the Cu-ATPase ATP7B in protein stability, trans-Golgi network retention, copper sensing, and retrograde trafficking', *American Journal of Physiology-Gastrointestinal and Liver Physiology*, 301(1), pp. G69–G81. doi: 10.1152/ajpgi.00038.2011.

Brown, H. R. *et al.* (2002) 'Correlation of simultaneous differential gene expression in the blood and heart with known mechanisms of adriamycin-induced cardiomyopathy in the rat', *Toxicologic Pathology*, 30(4), pp. 452–469. doi: 10.1080/01926230213169.

Buhrke, T., Lengler, I. and Lampen, A. (2011) 'Analysis of proteomic changes induced upon cellular differentiation of the human intestinal cell line Caco-2', pp. 411–426. doi: 10.1111/j.1440-169X.2011.01258.x.

Byrne, L. A. (2010) *Analytical assessment of metal interactions and subsequent stability*. Doctoral Dissertation. National University of Ireland. Available at: http://mural.maynoothuniversity.ie/4080/1/Laura_Anne_Byrne_Ph.D_thesis_SEC.pdf.

Cabras, T. *et al.* (2015) 'Proteomic investigation of whole saliva in Wilsons disease', *Journal of Proteomics*. Elsevier B.V., 128, pp. 154–163. doi: 10.1016/j.jprot.2015.07.033.

Cahill, D. P. *et al.* (1999) 'Characterization of MAD2B and other mitotic spindle checkpoint genes', *Genomics*, 58(2), pp. 181–187. doi: 10.1006/geno.1999.5831.

Calabrese, E. J. *et al.* (2001) 'Hormesis : A Generalizable and Unifying Hypothesis', *Critical Reviews in Toxicology*, 8444(31), pp. 353–424. doi: 10.1080/20014091111730.

Calabrese, E. J. (2013) 'Hormetic mechanisms', *Critical Reviews in Toxicology*, 43(7), pp. 580–606. doi: 10.3109/10408444.2013.808172.

Calabrese, E. J. (2014) 'Hormesis: from mainstream to therapy', *Journal of Cell*

Communication and Signaling, 8(4), pp. 289–291. doi: 10.1007/s12079-014-0255-5.

Calabrese, E. J. *et al.* (2016) 'HORMESIS: A fundamental concept with widespread biological and biomedical applications', *Gerontology*, 62(5), pp. 530–535. doi: 10.1159/000441520.

Calabrese, E. J. and Blain, R. (2004) 'Metals in Perspective Metals and hormesis', *J. Environ. Monit., The Royal Society of Chemistry*, (6), pp. 14N-19N.

Caro, I. *et al.* (1995) 'Characterisation of a newly isolated Caco-2 clone (TC-7), as a model of transport processes and biotransformation of drugs', *International Journal of Pharmaceutics*, 116(2), pp. 147–158. doi: 10.1016/0378-5173(94)00280-I.

Carpenter, A. R. *et al.* (2016) 'Uroplakin 1b is critical in urinary tract development and urothelial differentiation and homeostasis', *Kidney International*. Elsevier, 89(3), pp. 612–624. doi: 10.1016/j.kint.2015.11.017.

Chambers, A. *et al.* (2010) 'An exposure-response curve for copper excess and deficiency.', *Journal of toxicology and environmental health. Part B, Critical reviews*, 13(7–8), pp. 546–78. doi: 10.1080/10937404.2010.538657.

Chan, N. *et al.* (2017) 'Influencing the tumor microenvironment: A phase II study of copper-depletion using tetrathiomolybdate (TM) in patients with breast cancer at high risk for recurrence and in preclinical models of lung metastases', *Clin Cancer Res*, 23(10), pp. 666–677. doi: 10.1158/1078-0432.CCR-16-1326.

Chattopadhyay, M. K., Myung, H. P. and Tabor, H. (2008) 'Hypusine modification for growth is the major function of spermidine in Saccharomyces cerevisiae polyamine auxotrophs grown in limiting spermidine', *Proceedings of the National Academy of Sciences of the United States of America*, 105(18), pp. 6554–6559. doi: 10.1073/pnas.0710970105.

Chaube, R., Mishra, S. and Singh, R. K. (2010) 'In vitro effects of lead nitrate on steroid profiles in the post-vitellogenic ovary of the catfish Heteropneustes fossilis', *Toxicology in Vitro*. Elsevier Ltd, 24(7), pp. 1899–1904. doi: 10.1016/j.tiv.2010.07.021.

Chen, A. and Donovan, S. (2004) 'Genistein at a concentration present in soy infant formula inhibits Caco-2BBe cell proliferation by causing G2/M cell cycle arrest', *The*

Journal of nutrition, 134(6), pp. 1303–8. Available at: http://www.ncbi.nlm.nih.gov/pubmed/15173388%5Cnhttp://jn.nutrition.org/content/134/6/1303.short.

Chen, X.-M., Elisia, I. and Kitts, D. D. (2010) 'Defining conditions for the co-culture of Caco-2 and HT29-MTX cells using Taguchi design.', *Journal of pharmacological and toxicological methods*. Elsevier Inc., 61(3), pp. 334–42. doi: 10.1016/j.vascn.2010.02.004.

Chen, Y. *et al.* (2015) 'Robust bioengineered 3D functional human intestinal epithelium', *Nature Publishing Group*. Nature Publishing Group, pp. 1–11. doi: 10.1038/srep13708.

Chimienti, F. *et al.* (2001) 'Zinc resistance impairs sensitivity to oxidative stress in HeLa cells: Protection through metallothioneins expression', *Free Radical Biology and Medicine*, 31(10), pp. 1179–1190. doi: 10.1016/S0891-5849(01)00701-8.

Chovatiya, R. and Medzhitov, R. (2014) 'Stress, inflammation, and defense of homeostasis', *Molecular Cell*. Elsevier Inc., 54(2), pp. 281–288. doi: 10.1016/j.molcel.2014.03.030.

Chun, H. *et al.* (2017) 'Organ-specific regulation of ATP7A abundance is coordinated with systemic copper homeostasis', *Scientific Reports*, 7(1), pp. 1–13. doi: 10.1038/s41598-017-11961-z.

Coleman, O. *et al.* (2017) 'Filter-Aided Sample Preparation (FASP) for Improved Proteome Analysis of Recombinant Chinese Hamster Ovary Cells BT - Heterologous Protein Production in CHO Cells: Methods and Protocols', in Meleady, P. (ed.). New York, NY: Springer New York, pp. 187–194. doi: 10.1007/978-1-4939-6972-2_12.

Coleman, O. *et al.* (2018) 'A comparative quantitative LC-MS/MS profiling analysis of human pancreatic adenocarcinoma, adjacent-normal tissue, and patient-derived tumour xenografts', *Proteomes*, 6(4), pp. 1–20. doi: 10.3390/proteomes6040045.

Coleman, O. *et al.* (2019) 'Increased growth rate and productivity following stable depletion of miR-7 in a mAb producing CHO cell line causes an increase in proteins associated with the Akt pathway and ribosome biogenesis', *Journal of Proteomics*. Elsevier, 195(December 2018), pp. 23–32. doi: 10.1016/j.jprot.2019.01.003.

Collins, J. F. and Knutson, M. D. (2010) 'Metabolic crossroads of iron and copper', *Nutrition reviews*, 68(3), pp. 133–147. doi: 10.1111/j.1753-4887.2010.00271.x.Metabolic.

Conolly, R. B. and Lutz, W. K. (2004) 'Nonmonotonic dose-response relationships: Mechanistic basis, kinetic modeling, and implications for risk assessment', *Toxicological Sciences*, 77(1), pp. 151–157. doi: 10.1093/toxsci/kfh007.

Costello, C. M. *et al.* (2014) 'Synthetic small intestinal scaffolds for improved studies of intestinal differentiation', *Biotechnology and Bioengineering*, 111(6), pp. 1222–1232. doi: 10.1002/bit.25180.

Damia, G. and Broggini, M. (2019) 'Platinum resistance in ovarian cancer: Role of DNA repair', *Cancers*, 11(1), pp. 1–15. doi: 10.3390/cancers11010119.

Danzeisen, R. *et al.* (2007) 'How reliable and robust are current biomarkers for copper status?', *The British journal of nutrition*, 98(4), pp. 676–683. doi: 10.1017/S0007114508958025.

Denoyer, D. *et al.* (2015) 'Targeting copper in cancer therapy: "Copper That Cancer"', *Metallomics*. Royal Society of Chemistry, 7(11), pp. 1459–1476. doi: 10.1039/c5mt00149h.

DiNicolantonio, J. J., Mangan, D. and O'Keefe, J. H. (2018) 'Copper deficiency may be a leading cause of ischaemic heart disease', *Open Heart*, 5(2), p. e000784. doi: 10.1136/openhrt-2018-000784.

Du, Z. *et al.* (1996) 'Utilization of Copper in Copper Proteinate, Copper Lysine, and Cupric Sulfate Using the Rat as an Experimental Model', *J. Anim. Sci.*, 74, pp. 1657–1663.

Ebert, M. S. and Sharp, P. A. (2010) 'MicroRNA sponges: Progress and possibilities', *Rna*, 16(11), pp. 2043–2050. doi: 10.1261/rna.2414110.

Erdman Jr., J. W. *et al.* (2014) *Present Knowledge in Nutrition: Tenth Edition (2012), Igarss 2014*. doi: 10.1007/s13398-014-0173-7.2.

Espinoza, A. *et al.* (2012) 'Iron , Copper , and Zinc Transport : Inhibition of Divalent Metal Transporter 1 (DMT1) and Human Copper Transporter 1 (hCTR1) by shRNA',

Biol Trace Elem Res, 1(146), pp. 281–286. doi: 10.1007/s12011-011-9243-2.

Fatfat, M. *et al.* (2014) 'Copper chelation selectively kills colon cancer cells through redox cycling and generation of reactive oxygen species', *BMC Cancer*, 14(1), pp. 1–12. doi: 10.1186/1471-2407-14-527.

Festa, R. A. and Thiele, D. J. (2011) 'Copper: An essential metal in biology', *Current Biology*. Elsevier, 21(21), pp. R877–R883. doi: 10.1016/j.cub.2011.09.040.

Fierro-González, J. C. *et al.* (2016) 'Defining the human copper proteome and analysis of its expression variation in cancers', *Metallomics*, 9(2), pp. 112–123. doi: 10.1039/c6mt00202a.

Finkbeiner, S. R. *et al.* (2015) 'Generation of tissue-engineered small intestine using embryonic stem cell-derived human intestinal organoids', *Biology Open*, pp. 1–11. doi: 10.1242/bio.013235.

Fischbach, M., Sabbioni, E. and Bromley, P. (1993) 'Induction of the human growth hormone gene placed under human hsp70 promoter control in mouse cells: A quantitative indicator of metal toxicity', *Cell Biology and Toxicology*, 9(2), pp. 177–188. doi: 10.1007/BF00757579.

Flora, S. J. S. and Pachauri, V. (2010) 'Chelation in metal intoxication.', *International journal of environmental research and public health*, 7(7), pp. 2745–88. doi: 10.3390/ijerph7072745.

Fogh, J. and Trempe, G. (1975) 'New Human Tumor Cell Lines', in Fogh, J. (ed.) *Human Tumor Cells in Vitro*. Boston, MA: Springer US, pp. 115–159. doi: 10.1007/978-1-4757-1647-4_5.

Freedman, J. H., Ciriolo, M. R. and Peisach, J. (1989) 'The role of glutathione in copper metabolism and toxicity.', *The Journal of biological chemistry*, 264(10), pp. 5598–5605. Available at: http://eutils.ncbi.nlm.nih.gov/entrez/eutils/elink.fcgi?dbfrom=pubmed&id=2564391&retmode=ref&cmd=prlinks%5Cnpapers3://publication/uuid/CCBF959B-2A64-4362-9393-61DFAB0DFB24.

Freedman, J. H. and Peisach, J. (1989) 'Resistance of cultured hepatoma cells to copper

toxicity. Purification and characterization of the hepatoma metallothionein', *BBA - General Subjects*, 992(2), pp. 145–154. doi: 10.1016/0304-4165(89)90003-2.

Freedman, J. H., Weiner, R. J. and Peisachst, J. (1986) 'Resistance to Copper Toxicity of Cultured Hepatoma Cells. Characterization of resistant cell lines.', *The Journal of biological chemistry*, 261(25), pp. 11840–11848.

Frey, A. G. *et al.* (2014) 'Iron chaperones PCBP1 and PCBP2 mediate the metallation of the dinuclear iron enzyme deoxyhypusine hydroxylase', *Proceedings of the National Academy of Sciences of the United States of America*, 111(22), pp. 8031–8036. doi: 10.1073/pnas.1402732111.

Fuqua, B. K., Vulpe, C. D. and Anderson, G. J. (2012) 'Intestinal iron absorption', *Journal of Trace Elements in Medicine and Biology*. Elsevier GmbH., 26(2–3), pp. 115–119. doi: 10.1016/j.jtemb.2012.03.015.

Gaetke, L. M., Chow-Johnson, H. S. and Chow, C. K. (2014) 'Copper: toxicological relevance and mechanisms', *Archives of Toxicology*, 88(11), pp. 1929–1938. doi: 10.1007/s00204-014-1355-y.

Gallagher, C. *et al.* (2014) 'Comparative transcriptomic analysis of cultivated limbal epithelium and donor corneal tissue reveals altered wound healing gene expression.', *Investigative ophthalmology & visual science*, 55(9), pp. 5795–5805. doi: 10.1167/iovs.14-14664.

Gan, J. *et al.* (2019) 'Highlighting the Proteasome : Using Fluorescence to Visualize Proteasome Activity and Distribution', *Frontiers in Molecular Biosciences*, 6(March), pp. 1–8. doi: 10.3389/fmolb.2019.00014.

Gao, C. *et al.* (2014) 'Effects of different sources of copper on Ctr1, ATP7A, ATP7B, MT and DMT1 protein and gene expression in Caco-2 cells', *Journal of Trace Elements in Medicine and Biology*. Elsevier GmbH., 28(3), pp. 344–350. doi: 10.1016/j.jtemb.2014.04.004.

Garrick, M. D. *et al.* (2006) 'DMT1: Which metals does it transport?', *Biological Research*, 39(1), pp. 79–85. doi: 10.4067/S0716-97602006000100009.

Garth J.S. Cooper (2011) 'Therapeutic Potential of Copper Chelation with

Triethylenetetramine in Managing Diabetes Mellitus and Alzheimer's Disease.', *Drugs*, 71(10), pp. 1281–1320. doi: 10.2165/11591370-000000000-00000.

Gerbe, F. and Jay, P. (2016) 'Intestinal tuft cells: Epithelial sentinels linking luminal cues to the immune system', *Mucosal Immunology*. Nature Publishing Group, 9(6), pp. 1353–1359. doi: 10.1038/mi.2016.68.

Gerbe, F., Legraverend, C. and Jay, P. (2012) 'The intestinal epithelium tuft cells: specification and function', *Cellular and Molecular Life Sciences*, 69(17), pp. 2907–2917. doi: 10.1007/s00018-012-0984-7.

Gioria, S. *et al.* (2018) 'Proteomics study of silver nanoparticles on Caco-2 cells', *Toxicology in Vitro*. Elsevier, 50(March), pp. 347–372. doi: 10.1016/j.tiv.2018.03.015.

Glahn, R. P. *et al.* (1998) 'Caco-2 Cell Ferritin Formation Predicts Nonradiolabeled Food Iron Availability in an In Vitro Digestion/Caco-2 Cell Culture Model', *The Journal of Nutrition*, 128(9), pp. 1555–1561. doi: 10.1093/jn/128.9.1555.

Goddard, W. P. *et al.* (1997) 'Iron Uptake by Isolated Human Enterocyte Suspensions In Vitro Is Dependent on Body Iron Stores and Inhibited by Other Metal Cations', *J. Nutr*, 127(September 1996), pp. 177–183.

Gomes, I. M., Maia, C. J. and Santos, C. R. (2012) 'STEAP proteins: From structure to applications in cancer therapy', *Molecular Cancer Research*, 10(5), pp. 573–587. doi: 10.1158/1541-7786.MCR-11-0281.

Gong, D. *et al.* (2009) 'Quantitative proteomic profiling identifies new renal targets of copper(II)-selective chelation in the reversal of diabetic nephropathy in rats', *Proteomics*, 9(18), pp. 4309–4320. doi: 10.1002/pmic.200900285.

Gotoh, T. *et al.* (2004) 'hsp70-DnaJ chaperone pair prevents nitric oxide- and CHOP-induced apoptosis by inhibiting translocation of Bax to mitochondria', *Cell Death and Differentiation*, 11(4), pp. 390–402. doi: 10.1038/sj.cdd.4401369.

Grabinger, T. *et al.* (2014) 'Ex vivo culture of intestinal crypt organoids as a model system for assessing cell death induction in intestinal epithelial cells and enteropathy', *Cell Death and Disease*. Nature Publishing Group, pp. 1–10. doi: 10.1038/cddis.2014.183.

Graham, R. J., Bhatia, H. and Yoon, S. (2019) ‘Consequences of trace metal variability and supplementation on Chinese hamster ovary (CHO) cell culture performance: A review of key mechanisms and considerations’, *Biotechnology and Bioengineering*, 116(12), pp. 3446–3456. doi: 10.1002/bit.27140.

Gray, L. W. *et al.* (2012) ‘Urinary copper elevation in a mouse model of Wilson’s disease is a regulated process to specifically decrease the hepatic copper load’, *PLoS ONE*, 7(6). doi: 10.1371/journal.pone.0038327.

Groba, S. R. *et al.* (2017) ‘Downregulation of hepatic multi-drug resistance protein 1 (MDR1) after copper exposure’, *Metallomics*, 9(9), pp. 1279–1287. doi: 10.1039/c7mt00189d.

Gulec, S. and Collins, J. (2014) ‘Molecular mediators governing iron-copper interactions.’, *Annual Review of Nutrition*, 34, pp. 95–116. doi: 10.1146/annurev-nutr-071812-161215.

Gullberg, E. *et al.* (2000) ‘Expression of specific markers and particle transport in a new human intestinal M-cell model.’, *Biochemical and biophysical research communications*, 279(3), pp. 808–813. doi: 10.1006/bbrc.2000.4038.

Guo, R. *et al.* (2001) ‘Chemical characteristics and relative bioavailability of supplemental organic copper sources for poultry’, *Journal of Animal Science*, 79(5), pp. 1132–1141.

Gupta, S. K. *et al.* (1993) ‘Serum and tissue trace elements in colorectal cancer’, *Journal of Surgical Oncology*, 52(3), pp. 172–175. doi: 10.1002/jso.2930520311.

Gutierrez, E. *et al.* (2013) ‘eif5A promotes translation of polyproline motifs’, *Molecular Cell*. Elsevier Inc., 51(1), pp. 35–45. doi: 10.1016/j.molcel.2013.04.021.

Harvey, L. J. and McArdle, H. J. (2008) ‘Biomarkers of copper status: a brief update.’, *The British journal of nutrition*, 99 Suppl 3, pp. S10–S13. doi: 10.1017/S0007114508006806.

Hasan, N. M. and Lutsenko, S. (2012) ‘Regulation of Copper Transporters in Human Cells’, in *Current Topics in Membranes*. Elsevier, pp. 137–161. doi: 10.1016/B978-0-12-394390-3.00006-9.

Hatori, Y. and Lutsenko, S. (2016) 'The Role of Copper Chaperone Atox1 in Coupling Redox Homeostasis to Intracellular Copper Distribution', *Antioxidants*, 5(3), p. 25. doi: 10.3390/antiox5030025.

Hayes, J. D. and McLellan, L. I. (1999) 'Glutathione and glutathione-dependent enzymes represent a co-ordinately regulated defence against oxidative stress', *Free Radical Research*, 31(4), pp. 273–300. doi: 10.1080/10715769900300851.

He, W. *et al.* (2008) 'Availability and toxicity of Fe (II) and Fe (III) in Caco-2 cells', *J Zhejiang Univ Sci B*, 9(9), pp. 707–712. doi: 10.1631/jzus.B0820023.

Heenan, M. *et al.* (1997) 'Isolation from a human MDR lung cell line of multiple clonal subpopulations which exhibit significantly different drug resistance', *International Journal of Cancer*, 71(5), pp. 907–915. doi: 10.1002/(SICI)1097-0215(19970529)71:5<907::AID-IJC33>3.0.CO;2-1.

Helander, H. F. and Fändriks, L. (2014) 'Surface area of the digestive tract - revisited.', *Scandinavian journal of gastroenterology*, 49(6), pp. 681–9. doi: 10.3109/00365521.2014.898326.

Helmestam, M., Stavreus-Evers, A. and Olovsson, M. (2010) 'Cadmium chloride alters mRNA levels of angiogenesis related genes in primary human endometrial endothelial cells grown in vitro', *Reproductive Toxicology*. Elsevier Inc., 30(3), pp. 370–376. doi: 10.1016/j.reprotox.2010.05.003.

Herst, P. M. *et al.* (2017) 'Functional mitochondria in health and disease', *Frontiers in Endocrinology*, 8(NOV). doi: 10.3389/fendo.2017.00296.

Hidalgo, I. J., Raub, T. J. and Borchardt, R. T. (1989) 'Characterization of the human colon carcinoma cell line (Caco-2) as a model system for intestinal epithelial permeability', *Gastroenterology*, 96(3), pp. 736–749.

Hilgendorf, C. *et al.* (2000) 'Caco-2 versus Caco-2/HT29-MTX Co-cultured Cell Lines: Permeabilities Via Diffusion, Inside-and Outside-Directed Carrier-Mediated Transport', *-tical Association J Pharm Sci*, 89(1), pp. 63–75. doi: 10.1002/(SICI)1520-6017(200001)89:1<63::AID-JPS7>3.0.CO;2-6.

Hill, C. E., Myers, J. P. and Vandenberg, L. N. (2018) 'Nonmonotonic dose–Response

curves occur in dose ranges that are relevant to regulatory decision-making', *Dose-Response*, 16(3), pp. 1–4. doi: 10.1177/1559325818798282.

Hoffman, H., Richard, C. and Phyliky, L. (1988) 'Zinc-induced copper deficiency', *Gastroenterology*. Elsevier Inc., 94(2), pp. 508–512. doi: 10.1016/0016-5085(88)90445-3.

Hofmann, S. *et al.* (2005) 'Functional and mutational characterization of human MIA40 acting during import into the mitochondrial intermembrane space', *Journal of Molecular Biology*, 353(3), pp. 517–528. doi: 10.1016/j.jmb.2005.08.064.

Hong, Y. *et al.* (2015) 'Glutathione and multidrug resistance protein transporter mediate a self-propelled disposal of bismuth in human cells', *Proceedings of the National Academy of Sciences*, 112(11), pp. 3211–3216. doi: 10.1073/pnas.1421002112.

Huet, C. *et al.* (1987) 'Absorptive and mucus-secreting subclones isolated from a multipotent intestinal cell line (HT-29) provide new models for cell polarity and terminal differentiation.', *The Journal of cell biology*, 105(1), pp. 345–57. doi: 10.1083/jcb.105.1.345.

Huppke, P. *et al.* (2012) 'Molecular and biochemical characterization of a unique mutation in CCS, the human copper chaperone to superoxide dismutase', *Human Mutation*, 33(8), pp. 1207–1215. doi: 10.1002/humu.22099.

Ighodaro, O. M. and Akinloye, O. A. (2018) 'First line defence antioxidants-superoxide dismutase (SOD), catalase (CAT) and glutathione peroxidase (GPX): Their fundamental role in the entire antioxidant defence grid', *Alexandria Journal of Medicine*. Alexandria University Faculty of Medicine, 54(4), pp. 287–293. doi: 10.1016/j.ajme.2017.09.001.

Inglett, G. E. and Solomons, N. W. (1998) 'Competitive Mineral — Mineral Interaction', in *Nutritional Bioavailablility of Zinc*, pp. 247–271.

Iolante, G. D. V *et al.* (2004) 'Short Term Caco-2 / TC7 Cell Culture : Comparison between of Conventional 21-d and a Commercially Available 3-d System', *Biol. Pharm. Bull.*, 27(12), pp. 1986–1992.

Jaiser, S. R. and Winston, G. P. (2010) 'Copper deficiency myelopathy', *Journal of*

Neurology, 257(6), pp. 869–881. doi: 10.1007/s00415-010-5511-x.

Jany, T. *et al.* (2015) 'Rational design of a cytotoxic dinuclear Cu2 complex that binds by molecular recognition at two neighboring phosphates of the dna backbone', *Inorganic Chemistry*, 54(6), pp. 2679–2690. doi: 10.1021/ic5028465.

Johnson, M. A. and Kays, S. E. (1990) 'Copper: Its role in human nutrition', *Nutrition Today*, pp. 6–14. doi: 10.1097/00017285-199001000-00003.

Joyce, H. *et al.* (2015) 'Influence of multidrug resistance and drug transport proteins on chemotherapy drug metabolism', *Expert Opinion on Drug Metabolism and Toxicology*, 11(5), pp. 795–809. doi: 10.1517/17425255.2015.1028356.

Juarez, J. C. *et al.* (2006) 'Copper Binding by Tetrathiomolybdate Attenuates Angiogenesis and Tumor Cell Proliferation through the Inhibition of Superoxide Dismutase 1', *Clinical Cancer Research*, 12(16), pp. 4974–4982. doi: 10.1158/1078-0432.CCR-06-0171.

Kaler, S. G. (2011) 'ATP7A-related copper transport diseases—emerging concepts and future trends', *Nat Rev Neurol.*, 7(1), pp. 15–16. doi: 10.1038/nrneurol.2010.180.ATP7A-related.

Katzmann, D. J., Babst, M. and Emr, S. D. (2001) 'Ubiquitin-Dependent Sorting into the Multivesicular Body Pathway Requires the Function of a Conserved Endosomal Protein Sorting Complex , ESCRT-I', *Cell*, 106, pp. 145–155. doi: 10.1016/s0092-8674(01)00434-2.

Keely, S. *et al.* (2005) 'In vitro and ex vivo intestinal tissue models to measure mucoadhesion of poly (methacrylate) and N-trimethylated chitosan polymers', *Pharmaceutical Research*, 22(1), pp. 38–49. doi: 10.1007/s11095-004-9007-1.

Keenan, J., O'Sullivan, F., *et al.* (2018) 'Acute exposure to organic and inorganic sources of copper: Differential response in intestinal cell lines', *Food Science and Nutrition*, 6(8), pp. 2499–2514. doi: 10.1002/fsn3.857.

Keenan, J., Horgan, K., *et al.* (2018) 'Unexpected fluctuations of trace element levels in cell culture medium in vitro: caveat emptor', *In Vitro Cellular & Developmental Biology - Animal*, 54(9), pp. 555–558. doi: 10.1007/s11626-018-0285-z.

Kidane, T. Z. *et al.* (2012) 'Uptake of copper from plasma proteins in cells where expression of CTR1 has been modulated', *BioMetals*, 25(4), pp. 697–709. doi: 10.1007/s10534-012-9528-8.

Kim, H. J. *et al.* (2012) 'Human gut-on-a-chip inhabited by microbial flora that experiences intestinal peristalsis-like motions and flow.', *Lab on a chip*, 12(12), pp. 2165–74. doi: 10.1039/c2lc40074j.

Klomp, A. E. M. *et al.* (2002) 'Biochemical characterization and subcellular localization of human copper transporter 1 (hCTR1).', *The Biochemical journal*, 364(Pt 2), pp. 497–505. doi: 10.1042/BJ20011803.

Koch, K. A., O Pena, M. M. and Thiele, D. J. (1997) 'Copper-binding and signaling motifs in catalysis , transport, detoxification and signalling', *Chemistry&Biology*, 4(8), pp. 549–560.

Kozlowski, H. *et al.* (2009) 'Copper, iron, and zinc ions homeostasis and their role in neurodegenerative disorders (metal uptake, transport, distribution and regulation)', *Coordination Chemistry Reviews*, 253(21–22), pp. 2665–2685. doi: 10.1016/j.ccr.2009.05.011.

Lafont, F. *et al.* (1998) 'Annexin XIIIb associates with lipid microdomains to function in apical delivery', *Journal of Cell Biology*, 142(6), pp. 1413–1427. doi: 10.1083/jcb.142.6.1413.

Lagarde, F. *et al.* (2015) 'Non-monotonic dose-response relationships and endocrine disruptors: a qualitative method of assessment.', *Environmental health : a global access science source*, 14(1), p. 13. doi: 10.1186/1476-069X-14-13.

Laurie, S. H. and Sarkar, B. (1977) 'Potentiometric and Spectroscopic Study of the Equilibria in the Aqueous Copper(11)-3,6-Diazaoctane-1,8-diamine System and an Equilibrium-dialysis Examination of the Ternary System of Human Serum AlbuminCopper(11)-3,6- Diazaoctane-I ,8-diamine', *J.C.S. Dalton*, IV, pp. 1822–1827.

Leblondel, G. and Allain, P. (1999) 'Manganese transport by caco-2 cells.', *Biological Trace Element Research*, 67(1), p. 13. Available at: http://search.ebscohost.com/login.aspx?direct=true&db=edb&AN=50082857&site=eds-live&scope=site.

Lee, B. H. *et al.* (2011) 'Proteomic analysis of the hepatic tissue of Long – Evans Cinnamon (LEC) rats according to the natural course of Wilson disease', pp. 3698–3705. doi: 10.1002/pmic.201100122.

Lesuffleur, T. *et al.* (1990) 'Growth adaptation to methotrexate of HT-29 human colon carcinoma cells is associated with their ability to differentiate into columnar absorptive and mucus-secreting cells', *Cancer Research*, 50(19), pp. 6334–6343.

Leung, T. K. *et al.* (1990) 'The human heat-shock protein family. Expression of a novel heat-inducible HSP70 (HSP70B') and isolation of its cDNA and genomic DNA.', *The Biochemical Journal*, 267(1), pp. 125–32. doi: 10.1042/bj2670125.

Levin, D. E. *et al.* (2013) 'Human tissue-engineered small intestine forms from postnatal progenitor cells', *Journal of Pediatric Surgery*, 48(1), pp. 129–137. doi: 10.1016/j.jpedsurg.2012.10.029.

Levy-Rimler, G. *et al.* (2001) 'The effect of nucleotides and mitochondrial chaperonin 10 on the structure and chaperone activity of mitochondrial chaperonin 60', *Eur. J. Biochem.*, 268, pp. 3465–3472. doi: 10.1046/j.1432-1327.2001.02243.x.

Li, Y. *et al.* (2017) 'Glutaredoxin 1 mediates the protective efect of steady laminar fow on endothelial cells against oxidative stress-induced apoptosis via inhibiting Bim', *Scientific Reports*, 7(1), pp. 1–11. doi: 10.1038/s41598-017-15672-3.

Lillig, C. H. and Berndt, C. (2009) 'Thioredoxins and Glutaredoxins. Functions and Metal Ion Interactions', *Met. Ions Life Sci.*, 5(14), pp. 413–439. doi: 10.1039/9781847558992-00413.

Linden, S. K. *et al.* (2008) 'Mucins in the mucosal barrier to infection', *Nature Mucosal Immunology*, 1(3), pp. 183–197. doi: 10.1038/mi.2008.5.

Linder, C. and Hazegh-Azam, M. (1996) 'Copper biochemistry and molecular biology', *American Journal of Clinical Nutrition*, (63), pp. 797s-811s.

Linder, M. C. (2012) 'The relationship of copper to DNA damage and damage prevention in humans', *Mutation Research/Fundamental and Molecular Mechanisms of Mutagenesis*. Elsevier B.V., 733(1–2), pp. 83–91. doi: 10.1016/j.mrfmmm.2012.03.010.

Linder, M. C. (2016) 'Ceruloplasmin and other copper binding components of blood

plasma and their functions : an update', *Metallomics*. Royal Society of Chemistry, 8, pp. 887–905. doi: 10.1039/C6MT00103C.

Liu, N. *et al.* (2007) 'Transcuprein is a Macroglobulin Regulated by Copper and Iron Availability', *J Nutr Biochem.*, 9(18), pp. 597–608. doi: 10.1016/j.cortex.2009.08.003.Predictive.

Liu, X. *et al.* (2015) 'Glutaredoxin 1 (Grx1) protects human retinal pigment epithelial cells from oxidative damage by preventing AKT glutathionylation', *Investigative Ophthalmology and Visual Science*, 56(5), pp. 2821–2832. doi: 10.1167/iovs.14-15876.

Livak, K. J. and Schmittgen, T. D. (2001) 'Analysis of relative gene expression data using real-time quantitative PCR and the 2-ΔΔCT method', *Methods*, 25(4), pp. 402–408. doi: 10.1006/meth.2001.1262.

Lönnerdal, B. (2008) 'Intestinal regulation of copper homeostasis : a developmental perspective', 88, pp. 846–850.

Lu, J. *et al.* (2010) 'Copper (II)-selective chelation improves function and antioxidant defences in cardiovascular tissues of rats as a model of diabetes : comparisons between triethylenetetramine and three less copper-selective transition-metal-targeted treatments', *Diabetologia*, (53), pp. 1217–1226. doi: 10.1007/s00125-010-1698-8.

Lu, J. (2010) 'Triethylenetetramine Pharmacology and Its Clinical Applications', *Molecular Cancer Therapeutics*, 9(9), pp. 2458–2467. doi: 10.1158/1535-7163.mct-10-0523.

Luo, J. *et al.* (2012) 'Comparative metabolite analysis to understand lactate metabolism shift in Chinese hamster ovary cell culture process', *Biotechnology and Bioengineering*, 109(1), pp. 146–156. doi: 10.1002/bit.23291.

Lutsenko, S. *et al.* (2007) 'Function and Regulation of Human Copper-Transporting ATPases', *Physiological Reviews*, 87(3), pp. 1011–1046. doi: 10.1152/physrev.00004.2006.

Mabbott, N. A. *et al.* (2013) 'Microfold (M) cells: important immunosurveillance posts in the intestinal epithelium.', *Mucosal immunology*. Nature Publishing Group, 6(4), pp. 666–77. doi: 10.1038/mi.2013.30.

Mahler, G. J., Shuler, M. L. and Glahn, R. P. (2009) 'Characterization of Caco-2 and HT29-MTX cocultures in an in vitro digestion/cell culture model used to predict iron bioavailability.', *The Journal of nutritional biochemistry*. Elsevier Inc., 20(7), pp. 494–502. doi: 10.1016/j.jnutbio.2008.05.006.

Majumder, S. *et al.* (2009) 'The role of copper in drug-resistant murine and human tumors', *BioMetals*, 22(2), pp. 377–384. doi: 10.1007/s10534-008-9174-3.

Mantha, M. and Jumarie, C. (2010) 'Cadmium-induced hormetic effect in differentiated caco-2 cells: ERK and p38 activation without cell proliferation stimulation', *Journal of Cellular Physiology*, 224(1), pp. 250–261. doi: 10.1002/jcp.22128.

Marshall, K. R. *et al.* (2005) 'The human apoptosis-inducing protein AMID is an oxidoreductase with a modified flavin cofactor and DNA binding activity', *Journal of Biological Chemistry*, 280(35), pp. 30735–30740. doi: 10.1074/jbc.M414018200.

Martin, A. and Clynes, M. (1991) 'Acid phosphatase: Endpoint for in vitro toxicity tests', *In Vitro Cell. Dev. Bio*, 27A(March), pp. 183–184. doi: 10.1016/j.nurpra.2014.09.017.

Martin, A. and Clynes, M. (1993) 'Comparison of 5 microplate colorimetric assays forin vitro cytotoxicity testing and cell proliferation assays', *Cytotechnology*, 11(1), pp. 49–58. doi: 10.1007/BF00749057.

Mason, K. E. (1979) 'A conspectus of research on copper metabolism and requirements of man.', *The Journal of nutrition*, 109(11), pp. 1979–2066.

Materia, S. *et al.* (2012) 'Clusterin and COMMD1 independently regulate degradation of the mammalian copper ATPases ATP7A and ATP7B', *Journal of Biological Chemistry*, 287(4), pp. 2485–2499. doi: 10.1074/jbc.M111.302216.

Mathews, M. B. and Hershey, J. W. B. (2015) 'The translation factor eIF5A and human cancer', *Biochim Biophys Acta*, 1849(7), pp. 836–844. doi: 10.1016/j.bbagrm.2015.05.002.

Mattie, M. D., McElwee, M. K. and Freedman, J. H. (2008) 'Mechanism of copper-activated transcription: activation of AP-1, and the JNK/SAPK and p38 signal transduction pathways.', *Journal of molecular biology*. Elsevier B.V., 383(5), pp. 1008–

18. doi: 10.1016/j.jmb.2008.08.080.

Maynard, C. J. *et al.* (2005) 'Metals and amyloid-β in Alzheimer's disease', *International Journal of Experimental Pathology*, 86(3), pp. 147–159. doi: 10.1111/j.0959-9673.2005.00434.x.

McGivern, T. J. P. *et al.* (2018) 'Innovative DNA-Targeted Metallo-prodrug Strategy Combining Histone Deacetylase Inhibition with Oxidative Stress', *Molecular Pharmaceutics*. American Chemical Society, 15(11), pp. 5058–5071. doi: 10.1021/acs.molpharmaceut.8b00652.

Meaney, C. and O'Driscoll, C. (1999) 'Mucus as a barrier to the permeability of hydrophilic and lipophilic compounds in the absence and presence of sodium taurocholate micellar systems using cell culture models', *European Journal of Pharmaceutical Sciences*, 8(3), pp. 167–175. doi: 10.1016/S0928-0987(99)00007-X.

Meguro, Y. *et al.* (1991) 'Changes of copper level and cytochrome c oxidase activity in the macular mouse with age', *Brain and Development*, 13(3), pp. 184–186. doi: 10.1016/S0387-7604(12)80027-1.

Michael Davis, J. and Svendsgaard, D. J. (1990) 'U-shaped dose-response curves: Their occurrence and implications for risk assessment', *Journal of Toxicology and Environmental Health*, 30(2), pp. 71–83. doi: 10.1080/15287399009531412.

Molloy, S. A. and Kaplan, J. H. (2009) 'Copper-dependent recycling of hCTR1, the human high affinity copper transporter', *Journal of Biological Chemistry*, 284(43), pp. 29704–29713. doi: 10.1074/jbc.M109.000166.

Muita, J. W. (2001) 'Micronutrients in health and disease.', *East African Medical Journal*, 78(9), pp. 449–450. doi: 10.1136/pgmj.2006.047670.

Mutoh, M. *et al.* (1997) 'Reversal of Heavy Metal Resistance in Multidrug-Resistant Human KB Carcinoma Cells', *Biochemical and Biophysical Research Communications*, 236(3), pp. 586–590. doi: 10.1006/bbrc.1997.7015.

Natoli, M. *et al.* (2009) 'Mechanisms of defence from Fe(II) toxicity in human intestinal Caco-2 cells', *Toxicology in Vitro*. Elsevier Ltd, 23(8), pp. 1510–1515. doi: 10.1016/j.tiv.2009.06.016.

Natoli, M. *et al.* (2011) ‘Cell growing density affects the structural and functional properties of Caco-2 differentiated monolayer.’, *Journal of cellular physiology*, 226(6), pp. 1531–43. doi: 10.1002/jcp.22487.

Neunlist, M. *et al.* (2013) ‘The digestive neuronal-glial-epithelial unit: a new actor in gut health and disease.’, *Nature reviews. Gastroenterology & hepatology*. Nature Publishing Group, 10(2), pp. 90–100. doi: 10.1038/nrgastro.2012.221.

Nguyen, T., Nioi, P. and Pickett, C. B. (2009) ‘The Nrf2-antioxidant response element signaling pathway and its activation by oxidative stress’, *Journal of Biological Chemistry*, 284(20), pp. 13291–13295. doi: 10.1074/jbc.R900010200.

Nishito, Y. and Kambe, T. (2018) ‘Absorption Mechanisms of Iron, Copper, and Zinc: An Overview’, *J Nutr Sci Vitaminol*, 64, pp. 1–7. doi: 10.3177/jnsv.64.1.

Nose, Y. *et al.* (2010) ‘Ctr1 is an apical copper transporter in mammalian intestinal epithelial cells in vivo that is controlled at the level of protein stability’, *Journal of Biological Chemistry*, 285(42), pp. 32385–32392. doi: 10.1074/jbc.M110.143826.

Nurchi, V. M. *et al.* (2013) ‘Complex formation equilibria of Cu(II) and Zn(II) with triethylenetetramine and its mono- and di-acetyl metabolites.’, *Dalton transactions (Cambridge, England : 2003)*, 42, pp. 6161–70. doi: 10.1039/c2dt32252h.

O’Doherty, C. *et al.* (2019) ‘Copper-induced non-monotonic dose response in Caco-2 cells’, *In Vitro Cellular & Developmental Biology - Animal*, 55(4), pp. 221–225. doi: 10.1007/s11626-019-00333-8.

O’Sullivan, F. *et al.* (2017) ‘Parallel mRNA, proteomics and miRNA expression analysis in cell line models of the intestine’, *World Journal of Gastroenterology*, 23(41), pp. 7369–7386. doi: 10.3748/wjg.v23.i41.7369.

O Doherty, C. *et al.* (2020) ‘Characterisation and proteomic profiling of continuously exposed Cu- resistant variants of the Caco-2 cell line’, *Toxicology in Vitro*. Elsevier, 65(January), p. 104773. doi: 10.1016/j.tiv.2020.104773.

Ogra, Y. (2011) ‘Research Tools and Techniques for Copper Metabolism in Mammals’, *Journal of Health Science*, 57(5), pp. 385–396. doi: 10.1248/jhs.57.385.

Ogra, Y. *et al.* (2016) ‘Changes in intracellular copper concentration and copper-

regulating gene expression after PC12 differentiation into neurons', *Scientific Reports*. Nature Publishing Group, 6(1), p. 33007. doi: 10.1038/srep33007.

Ogra, Y., Aoyama, M. and Suzuki, K. T. (2006) 'Protective role of metallothionein against copper depletion', *Archives of Biochemistry and Biophysics*, 451(2), pp. 112–118. doi: 10.1016/j.abb.2006.04.017.

Olivares, M. *et al.* (2008) 'Present situation of biomarkers for copper status', *American Journal of Clinical Nutrition*, 88(3), pp. 859–862.

Osredkar, J. and Sustar, N. (2011) 'Copper and Zinc , Biological Role and Significance of Copper / Zinc Imbalance', *Journal of Clinical Toxicology*, 3, pp. 1–18. doi: 10.4172/2161-0495.S3-001.

Park, J. *et al.* (2009) 'Proteomic analysis of sera of asymptomatic, early-stage patients with Wilsons disease', *Proteomics Clin. Appl.*, 3, pp. 1185–1190. doi: 10.1002/prca.200800057.

Peterson, L. W. and Artis, D. (2014) 'Intestinal epithelial cells: regulators of barrier function and immune homeostasis.', *Nature reviews. Immunology*. Nature Publishing Group, 14(3), pp. 141–53. doi: 10.1038/nri3608.

Peterson, M. D. and Mooseker, M. S. (1992) 'Characterization of the enterocyte-like brush border cytoskeleton of the C2BBe clones of the human intestinal cell line, Caco-2.', *Journal of cell science*, 102 (Pt 3, pp. 581–600. Available at: http://eutils.ncbi.nlm.nih.gov/entrez/eutils/elink.fcgi?dbfrom=pubmed&id=1506435&retmode=ref&cmd=prlinks%5Cnpapers3://publication/uuid/CD249B4D-020D-4742-B81B-C3776BBD6E5F.

Pettit, L. D., Powell, K. J. and Chemistry., I. U. of P. and A. (no date) 'The IUPAC stability constants database, SC-database and mini-SCDatabase.' Timble, Otley, Yorks, UK: Academic Software. Available at: http://www.acadsoft.co.uk/scdbase/scdbase.htm.

Pfeiffenberger, J. *et al.* (2018) 'The steady state pharmacokinetics of trientine in Wilson disease patients'. European Journal of Clinical Pharmacology.

Phillips-Krawczak, C. A. *et al.* (2015) 'COMMD1 is linked to the WASH complex and regulates endosomal trafficking of the copper transporter ATP7A', *Molecular Biology*

of the Cell, 26(1), pp. 91–103. doi: 10.1091/mbc.e14-06-1073.

Powell, J. J., Jugdaohsingh, R. and Thompson, R. P. (1999) 'The regulation of mineral absorption in the gastrointestinal tract.', *The Proceedings of the Nutrition Society*, 58(1999), pp. 147–153. doi: 10.1079/PNS19990020.

Prasad, A. S. (2012) 'Discovery of human zinc deficiency: 50 years later', *Journal of Trace Elements in Medicine and Biology*. Elsevier GmbH., 26(2–3), pp. 66–69. doi: 10.1016/j.jtemb.2012.04.004.

Prohaska, J. R. (2008) 'Role of copper transporters in copper homeostasis 1 – 4', *Am J Clin Nutr*, 1, pp. 826–829.

Prohaska, J. R., Broderius, M. and Brokate, B. (2003) 'Metallochaperone for Cu,Zn-superoxide dismutase (CCS) protein but not mRNA is higher in organs from copper-deficient mice and rats', *Archives of Biochemistry and Biophysics*, 417(2), pp. 227–234. doi: 10.1016/S0003-9861(03)00364-3.

Puckett, C. A., Ernst, R. J. and Barton, J. K. (2010) 'Exploring the cellular accumulation of metal complexes', *Dalton Transactions*, 39(5), pp. 1159–1170. doi: 10.1039/b922209j.

Puig, S. and Thiele, D. J. (2002) 'Molecular mechanisms of copper uptake and distribution', *Current Opinion in Chemical Biology*, 6(2), pp. 171–180. doi: 10.1016/S1367-5931(02)00298-3.

Purchase, R. (2013) 'The treatment of Wilson ' s disease , a rare genetic disorder of copper metabolism', *Science Progress*, 96(1), pp. 19–32. doi: 10.3184/003685013X13587771579987.

Qian, Y. *et al.* (2011) 'Cell culture and gene transcription effects of copper sulfate on Chinese hamster ovary cells', *Biotechnology Progress*, 27(4), pp. 1190–1194. doi: 10.1002/btpr.630.

Qian, Y. *et al.* (2014) 'Hypoxia influences protein transport and epigenetic repression of CHO cell cultures in shake flasks', *Biotechnology Journal*, 9(11), pp. 1413–1424. doi: 10.1002/biot.201400315.

Radons, J. (2016) 'The human HSP70 family of chaperones: where do we stand?', *Cell*

Stress and Chaperones, 21(3), pp. 379–404. doi: 10.1007/s12192-016-0676-6.

Raghunath, A. *et al.* (2018) 'Antioxidant response elements: Discovery, classes, regulation and potential applications', *Redox Biology*. Elsevier B.V., 17(March), pp. 297–314. doi: 10.1016/j.redox.2018.05.002.

Rakshit, A. *et al.* (2018) 'Cu2+ selective chelators relieve copper-induced oxidative stress in vivo', *Chem. Sci.* Royal Society of Chemistry, 9, pp. 7916–7930. doi: 10.1039/c8sc04041a.

Ramos, D. *et al.* (2016) 'Mechanism of copper uptake from blood plasma ceruloplasmin by mammalian cells', *PLoS ONE*, 11(3), pp. 1–23. doi: 10.1371/journal.pone.0149516.

Reed, E., Lutsenko, S. and Bandmann, O. (2019) 'Animal models of Wilson disease', *Journal of Neurochemistry*, 146(4), pp. 356–373. doi: 10.1111/jnc.14323.Animal.

des Rieux, A. *et al.* (2007) 'An improved in vitro model of human intestinal follicle-associated epithelium to study nanoparticle transport by M cells.', *European journal of pharmaceutical sciences : official journal of the European Federation for Pharmaceutical Sciences*, 30(5), pp. 380–91. doi: 10.1016/j.ejps.2006.12.006.

de Romaña, D. L. *et al.* (2011) 'Risks and benefits of copper in light of new insights of copper homeostasis', *Journal of Trace Elements in Medicine and Biology*, 25(1), pp. 3–13. doi: 10.1016/j.jtemb.2010.11.004.

Ross, D. and Siegel, D. (2018) 'NQO1 in protection against oxidative stress', *Current Opinion in Toxicology*. Elsevier Ltd, 7, pp. 67–72. doi: 10.1016/j.cotox.2017.10.005.

Rossi, D. *et al.* (2016) 'Evidence for a negative cooperativity between eIF5A and eEF2 on binding to the ribosome', *PLoS ONE*, 11(4), pp. 1–18. doi: 10.1371/journal.pone.0154205.

Rousselet, E., Richaud, P., *et al.* (2008) 'A zinc-resistant human epithelial cell line is impaired in cadmium and manganese import', *Toxicology and Applied Pharmacology*, 230(3), pp. 312–319. doi: 10.1016/j.taap.2008.02.025.

Rousselet, E., Martelli, A., *et al.* (2008) 'Zinc adaptation and resistance to cadmium toxicity in mammalian cells: Molecular insight by proteomic analysis', *Proteomics*, 8(11), pp. 2244–2255. doi: 10.1002/pmic.200701067.

Ruttkay-Nedecky, B. *et al.* (2013) 'The role of metallothionein in oxidative stress.', *International journal of molecular sciences*, 14(3), pp. 6044–66. doi: 10.3390/ijms14036044.

Sambuy, Y. *et al.* (2005) 'The Caco-2 cell line as a model of the intestinal barrier: Influence of cell and culture-related factors on Caco-2 cell functional characteristics', *Cell Biology and Toxicology*, 21(1), pp. 1–26. doi: 10.1007/s10565-005-0085-6.

De Santa Barbara, P., Van Den Brink, G. R. and Roberts, D. J. (2003) 'Development and differentiation of the intestinal epithelium', *Cellular and Molecular Life Sciences*, 60(7), pp. 1322–1332. doi: 10.1007/s00018-003-2289-3.

Santoro, M. G. (2000) 'Heat Shock Factors and the Control of the Stress Response', *Biochemical Pharmacology*, 59(99), pp. 55–63.

Santra, M., Dill, K. A. and de Graff, A. M. R. (2018) 'How Do Chaperones Protect a Cell's Proteins from Oxidative Damage?', *Cell Systems*. Elsevier Inc., 6(6), pp. 743-751.e3. doi: 10.1016/j.cels.2018.05.001.

Sarkar, B. and Clarke, R. (1969) 'A Comparative Study of in vitro and in vivo Interaction of D-penicillamine and Triethylenetetramine with Copper'.

Sato, T. *et al.* (2009) 'Single Lgr5 stem cells build crypt-villus structures in vitro without a mesenchymal niche.', *Nature*. Nature Publishing Group, 459(7244), pp. 262–5. doi: 10.1038/nature07935.

Sauer, A. K. *et al.* (2017) 'Characterization of zinc amino acid complexes for zinc delivery in vitro using Caco-2 cells and enterocytes from hiPSC', *BioMetals*, (Prasad 2014), pp. 1–19. doi: 10.1007/s10534-017-0033-y.

Scheers, N. M., Almgren, A. B. and Sandberg, A.-S. (2014) 'Proposing a Caco-2/HepG2 cell model for in vitro iron absorption studies.', *The Journal of nutritional biochemistry*. The Authors, 25(7), pp. 710–5. doi: 10.1016/j.jnutbio.2014.02.013.

Schilsky, M. L. *et al.* (1998) 'Copper resistant human hepatoblastoma mutant cell lines without metallothionein induction overexpress ATP7B', *Hepatology*, 28(5), pp. 1347–1356. doi: 10.1002/hep.510280525.

Schmidt, P. J., Kunst, C. and Culotta, V. C. (2000) 'Copper activation of superoxide

dismutase 1 (SOD1) in vivo: Role for protein-protein interactions with the copper chaperone for SOD1', *Journal of Biological Chemistry*, 275(43), pp. 33771–33776. doi: 10.1074/jbc.M006254200.

Schuller, A. P. *et al.* (2017) 'eIF5A Functions Globally in Translation Elongation and Termination', *Molecular Cell*. Elsevier Inc., 66(2), pp. 194-205.e5. doi: 10.1016/j.molcel.2017.03.003.

Schulz, H. (1888) 'Ueber Hefegifte', *Pfluger, Archiv fur die Gesammte Physiologie des Menschen und der Thiere*, 42(1), pp. 517–541. doi: 10.1007/BF01669373.

Shah, P. *et al.* (2006) 'Role of Caco-2 cell monolayers in prediction of intestinal drug absorption', *Biotechnology Progress*, 22(1), pp. 186–198. doi: 10.1021/bp050208u.

Shao, Y. *et al.* (2017) 'Zinc enhances intestinal epithelial barrier function through the PI3K/AKT/mTOR signaling pathway in Caco-2 cells', *The Journal of Nutritional Biochemistry*. Elsevier Inc., 43, pp. 18–26. doi: 10.1016/j.jnutbio.2017.01.013.

Shomura, Y. *et al.* (2005) 'Regulation of Hsp70 Function by HspBP1 : Structural Analysis Reveals an Alternate Mechanism for Hsp70 Nucleotide Exchange', *Molecular Cell*, 17, pp. 367–379. doi: 10.1016/j.molcel.2004.12.023.

Siegemund, R. *et al.* (1991) 'Mode of action of triethylenetetramine dihydrochloride on copper metabolism in Wilson's disease', *Acta Neurologica Scandinavica*, 83(6), pp. 364–366. doi: 10.1111/j.1600-0404.1991.tb03964.x.

Simmons, S. O. *et al.* (2011) 'NRF2 Oxidative Stress Induced by Heavy Metals is Cell Type Dependent.', *Current chemical genomics*, 5, pp. 1–12. doi: 10.2174/1875397301105010001.

Smith, A. T., Smith, K. P. and Rosenzweig, A. C. (2014) 'Diversity of the metal-transporting P1B-type ATPases', *JBIC Journal of Biological Inorganic Chemistry*, 19(6), pp. 947–960. doi: 10.1007/s00775-014-1129-2.

Sone, H. *et al.* (1996) 'Inhibition of Hereditary Hepatitis and Liver Tumor Development in Long-Evans Cinnamon Rats by the Copper- Chelating Agent Trientine Dihydrochloride', *HEPATOLOGY*, 23(4), pp. 764–770.

Song, M. O. *et al.* (2014) 'The Role of Nrf1 and Nrf2 in the Regulation of Copper-

responsive Transcription', 154(11), pp. 2262–2265. doi: 10.1016/j.pain.2013.06.005.Re-Thinking.

Spence, J. R. *et al.* (2011) 'Directed differentiation of human pluripotent stem cells into intestinal tissue in vitro.', *Nature*. Nature Publishing Group, 470(7332), pp. 105–9. doi: 10.1038/nature09691.

Stefani, M. and Dobson, C. M. (2003) 'Protein aggregation and aggregate toxicity: New insights into protein folding, misfolding diseases and biological evolution', *Journal of Molecular Medicine*, 81(11), pp. 678–699. doi: 10.1007/s00109-003-0464-5.

Suazo, M. *et al.* (2008) 'CCS and SOD1 mRNA are reduced after copper supplementation in peripheral mononuclear cells of individuals with high serum ceruloplasmin concentration', *Journal of Nutritional Biochemistry*, 19(4), pp. 269–274. doi: 10.1016/j.jnutbio.2007.04.003.

Sutherland, J. D. and Barrio, R. (2018) 'Putting the stress on UFM1 (ubiquitin-fold modifier 1): Protein ufmylation as a novel regulator of endoplasmic reticulum stress in cardiac health and disease', *Circulation: Heart Failure*, 11(10), pp. 1–4. doi: 10.1161/CIRCHEARTFAILURE.118.005455.

Szklarczyk, D. *et al.* (2019) 'STRING v11: Protein-protein association networks with increased coverage, supporting functional discovery in genome-wide experimental datasets', *Nucleic Acids Research*. Oxford University Press, 47(D1), pp. D607–D613. doi: 10.1093/nar/gky1131.

Takahashi, K. and Yamanaka, S. (2006) 'Induction of Pluripotent Stem Cells from Mouse Embryonic and Adult Fibroblast Cultures by Defined Factors', *Cell*, 126(4), pp. 663–676. doi: 10.1016/j.cell.2006.07.024.

Taupin, D. and Podolsky, D. K. (2003) 'Trefoil factors: Initiators of mucosal healing', *Nature Reviews Molecular Cell Biology*, 4(9), pp. 721–732. doi: 10.1038/nrm1203.

Taymaz-nikerel, H. *et al.* (2018) 'Doxorubicin induces an extensive transcriptional and metabolic rewiring in yeast cells', (August), pp. 1–14. doi: 10.1038/s41598-018-31939-9.

Tegoni, M. *et al.* (2014) 'Copper Chelators: Chemical Properties and Bio-medical

Applications', *Current Medicinal Chemistry*, 21(33), pp. 3785–3818. doi: 10.2174/09298673216661406011619 39.

Tennant, J. *et al.* (2002) 'Effects of copper on the expression of metal transporters in human intestinal Caco-2 cells', *FEBS Letters*, 527, pp. 239–244. doi: 10.1016/S0014-5793(02)03253-2.

Thorn, C. F. *et al.* (2011) 'Doxorubicin pathways: pharmacodynamics and adverse effects', *Pharmacogenet Genomics*, 21(7), pp. 440–446. doi: 10.1097/FPC.0b013e32833ffb56.Doxorubicin.

Titma, T. *et al.* (2016) 'Toxicity of antimony, copper, cobalt, manganese, titanium and zinc oxide nanoparticles for the alveolar and intestinal epithelial barrier cells in vitro', *Cytotechnology*. Springer Netherlands, 68(6), pp. 2363–2377. doi: 10.1007/s10616-016-0032-9.

Tlaskalová-Hogenová, H. *et al.* (2004) 'Commensal bacteria (normal microflora), mucosal immunity and chronic inflammatory and autoimmune diseases', *Immunology Letters*, 93(2–3), pp. 97–108. doi: 10.1016/j.imlet.2004.02.005.

Tsuruta, T. *et al.* (2016) 'Biochemical and Biophysical Research Communications Organoids as an ex vivo model for studying the serotonin system in the murine small intestine and colon epithelium', *Biochemical and Biophysical Research Communications*. Elsevier Ltd, 474(1), pp. 161–167. doi: 10.1016/j.bbrc.2016.03.165.

Umar, S. (2011) 'Intestinal Stem Cells', 12(5), pp. 340–348. doi: 10.1007/s11894-010-0130-3.Intestinal.

Valko, M., Morris, H. and Cronin, M. (2005) 'Metals, Toxicity and Oxidative Stress', *Current Medicinal Chemistry*, 12(10), pp. 1161–1208. doi: 10.2174/0929867053764635.

Vandenberg, L. N. *et al.* (2012) 'Hormones and endocrine-disrupting chemicals: Low-dose effects and nonmonotonic dose responses', *Endocrine Reviews*, 33(3), pp. 378–455. doi: 10.1210/er.2011-1050.

Vernhet, L. *et al.* (2002) 'Overexpression of the multidrug resistance-associated protein (MRP1) in human heavy metal-selected tumor cells', *FEBS Letters*, 443(3), pp. 321–

325. doi: 10.1016/s0014-5793(98)01716-5.

Vu, V. V. *et al.* (2009) 'Human deoxyhypusine hydroxylase, an enzyme involved in regulating cell growth, activates O2 with a nonheme diiron center', *Proceedings of the National Academy of Sciences of the United States of America*, 106(35), pp. 14814–14819. doi: 10.1073/pnas.0904553106.

Waggoner, D. J., Bartnikas, T. B. and Gitlin, J. D. (1999) 'The Role of Copper in Neurodegenerative Disease', *Pharmacology & Therapeutics*, 81(6), pp. 221–230. doi: 10.1016/S0163-7258(98)00042-4.

Wallach, T. E. and Bayrer, J. R. (2017) 'Intestinal Organoids: New Frontiers in the Study of Intestinal Disease and Physiology', *Journal of Pediatric Gastroenterology and Nutrition*, 64(2), pp. 180–185. doi: 10.1097/MPG.0000000000001411.

Walter, E. *et al.* (1996) 'HT29-MTX/Caco-2 cocultures as an in vitro model for the intestinal epithelium: in vitro-in vivo correlation with permeability data from rats and humans.', *Journal of pharmaceutical sciences*, 85(10), pp. 1070–6. doi: 10.1021/js960110x.

Wang, Q. *et al.* (2018) 'Suckling Piglet Intestinal Enterocyte Nutrient Metabolism Changes', *Cellular Physiology and Biochemistry*, 48(5), pp. 2103–2113. doi: 10.1159/000492552.

Wang, X. *et al.* (2018) 'Ex Vivo Enteroids Recapitulate In Vivo Citrulline Production in Mice', (10), pp. 1–6. doi: 10.1093/jn/nxy126.

Wang, Y. *et al.* (2017) 'Copper or/and arsenic induce oxidative stress-cascaded, nuclear factor kappa B-dependent inflammation and immune imbalance, trigging heat shock response in the kidney of chicken', *Oncotarget*, 8(58), pp. 98103–98116. doi: 10.18632/oncotarget.21463.

Wang, Y. *et al.* (2018) 'Copper or/and arsenic induces autophagy by oxidative stress-related PI3K/AKT/mTOR pathways and cascaded mitochondrial fission in chicken skeletal muscle', *Journal of Inorganic Biochemistry*. Elsevier, 188(July), pp. 1–8. doi: 10.1016/j.jinorgbio.2018.08.001.

Watson, C. L. *et al.* (2014) 'An in vivo model of human small intestine using

pluripotent stem cells', *Nature Medicine*, 20(11). doi: 10.1038/nm.3737.

Wells, J. M. and Spence, J. R. (2014) 'How to make an intestine.', *Development (Cambridge, England)*, 141(4), pp. 752–60. doi: 10.1242/dev.097386.

Weydert, C. J. and Cullen, J. J. (2010) 'Measurement of superoxide dismutase, catalase and glutathione peroxidase in cultured cells and tissue', *Nature protocols*, 5(1), pp. 51–66. doi: 10.1038/nprot.2009.197.MEASUREMENT.

Wice, B. M. and Gordon, J. I. (1992) 'A strategy for isolation of cDNAs encoding proteins affecting human intestinal epithelial cell growth and differentiation: Characterization of a novel gut-specific N-myristoylated annexin', *Journal of Cell Biology*, 116(2), pp. 405–422. doi: 10.1083/jcb.116.2.405.

Wikman-Larhed, A. and Artursson, P. (1995) 'Co-cultures of human intestinal goblet (HT29-H) and absorptive (Caco-2) cells for studies of drug and peptide absorption', *European Journal of Pharmaceutical Sciences*, 3, pp. 171–183.

Wikman, A. *et al.* (1993) 'A Drug Absorption Model Based on the Mucus Layer Producing Human Intestinal Goblet Cell Line HT29-H', *Pharmaceutical Research: An Official Journal of the American Association of Pharmaceutical Scientists*, pp. 843–852. doi: 10.1023/A:1018905109971.

Wingler, K. *et al.* (2000) 'Gastrointestinal glutathione peroxidase prevents transport of lipid hydroperoxides in CaCo-2 cells', *Gastroenterology*, 119(2), pp. 420–430. doi: 10.1053/gast.2000.9521.

Wollert, T. *et al.* (2009) 'The ESCRT machinery at a glance', *J Cell Sci.*, 122(13), pp. 2163–2166. doi: 10.1242/jcs.029884.

Woodcock, S. *et al.* (1991) 'Isolation and characterisation of clones from the Caco-2 cell line displaying increased taurocholic acid transport', *J Cell Sci.*, Mar;98 (P(82), pp. 323–32.

Wosen, J. E. *et al.* (2019) 'Human Intestinal Enteroids Model MHC-II in the Gut Epithelium', 10(August), pp. 1–8. doi: 10.3389/fimmu.2019.01970.

Wray, S. H., Kuwabara, T. and Sanderson, P. (1976) 'Menkes' kinky hair disease: a light and electron microscopic study of the eye', *Investigative Ophthalmology*, 15(2),

pp. 128–138.

Youness, R. A. *et al.* (2016) ‘MicroRNA-486-5p enhances hepatocellular carcinoma tumor suppression through repression of IGF-1R and its downstream mTOR , STAT3 and c-Myc’, *ONCOLOGY LETTERS*, 12, pp. 2567–2573. doi: 10.3892/ol.2016.4914.

Yu, J. *et al.* (2012) ‘In vitro 3D human small intestinal villous model for drug permeability determination’, *Biotechnology and Bioengineering*, 109(9), pp. 2173–2178. doi: 10.1002/bit.24518.

Yuk, I. H. *et al.* (2015) ‘Effects of copper on CHO cells: Cellular requirements and product quality considerations’, *Biotechnology Progress*, 31(1), pp. 226–238. doi: 10.1002/btpr.2004.

Zerounian, N. R. *et al.* (2003) ‘Regulation of copper absorption by copper availability in the Caco-2 cell intestinal model.’, *American journal of physiology. Gastrointestinal and liver physiology*, 284(5), pp. G739-47. doi: 10.1152/ajpgi.00415.2002.

Zerounian, N. R. and Linder, M. C. (2002) ‘Effects of copper and ceruloplasmin on iron transport in the Caco 2 cell intestinal model’, *Journal of Nutritional Biochemistry*, 13, pp. 138–148.

Zhang, Y. *et al.* (2012) ‘Transcriptional Regulation of the Ufm1 Conjugation System in Response to Disturbance of the Endoplasmic Reticulum Homeostasis and Inhibition of Vesicle Trafficking’, *PLoS ONE*, 7(11), pp. 1–11. doi: 10.1371/journal.pone.0048587.

Zhang, Y. *et al.* (2018) ‘miR-486-5p regulates the migration and invasion of colorectal cancer cells through targeting PIK3R1’, (10), pp. 7243–7248. doi: 10.3892/ol.2018.8233.

Zheng, H. *et al.* (2008) ‘Data mining of metal ion environments present in protein structures’, *Journal of Inorganic Biochemistry*, 102(9), pp. 1765–1776. doi: 10.1016/j.jinorgbio.2008.05.006.

Zimnicka, A. M., Maryon, E. B. and Kaplan, J. H. (2007) ‘Human copper transporter hCTR1 mediates basolateral uptake of copper into enterocytes: Implications for copper homeostasis’, *Journal of Biological Chemistry*, 282(36), pp. 26471–26480. doi: 10.1074/jbc.M702653200.

Zödl, B. *et al.* (2003) 'Toxic and biochemical effects of zinc in Caco-2 cells', *Journal of Inorganic Biochemistry*, 97(4), pp. 324–330. doi: 10.1016/S0162-0134(03)00312-X.

Appendices

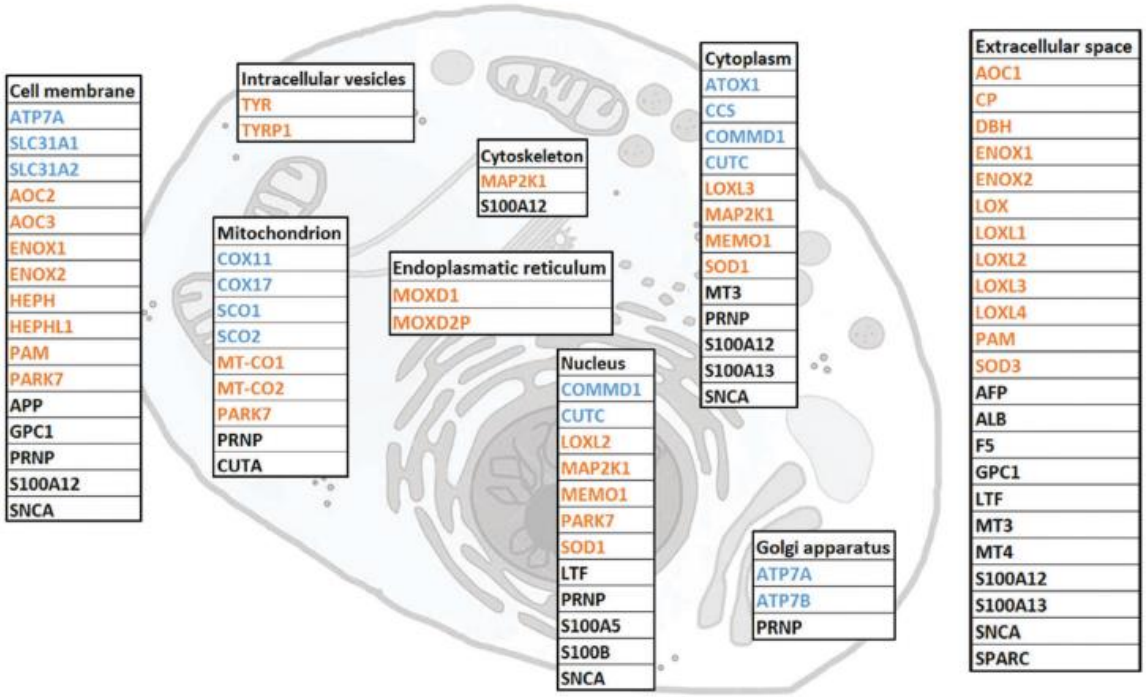

Appendix Figure 1: *The Cu binding proteome indicating cellular localization for 54 Cu-binding proteins. Colours indicate protein function: blue - transporter; orange - enzyme; and black - protein with other or unknown function (From Fierro-González et. al 2016)*

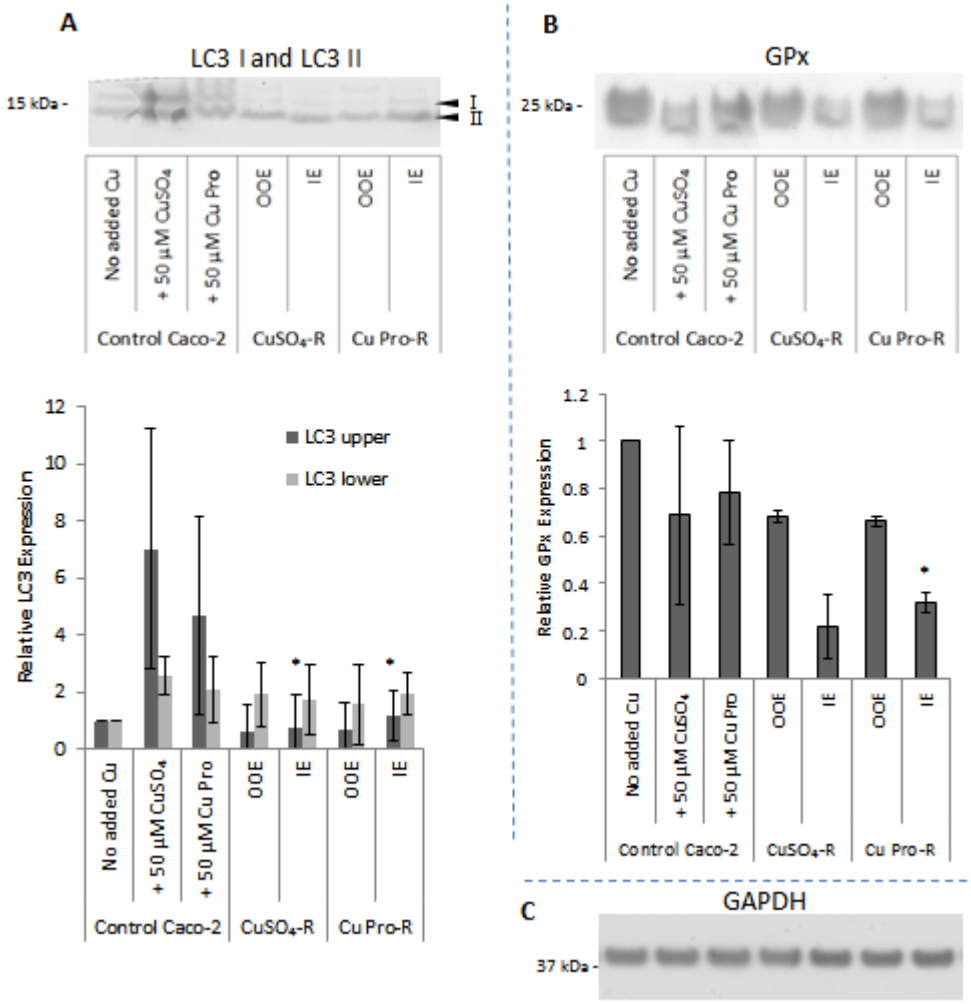

Appendix Figure 2. *Representative Western blots for A: Microtubule-associated proteins 1A/1B light chain 3B (LC3) upper band (LC3-I) and lower band (LC3-II), B: Glutathione peroxidase 1 (GPx), and C: endogenous control - GAPDH in parental Caco-2, $CuSO_4$-R and Cu Pro-R cells exposed to basal growth media "out-of-exposure" (OOE) and during exposure to 50 µM $CuSO_4$ or 50 µM Cu Pro "in-exposure" (IE) for 96 hours. Densitometry expressed relative to unexposed control and normalised to GAPDH (N=3). Asterisk indicates that there are significant differences (* $P < 0.05$) between the Cu-treated resistant cells and the Cu-treated control group at the same concentration (50 µM).*

Sample ID	Biological Rep.	Conc. (ng/µl)	A 260/280	A 260/230	RIN (From Bioanalyser)
Control Caco-2	REP 1	759.55	2.12	2.03	8.3
Clone In1		467.86	2.02	1.21	8.3
Clone In2		503.22	2.13	2.1	7.9
Cone Or1		444.61	2.03	1.64	8.2
Clone Or2		513.08	2.11	0.98	8
Clone Or3		639.68	2.12	1.78	8.1
Control Caco-2	REP 2	810.96	2.08	1.99	8.4
Clone In1		534.23	2.09	2.09	8.9
Clone In2		548.64	2.1	1.9	8.5
Clone Or1		641.97	2.1	2	8.8
Clone Or2		666.19	2.13	2.09	8.7
Cone Or3		816.56	2.11	1.22	8.8
Control Caco-2	REP 3	659.02	2.08	2.03	8.3
Clone In1		712.96	2.09	2.02	8.3
Clone In2		518.8	2.12	1.94	8.3
Cone Or1		684.72	2.09	1.91	8.5
Clone Or2		662.03	2.08	1.43	8.7
Clone Or3		967.2	2.08	2.02	8.2

Appendix Figure 3: *Quality control for mRNA extracted from parental Caco-2 cells and isolated Cu-resistant Caco-2 clones (In1, In2, Or1, Or2 and Or3). RIN = RNA integrity number, output from bioanalyser and used to threshold samples for passing QC check before running on human gene microarrays (minimum 7.9).*

A

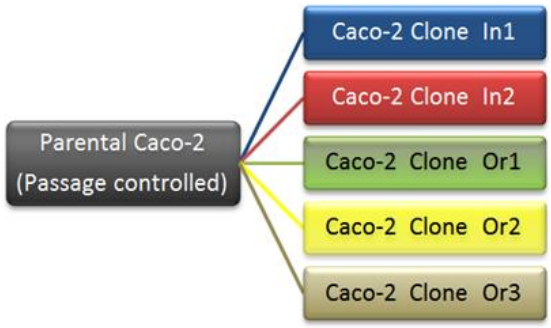

B

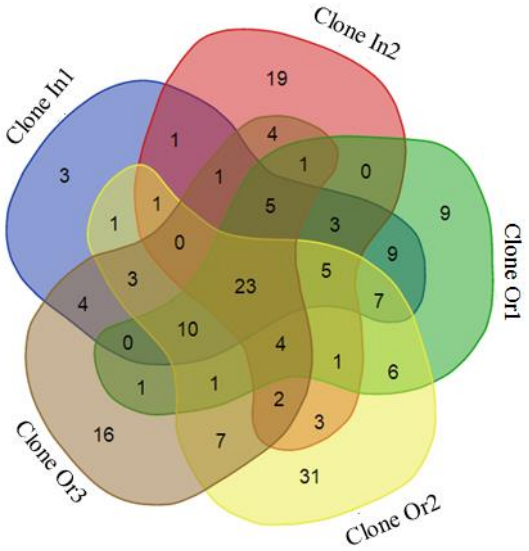

C

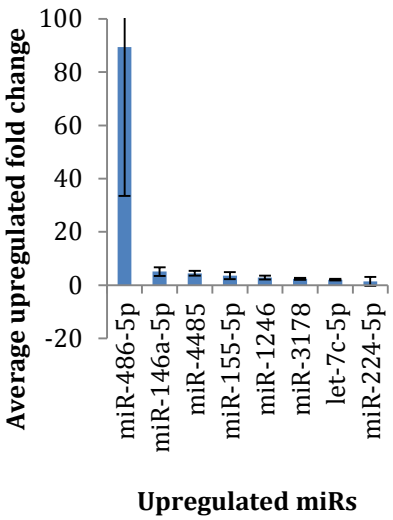

D

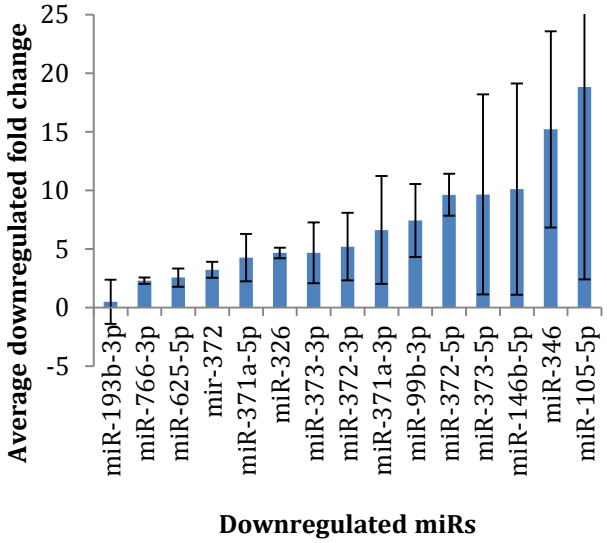

Appendix Figure 4: *A: Design schematic for miRNA microarray analysis; B: 5-set Venn diagram showing overlap of differentially expressed miRNA identified between Cu-resistant clones and parental Caco-2 cells; C/ D: Bar chart of relative expression for 8 upregulated and 15 downregulated miRNA in common between all Cu-resistant Caco-2 clones*